Alternative Theories of Gravity and their Application to Cosmology

Jannie A. Leach

Thesis presented for the degree of

DOCTOR OF PHILOSOPHY

in the Department of Mathematics and Applied Mathematics

at the

University of Cape Town

February 2008

Declaration

The work presented in this thesis is partly based on collaboration with Iain Brown (Institut für Theoretiche Physik, Universität Heidelberg, Germany), Salvatore Capozziello (Dipartimento di Scienze Fisiche and INFN Sez. di Napoli, Università di Napoli 'Federico II', Italy), and Kishore Ananda, Sante Carloni, Peter Dunsby and Naureen Goheer (Department of Mathematics and Applied Mathematics, University of Cape Town). The list below identifies sections or paragraphs which are partially based on the listed publications (or article in preparation):

- Chapter 3:

  J. A. Leach, S. Carloni and P. K. S. Dunsby
  Class. Quantum Grav. **23** (2006) 4915

- Chapter 4:

  N. Goheer, J. A. Leach and P. K. S. Dunsby
  Class. Quantum Grav. **24** (2007) 5689

- Chapter 5:

  N. Goheer, J. A. Leach and P. K. S. Dunsby
  Class. Quantum Grav. **25** (2008) 035013

- Chapter 6:

  S. Carloni, J. A. Leach, S. Capozziello and P. K. S. Dunsby
  Class. Quantum Grav. **25** (2008) 035008

- Chapter 7:

  J. A. Leach, I. A. Brown, K. N. Ananda and P. K. S. Dunsby
  In progress.

I hereby declare that this thesis has not been submitted, either in the same or different form, to this or any other university for a degree and that it represents my own work.

Jannie Leach

Abstract

In this thesis we study extended theories of gravity in the context of cosmology. The first part is dedicated to the application of the theory of dynamical systems, which allow us to investigate the global dynamics of some cosmological models resulting from scalar-tensor and higher-order theories of gravity.

We use the dynamical systems approach with non–compact expansion normalised variables to study the isotropisation of Bianchi type I models in R^n–gravity. We find that these type of models can isotropise faster or slower than their general relativity counterparts. We extend this analysis to the full class of orthogonal spatially homogeneous Bianchi models to study the effect of spatial curvature on the isotropisation of these models. A compact state space is constructed by dividing the state space into different sectors, that allows us to also investigate static solutions and bouncing or recollapsing behaviours which is not possible when using non-compact expansion normalised variables. We find no Einstein static solutions, but there do exist cosmologies with bounce behaviours. We also find that all isotropic points are flat Friedmann like. We discuss the advantages and disadvantages of compactifying the state space, and illustrate this using two examples.

We next study the phase-space of Friedmann models derived from scalar-tensor gravity where the non-minimal coupling is $F(\phi) = \xi\phi^2$ and the self-interaction potential is $V(\phi) = \lambda\phi^n$. Transient almost-Friedmann phases evolving towards accelerated expansion and unstable inflationary phases evolving towards stable ones are found.

In the last part of this work, we set out a framework to analyse tensor anisotropies in the cosmic microwave background of scalar-tensor cosmologies. As an example, we consider one of the exact solutions found for the class of scalar-tensor theories considered above.

Acknowledgements

For three years I have been grinding away in my office and now, finally, all this work has culminated in this thesis. During this time I have had some of the best moments of my life. This is in no small part due to a number of people, who inspired, supported and encouraged me on this journey. It has been a great pleasure and I wish to thank some of them here.

I thank my supervisor, Peter for his help, guidance and all round facilitation of this PhD. Through your efforts have I not only been introduced to many exciting concepts but also have developed as a scientist and introduced to the greater scientific community. My deepest gratitude to you.

To all my collaborators a special thanks for their individual contributions without which this thesis would not have been possible. Naureen, my cute slave driver, who taught me so much about dynamical systems and how to be more sensitive by providing her with a shoulder to cry on. We really nailed this dynamical systems thing hey! I also thank Sante and Salvatore for introducing me to alternative theories of gravity and Kishore for his help on tensor anisotropies. Ian, apparently both of us like to rock the boat so here's to rocking the boat!

Of course no journey is worth taking without companions, i.e. my fellow cosmostringy people. Gerry, my man, thanks for all the coffee's and many interesting conversations. Teresa, well what can I say, thank you for all our 'play' time, it really helped when I needed a break from work. Bob, my comrade in arms, were finished our struggle!! Jeff, dude, thanks for all the advise and the many discussions on string theory, dual groups etc., I really enjoyed it. Big thanks to my office mates, Andy, Anslyn and Jacques for many a good laugh. To the rest of the cosmo crew, Kishore, Chris, Charles, Alex, Reneé, Bruce and George, many thanks for your various inputs

as well.

Many in the Mathematics department at UCT also made a contribution to my work and social well being. Di, I don't know how I would have managed without you. Your willingness to go out of your way to help and the countless times you sorted out problems with the NRF and post graduate funding, is greatly appreciated. To Alan, Rory, Oliver, William, Francois and all the others that were involved in the various courses that I tutored, a special thanks, it was a great pleasure working with you. Penny, thanks for all you help as well.

Now although my athletics has not been up to scratch over the past few years (and I am constantly being reminded of this!), the UCT Athletics Club played an important part in my life over the past few years. I had lots of fun, both as a social runner and SASSU manager. James, (maid) Marion, Will (power), Ian (Noddie), Helen, the two Nicci's, Lauren, Amy, Penny, Sean, Deon, the Benno's, Jarvis and the rest of the gang, you really made this one of the best experiences of my life, I thank you all.

I also wish to thank the group at the University of Naples, Federico II, for their help and hospitality during my stay in Naples: Claudio, Salvatore, Paolo, Venchenzo, Ester and Antonio, thank you all for making my visits memorable, I enjoyed them thoroughly!

I thank the National Research Foundation (South Africa) and the Italian *Ministero Degli Affari Esteri-DG per la Promozione e Cooperazione Culturale* which supported my research under the joint Italy/ South Africa Science and Technology agreement.

Lastly, and most importantly, I wish to thank my parents, Willem and Elize, my brother Kobus, sister Annelize, and other family members, for the years of support and encouragement. *Ma, dankie vir al die jare se bystand en vir die mooi voorbeeld wat jy daar vir my gestel het. Jou deursettings vermoë was vir my 'n inspirasie om deur te druk teen spyte van omstandighede. Pa, waar moet ek begin. Jou voorbeeld van manlikheid en vaderskap, vorm die basis van my wese. Deur jou voorbeeld het ek geleer dat rede is die lig van die wêreld en dat dit slegs kan seëvier deur die individue what die fakkel van die self dra. Kobus, dankie vir al jou ondersteuning, jy is 'n vriend duisend!*

Ek woon in my eie huis, het niemand nog nagemaak nie, en ek lag vir elke meester, wat nie vir homself kan lag nie.
-Nietzsche, *Die fröhliche Wissenschaft.*

Contents

List of Figures

List of Tables

Chapter 1

Introduction

1.1 The standard model of cosmology

The standard model of cosmology (see for example [1]) based on Einstein's theory of General Relativity (GR) is one of the great success stories in modern theoretical physics. This model describes a universe that is isotropic and homogeneous on large scales; the so-called Friedmann-Lemaître-Robertson-Walker (FLRW) model. It describes the universe from around one second after the big bang to the present matter dominated era ($\sim$ 13 billion years). During this very long history, the universe changed dramatically. Approximately three minutes after the big bang, *nucleosynthesis* took place, that is hydrogen and helium nuclei formed from protons and neutrons. For the next 10^5 years, the universe was in a radiation dominated phase in which matter and radiation was coupled through Thompson scattering. After 10^5 years the temperature cooled down to around 3000 K, which allowed *recombination* of protons and electrons, leading to the formation of neutral hydrogen. Photons decoupled from matter and could travel almost unhindered till the present day, loosing energy as the universe continued to expand. The radiation due to these photons, are presently observed with a temperature of 2.73 K, known as the Cosmic Microwave Background (CMB) radiation. After recombination, density fluctuations grew since radiation could no longer prevent gravitational instabilities and so the universe entered the matter dominated phase in which we find ourselves at present.

The standard model's success is in part due to several of its predictions having been verified by observations. For example, the abundances of helium with respect to other light elements observed in the universe agrees well with predictions of this

model. The period of recombination is strongly supported by the CMB which is arguably the strongest evidence supporting the standard model.

There are however several problems with the standard model. The universe appears to be homogeneous, isotropic and (almost) flat, which requires very special initial conditions. Also, the formation of large scale structure is believed to be due to initial density fluctuations. These fluctuations must have a very special spectrum in order to produce the structure we observe today. One possible answer to these problems, is that the early universe underwent a brief period of rapid expansion or *inflation*. This inflationary phase could smooth out all inhomogeneities and inflate the universe so that it is almost flat. It can furthermore provide us with the initial density fluctuations which we require for structure formation. However, inflation is believed to be caused by a light or massless scalar-field, the *inflaton*, which has not been observed as yet.

The present day observed universe also possesses some problems for the standard model. The behaviour of galactic rotation curves and the mass discrepancy in galactic clusters, seem to suggest the existence of non–baryonic matter, commonly known as *dark matter*. This dark matter whose origin is still unclear, does not interact with baryonic matter or neutrinos. It also has a negligible velocity dispersion and is thus usually referred to as Cold Dark Matter (CDM). Current estimates, seem to indicate that over twenty percent of total energy content of the universe consists of dark matter. A second, and even more alarming problem for the standard model, is the one posed by the current observations, using both type Ia supernovae and the CMB, which seems to indicate that the universe has entered an accelerated expansion phase. This late time accelerated behaviour requires some unknown source of energy, dubbed *dark energy*, to drive it. Dark energy accounts for just over 70% of the universes energy content. In fact standard matter only seem to account for about five percent, so the nature of most of the universes content is completely unknown to us!

The standard model, despite its successes, has several unanswered problem facing it. In the next section we will look at one possible way of resolving these problems.

1.2 Alternative theories of gravity

The standard model assumes that the laws of gravity described by GR are the same on all scales in the universe, that is Newton's gravitational constant G remains constant across the universe. However, GR has only been tested up to solar system scales and we can therefore not necessarily assume that gravity behaves the same on larger scales.

The 'dark' problems discussed above, both apply to larger scales; dark matter on galactic and supergalactic scales and dark energy on cosmic scales. In fact, Milgrom and others [2, 3] realised that by modifying gravity on galactic scales, one could explain the galactic rotation curves of galaxies. This phenomenological approach is known as Modified Newtonian Dynamics (MOND) (see [4] for a review) and has over the last decade been revived in a number of forms [5–9], most notably Bekenstein's Tensor-Vector-Scalar theory (TeVeS) [10]. MOND has also been used in the context of braneworld models [11–14].

Thus a possible way around the problems facing the standard model, may be to assume that gravity gets modified on larger scales. These modifications include the adding of extra dimensions like in the brane world models [15], the adding of a minimally or non-minimally coupled scalar field [16], or modifications of the underlying field equations by either adding higher order corrections to the curvature [17–49] or changing the equation of state [50–52]. In this thesis we will consider the addition of scalar fields and higher order corrections, collectively known as *Extended Theories of Gravity* (ETG).

One of the most fruitful theories of this type is Scalar–Tensor Gravity (STG), in which scalar field(s) are introduced that are non–minimally coupled to gravity. These type of theories were proposed nearly half a century ago by Jordan [53] and later refined by Brans and Dicke [54]. The original motivation behind Brans-Dicke theory (BD) came from Mach's principle, but over the years, BD and STG have gained interest in a wide number of scenarios. For example, in unification schemes such as superstrings, supergravity or grand unified theories, the one–loop or higher–loop corrections in the high–curvature regime take the form of non–minimal couplings to the geometry or higher–order curvature invariants in their low energy effective actions [55].

In cosmology, STG acquired considerable interest because they naturally introduce a scalar field and scalar fields are capable of giving rise to inflationary behaviour, which overcome some of the shortcomings of the standard model of cosmology [56]. In GR the introduction of this type of field has the drawback of raising the issue of explaining its origin. Instead, in STG this problem finds a natural solution, because the scalar field can be considered an additional degree of freedom of the gravitational interaction. For these reasons, among others, inflationary models based on STG have been widely studied [57, 58].

Recently, STG has also been used to model dark energy, because scalar fields are also the natural candidates for phantom and quintessence fields (see [59] for a review).

This suggests that both inflation and dark energy could be the result of the action of the same scalar field. STG offers, in this sense, the ideal framework to implement this intriguing idea and might even allow us to overcome the problems due to the energy scale difference between the dark energy scalar fields and the inflaton [60].

Cosmological models in STG also satisfy current observational constraints, such as the late time accelerated behaviour [61–64]. The parameters of these type of models have also been constrained using the post Newtonian limit, nucleosynthesis [62] and cosmic clocks [65]. The Ehlers-Geren-Sachs (EGS) theorem has also been generalised for STG [66]. Recently, scalar and tensor perturbations have been investigated for specific STG in FLRW backgrounds [67, 68].

Over the past few years, there has been growing interest in higher order theories of gravity (HOTG). This is in part due to the fact that these theories contain extra curvature terms in their equations of motion, resulting in a dynamical behaviour which can be different to GR. In particular these additional terms can mimic cosmological evolution which is usually associated with dark energy [17–49], dark matter [69–71] or a cosmological constant [72].

The study of HOTG, where the linear Einstein-Hilbert Lagrangian is augmented by the addition of terms of quadratic or higher order in R, was first considered by Eddington [73]. It was later revived to study quantum effects in gravity [74, 75] and as a possible mechanism for inflation, the so called R^2-inflation [76–78].

Most of the current interest has been in theories of gravity where the gravitational Lagrangian is a non-linear function of the scalar curvature, mainly due to their simplicity. These $f(R)$-*theories of gravity* can take on a number of forms, the majority of the functions considered being of the type $R+\epsilon R^m$. Theories with $m = -1$ have been proposed as possible alternatives to sources of dark energy to explain the observed cosmic acceleration [17–19]. Solar system experiments do however constrain these type of theories for any corrections higher than R^2 (quadratic gravity) [79]. In these theories corrections to the characteristic length scale of General Relativity (GR) are introduced through the addition of a new length scale which is determined by the constant ϵ.

There are however forms of $f(R)$ which do not alter the characteristic length scale, for example R^n, in which GR is recovered when $n = 1$. These R^n-gravity theories have many attractive features, such as simple exact solutions which allows for comparison with observations [20,80]. Clifton and Barrow [81] used the dynamical systems approach to determine the extent to which exact solutions can be considered as attractors of spatially flat universes at late times. They compared the predictions

of these results with a range of observations and were able to show that the parameter n in FLRW may only deviate from GR by a very small amount ($n-1 \sim 10^{-19}$).

The isotropisation of anisotropic cosmologies can also be significantly altered by these higher-order corrections. In [82] (see Chapter 3), the existence of an isotropic past attractor within the class of Bianchi type I models was found for a power law Lagrangian of the form R^n. This feature was also found for Bianchi type I, II and IX models in quadratic theories of gravity [83, 84]. In these cases the extra curvature terms can dominate at early times and consequently allow for isotropic initial conditions. This is not possible in GR, where the shear term dominates at early times.

The study of these ETG can therefore lead to new insight into the behaviour of cosmological models when the underlying gravity is altered.

1.3 The $1+3$ covariant formalism

We start by introducing the $1+3$-covariant formalism as reviewed by Ellis and van Elst [85] (also see Ellis [86]). The following conventions will be used in this thesis: the metric signature is $(-+++)$; Latin indices run from 0 to 3; ∇ represents the usual covariant derivatives which may be split ($1+3$–covariantly) with the spatial covariant derivative being denoted by $\tilde{\nabla}$ and the time derivative by a dot; ∂^a denotes a partial derivative with respect to the coordinate x^a; units are used in which $c = 8\pi G = 1$.

1.3.1 Kinematical and dynamical quantities

Average 4-velocity of matter

We shall represent the average velocity of matter by a *4-velocity vector field* u^a which is given in terms of general coordinates $\{x^a\}$ by

$$u^a = \frac{dx^a}{d\tau}\,, \quad u_a u^a = -1, \tag{1.1}$$

where τ is proper time measured along the fundamental worldlines. The second part states that u^a is normalised.

For any given 4-velocity field u^a, the *projection tensor* h_{ab}, defined by

$$h_{ab} = g_{ab} + u_a u_b\,, \tag{1.2}$$

projects into the instantaneous rest-space of an observer moving with 4-velocity u^a.

This tensor is effectively the spatial metric for observers moving with 4-velocity u^a.[1]

Kinematical quantities

One can decompose the first covariant derivative of u_a into its irreducible parts,

$$\nabla_a u_b = -\,u_a\,\dot{u}_b + \tilde{\nabla}_a u_b = -\,u_a\,\dot{u}_b + \tfrac{1}{3}\,\Theta\,h_{ab} + \sigma_{ab} + \omega_{ab}\ , \tag{1.3}$$

where

$\Theta = \tilde{\nabla}_a u^a$ (volume) *rate of expansion*,

$\sigma_{ab} = \tilde{\nabla}_{\langle a} u_{b\rangle}$ *rate of shear* ($\sigma_{ab} = \sigma_{(ab)}$, $\sigma_{ab}\,u^b = 0$, $\sigma^a{}_a = 0$),

$\omega_{ab} = \tilde{\nabla}_{[a} u_{b]}$ *vorticity* ($\omega_{ab} = \omega_{[ab]}$, $\omega_{ab}\,u^b = 0$),

$\dot{u}_b = \nabla_a u_b u^a$ *acceleration vector* ($\dot{u}_a u^a = 0$).

We use angle brackets to denote orthogonal projections of vectors and the orthogonally projected symmetric trace-free part of tensors (PSTF). They are also used to denote othogonal projections of covariant time derivatives along u^a ('*Fermi derivatives*').

Energy-momentum tensor

In extended theories of gravity, it is useful to define an *effective energy-momentum tensor* $\tilde{T}_{ab}$. This effective fluid usually has a matter part (T_{ab}) and a 'curvature fluid' part (T^R_{ab}) for HOTG or scalar-field part (T^ϕ_{ab}) for STG (see Chapter 2).

We can decomposed $\tilde{T}_{ab}$ relative to u^a in the form

$$\begin{gathered}\tilde{T}_{ab} = \tilde{\mu}\,u_a\,u_b + \tilde{q}_a\,u_b + u_a\,\tilde{q}_b + \tilde{p}\,h_{ab} + \tilde{\pi}_{ab}\ , \\ \tilde{q}_a\,u^a = 0\ ,\ \tilde{\pi}^a{}_a = 0\ ,\ \tilde{\pi}_{ab} = \tilde{\pi}_{(ab)}\ ,\ \tilde{\pi}_{ab}\,u^b = 0\ ,\end{gathered} \tag{1.4}$$

where

$\tilde{\mu} = (\tilde{T}_{ab}u^a u^b)$ is the *relativistic energy density* relative to u^a,

$\tilde{q}^a = -\,\tilde{T}_{bc}\,u^b\,h^{ca}$ is the *energy flux* relative to u^a,

$\tilde{p} = \frac{1}{3}\,(\tilde{T}_{ab}h^{ab})$ is the *isotropic pressure*,

$\tilde{\pi}_{ab} = \tilde{T}_{cd}\,h^c{}_{\langle a}\,h^d{}_{b\rangle}$ is the trace-free *anisotropic pressure* (stress).

[1] This is only valid for $\omega^a = 0$, i.e. irrotational flow. See §1.3.2 below.

The kinematical quantities of the matter part of $\tilde{T}_{ab}$, are the same as above but expressed without the tilde.

Maxwell field strength tensor

The *Maxwell field strength tensor* F_{ab} of an electromagnetic field is split relative to u^a into *electric* and *magnetic field* parts by the relations

$$E_a = F_{ab}\, u^b \quad \Rightarrow \quad E_a u^a = 0 \ , \tag{1.5}$$

$$H_a = \tfrac{1}{2}\, \eta_{abc}\, F^{bc} \quad \Rightarrow \quad H_a u^a = 0 \ . \tag{1.6}$$

We have defined the *volume element* for the rest-spaces as

$$\varepsilon_{abc} = u^d\, \eta_{dabc} \qquad \Rightarrow \qquad \varepsilon_{abc} = \varepsilon_{[abc]} \ , \ \varepsilon_{abc}\, u^c = 0 \ , \tag{1.7}$$

where η_{abcd} is the 4-dimensional volume element ($\eta_{abcd} = \eta_{[abcd]}$, $\eta_{0123} = \sqrt{|\det\, g_{ab}\,|}$).

Weyl curvature tensor

The *Weyl conformal curvature tensor* C_{abcd} can also be split relative to u^a into a electric and magnetic parts:

$$E_{ab} = C_{acbd}\, u^c\, u^d \quad \Rightarrow \quad E^a{}_a = 0 \ , \ E_{ab} = E_{(ab)} \ , \ E_{ab}\, u^b = 0 \ , \tag{1.8}$$

$$H_{ab} = \tfrac{1}{2}\, \varepsilon_{ade}\, C^{de}{}_{bc}\, u^c \quad \Rightarrow \quad H^a{}_a = 0 \ , \ H_{ab} = H_{(ab)} \ , \ H_{ab}\, u^b = 0 \ . \tag{1.9}$$

Auxiliary quantities

It is useful to define the following auxiliary quantities: The *vorticity vector* is given by

$$\omega^a = \tfrac{1}{2}\, \varepsilon^{abc}\, \omega_{bc} \qquad \Rightarrow \qquad \omega_a\, u^a = 0 \ , \ \omega_{ab}\, \omega^b = 0 \ , \tag{1.10}$$

and the magnitudes for the vorticity and shear are respectively given by

$$\omega^2 = \tfrac{1}{2}\, (\omega_{ab}\omega^{ab}) \geq 0 \ , \quad \sigma^2 = \tfrac{1}{2}\, (\sigma_{ab}\sigma^{ab}) \geq 0 \ . \tag{1.11}$$

The *average length scale* a is determined by

$$\frac{\dot{a}}{a} = \tfrac{1}{3}\, \Theta = H \ , \tag{1.12}$$

where H is the Hubble parameter.

1.3.2 Propagation and constraint equations

We can now introduce the equations which govern the evolution of the universe. These are determined from the Ricci and Bianchi identities.

Ricci Identities

The *Ricci identity* for the vector field u_a is given by

$$\nabla_a\nabla_b u_c - \nabla_b\nabla_a u_c = R_{abcd}u^d. \tag{1.13}$$

Multiplying equation (1.13) by u^b, one obtains

$$\nabla_a\dot{u}_c - (\nabla_b u_c)(\nabla_a u^b) - \nabla_b\left(\nabla_a u_c\right)u^b = R_{abcd}u^d u^b. \tag{1.14}$$

Projecting on a and c and making use of equation (1.3) yields

$$\tilde{\nabla}_a\dot{u}_b - (\tilde{\nabla}_d u_b)(\tilde{\nabla}_a u^d) + \dot{u}_a\dot{u}_b - h^c_a h^d_b\nabla_f(\tilde{\nabla}_c u_d)u^f = h^c_a h^d_b R_{cedf}u^e u^f \tag{1.15}$$

which is the propagation equation of $\tilde{\nabla}_c u_d$ along the fluid flow lines. On substitution of equation (1.3) and separating into trace, trace-free and skew symmetric parts, we obtain three *propagation equations*. When we separate the parallel part of (1.13) into trace, trace-free and skew symmetric parts we obtain three *constraint equations*.

Propagation equations

The trace of equation (1.15) yields the propagation equation of Θ,

$$\dot{\Theta} - \tilde{\nabla}_a\dot{u}^a + \tfrac{1}{3}\Theta^2 - (\dot{u}_a\dot{u}^a) + 2\,\sigma^2 - 2\,\omega^2 + \tfrac{1}{2}(\tilde{\mu} + 3\tilde{p}) = 0, \tag{1.16}$$

which is the basic equation of gravitational attraction. This equation is the *Raychaudhuri equation*.

The skew part of equation (1.15) is the *vorticity propagation equation*, which is identical to the Einstein's case,

$$\dot{\omega}^{\langle a\rangle} - \tfrac{1}{2}\,\varepsilon^{abc}\,\tilde{\nabla}_b\dot{u}_c + \tfrac{2}{3}\,\Theta\,\omega^a - \sigma^a{}_b\,\omega^b = 0. \tag{1.17}$$

The symmetric trace-free part of equation (1.15) is the *shear propagation equation*

$$\dot{\sigma}_{\langle ab\rangle} - \tilde{\nabla}_{\langle a}\dot{u}_{b\rangle} + \tfrac{2}{3}\,\Theta\,\sigma_{ab} - \dot{u}_{\langle a}\,\dot{u}_{b\rangle} + \sigma^c{}_{\langle a}\,\sigma_{b\rangle c} + \omega_{\langle a}\,\omega_{b\rangle} + E_{ab} - \tfrac{1}{2}\tilde{\pi}_{ab} = 0\ . \tag{1.18}$$

Constraint equations

The components of the Ricci identity (1.13) which are perpendicular to u^a are equivalent to three sets of constraint equations.

The $(0\alpha) - equation$ (which is equivalent to the space-time components of the field equations) is given by

$$\tilde{\nabla}^b\sigma_{ab} - \tfrac{2}{3}\tilde{\nabla}_a\Theta + \varepsilon_{abc}\left[\tilde{\nabla}^b\omega^c + 2\dot{u}^b\omega^c\right] + \tilde{q}_a = 0. \tag{1.19}$$

The *divergence of the vorticity identity* is

$$\tilde{\nabla}_a\omega^a - \dot{u}_a\omega^a = 0. \tag{1.20}$$

The *magnetic part of the Weyl tensor* (or H_{ab}-equation) is given by

$$H_{ab} + 2\dot{u}_{\langle a}\omega_{b\rangle} + \tilde{\nabla}_{\langle a}\omega_{b\rangle} - \text{curl }\sigma_{ab} = 0, \tag{1.21}$$

where the 'curl' of the shear is curl $\sigma_{ab} = \eta_{cd\langle a}\tilde{\nabla}^c\sigma^d_{b\rangle}$.

Twice-contracted Bianchi identities

As pointed out in [87], no matter how complicated the effective stress energy momentum tensor $\tilde{T}_{ab}$ for an extended theory of gravity, it is always divergence free if $\nabla^b T_{ab} = 0$ (see §2.1.2 for a complete discussion). The total conservation equations are thus just the ones for standard matter, namely

$$\dot{\mu} + \tilde{\nabla}_a q^a + \Theta(\mu + p) + 2(\dot{u}_a q^a) + (\sigma^a{}_b\pi^b{}_a) = 0, \tag{1.22}$$

$$\dot{q}^{\langle a\rangle} + \tilde{\nabla}^a p + \tilde{\nabla}_b\pi^{ab} + \tfrac{4}{3}\Theta\, q^a + \sigma^a{}_b\, q^b + (\mu + p)\,\dot{u}^a - \dot{u}_b\,\pi^{ab} + \omega^{ab}q_b = 0. \tag{1.23}$$

When we assume that standard matter behaves as a perfect fluid, we can impose the restrictions $q^a = \pi_{ab} = 0$, so that the equations above reduce to

$$\dot{\mu} = -\Theta(\mu + p) \tag{1.24}$$

$$\tilde{\nabla}^a p + (\mu + p)\,\dot{u}^a = 0, \tag{1.25}$$

which are the *energy-* and *momentum conservation equations* respectively.

Other Bianchi identities

We can obtain a further set of equations, from the *Bianchi identities*

$$\nabla_{[a}R_{bc]de} = 0, \tag{1.26}$$

which consist of two propagation and two constraint equations.

The propagation equations are the *$\dot{E}$-equation*

$$\dot{E}^{\langle ab\rangle} + \tfrac{1}{2}\,\dot{\tilde{\pi}}^{\langle ab\rangle} - \text{curl}\ H^{ab} + \tfrac{1}{2}\,\tilde{\nabla}^{\langle a}\tilde{q}^{b\rangle} + \tfrac{1}{2}\,(\tilde{\mu}+\tilde{p})\,\sigma^{ab} + \Theta\,(E^{ab} + \tfrac{1}{6}\,\tilde{\pi}^{ab}) \qquad (1.27)$$
$$- \,3\,\sigma^{\langle a}{}_{c}\,(E^{b\rangle c} - \tfrac{1}{6}\,\tilde{\pi}^{b\rangle c}) + \dot{u}^{\langle a}\,\tilde{q}^{b\rangle} - \ \varepsilon^{cd\langle a}\,[\ 2\,\dot{u}_c\,H^{b\rangle}{}_{d} + \omega_c\,(E^{b\rangle}{}_{d} + \tfrac{1}{2}\,\tilde{\pi}^{b\rangle}{}_{d})\ ] = 0\ ,$$

and the *$\dot{H}$-equation*

$$\dot{H}^{\langle ab\rangle} + \text{curl}\ E^{ab} - \tfrac{1}{2}\text{curl}\ \tilde{\pi}^{ab} \ = \ -\,\Theta\,H^{ab} + 3\,\sigma^{\langle a}{}_{c}\,H^{b\rangle c} + \tfrac{3}{2}\,\omega^{\langle a}\,\tilde{q}^{b\rangle} \qquad (1.28)$$
$$- \,\varepsilon^{cd\langle a}\,[\ 2\,\dot{u}_c\,E^{b\rangle}{}_{d} - \tfrac{1}{2}\,\sigma^{b\rangle}{}_{c}\,\tilde{q}_d - \omega_c\,H^{b\rangle}{}_{d}\ ]\ ,$$

where we have defined the 'curls'

$$\text{curl}\ H^{ab} \ = \ \varepsilon^{cd\langle a}\,\tilde{\nabla}_c H^{b\rangle}{}_{d}\ , \qquad (1.29)$$

$$\text{curl}\ E^{ab} \ = \ \varepsilon^{cd\langle a}\,\tilde{\nabla}_c E^{b\rangle}{}_{d}\ , \qquad (1.30)$$

$$\text{curl}\ \tilde{\pi}^{ab} \ = \ \varepsilon^{cd\langle a}\,\tilde{\nabla}_c \tilde{\pi}^{b\rangle}{}_{d}\ . \qquad (1.31)$$

The *constraint equations* are the div *E-equation*

$$0 \ = \ \tilde{\nabla}_b(E^{ab} + \tfrac{1}{2}\,\tilde{\pi}^{ab}) - \tfrac{1}{3}\,\tilde{\nabla}^a\tilde{\mu} + \tfrac{1}{3}\,\Theta\,\tilde{q}^a - \tfrac{1}{2}\,\sigma^a{}_b\,\tilde{q}^b - 3\,\omega_b\,H^{ab}$$
$$- \,\varepsilon^{abc}\,[\ \sigma_{bd}\,H^d{}_c - \tfrac{3}{2}\,\omega_b\,\tilde{q}_c\ ]\ , \qquad (1.32)$$

and the div *H-equation*

$$0 \ = \ \tilde{\nabla}_b H^{ab} + (\tilde{\mu}+\tilde{p})\,\omega^a + 3\,\omega_b\,(E^{ab} - \tfrac{1}{6}\,\tilde{\pi}^{ab})$$
$$+ \,\varepsilon^{abc}\,[\ \tfrac{1}{2}\,\tilde{\nabla}_b\,\tilde{q}_c + \sigma_{bd}\,(E^d{}_c + \tfrac{1}{2}\,\tilde{\pi}^d{}_c)\ ]\ . \qquad (1.33)$$

Irrotational flow

In the case of zero rotation ($\omega = 0$):

- Fluid flow is hypersurface-orthogonal, and there exists a cosmic time function t such that
$$u_a = -g(x^b)\nabla_a t.$$
When $\dot{u}_a = 0$, we can set $g = 1$.

- h_{ab} is the metric of the orthogonal 3–spaces.

- Gauss's equation and the Ricci identities for u^a, implies that the Ricci tensor

of the 3-spaces is given by

$$ {}^3R_{ab} = -\dot{\sigma}_{\langle ab\rangle} - \Theta\,\sigma_{ab} + \tilde{\nabla}_{\langle a}\dot{u}_{b\rangle} + \dot{u}_{\langle a}\,\dot{u}_{b\rangle} + \tilde{\pi}_{ab} + \tfrac{1}{3}h_{ab}\left[2\tilde{\mu} - \tfrac{2}{3}\Theta^2 + 2\sigma^2\right] \quad (1.34) $$

and their Ricci scaler is given by

$$ {}^3R = 2\tilde{\mu} - \tfrac{2}{3}\Theta^2 + 2\sigma^2, \quad (1.35) $$

which is a generalised Friedmann equation. The *Gauss-Codazzi equations* are thus given by

$$ {}^3R_{ab} - \tfrac{1}{3}({}^3R)h_{ab} = -\dot{\sigma}_{\langle ab\rangle} - \Theta\,\sigma_{ab} + \tilde{\nabla}_{\langle a}\dot{u}_{b\rangle} + \dot{u}_{\langle a}\,\dot{u}_{b\rangle} + \tilde{\pi}_{ab}. \quad (1.36) $$

1.4 Dynamical systems in cosmology

The implementation of the theory of Dynamical Systems (DS) (see for example [88–90]) has proven to be useful to gain a qualitative understanding of a given class of cosmological models. This dynamical systems approach does not require the knowledge of any exact solutions. However, the equilibrium points of the dynamical system correspond to the interesting cosmological solutions. This approach helps identifying exact solutions with special symmetries, which is particularly useful when studying complicated field equations.

In recent times, this approach has been used to investigate alternative theories of gravity such as Brans-Dicke theory [91–95], scalar-tensor theories [96–104], and higher order gravity [81–83, 87, 105–110]. It has also proven useful in theories with non-linear equations of state [111,112] and brane world models [113–118]. In general, these modified theories of gravity have more complicated effective evolution equations, and it can be more difficult to find exact analytical solutions. The dynamical systems approach can therefore be useful in studying modified theories such as ETG.

We will now proceed to give a brief general prescription for the use of dynamical systems in cosmology.

1.4.1 Prescription for the dynamical systems approach

The starting point for a DS analysis in cosmology is to write the field equations in such a way that we can study the behaviour of the various physical and geometric quantities relative to the rate of expansion of the universe. This can be done by defining a set of expansion normalised variables [88–90]. Note that this is not the only method

to perform a DS analysis in cosmology (see for example Burd and Barrow [91]). In chapter 5 we compare two such methods to study their similarities and differences. In this section we will however concentrate on the first.

Autonomous system

The evolution equations for a given cosmological model are given by

$$\dot{\mathbf{x}} = \mathbf{F}\left(\mathbf{x}, \Theta\right), \quad \mathbf{F} = (F_1, ..., F_n), \tag{1.37}$$

which is constrained by the Friedmann equation:

$$\tfrac{1}{3}\Theta^2 - \mathbf{x} = 0, \tag{1.38}$$

where $\mathbf{x}$ is the set of physical and geometric variables (other than Θ) which appear in the Friedmann equation. For example in (1.35), they are the shear, energy density and 3-curvature terms. For modified theories there will be additional terms.

The next step is to obtain a set of expansion normalised variables which are dimensionless, and defined as:

$$\mathbf{y} = \frac{3\mathbf{x}}{\Theta^2}. \tag{1.39}$$

Each dimensionless state $\mathbf{y}$ determines a single parameter family of physical states $(\mathbf{x}, \Theta)$. The *deceleration parameter* q plays an important role in deriving the evolution equations of $\mathbf{y}$ from $\mathbf{x}$. We can express the expansion rate in terms of the deceleration parameter $q = -\frac{\ddot{a}a}{\dot{a}^2}$ as follows:

$$\dot{\Theta} = -\tfrac{1}{3}(1+q)\Theta^2. \tag{1.40}$$

Together with the dimensionless variables (1.39), we need to define a dimensionless time variable according to

$$' = \frac{3}{|\Theta|}\frac{d}{dt}, \tag{1.41}$$

so that the evolution equation (1.40) can be written as

$$\Theta' = -\epsilon(1+q)\Theta, \tag{1.42}$$

where ϵ is the sign of Θ and $|\Theta| = \epsilon\Theta$. The normalisation in (1.41) must be strictly positive in order for the time variable to be increasing monotonically and therefore for expanding models we have $\epsilon = 1$ and for collapsing models $\epsilon = -1$.

The evolution equations for $\mathbf{y}$ can now be derived from those for $\mathbf{x}$, yielding a

autonomous system of differential equations:

$$\mathbf{y}' = \mathbf{f}(\mathbf{y}), \quad \mathbf{f} = (f_1, ..., f_n). \tag{1.43}$$

The Friedmann constraint (1.38) now takes on the form

$$1 = \mathbf{y}. \tag{1.44}$$

When the set of variables $\mathbf{y}$ are all strictly positive, the the state space defined by these dimensionless variables is *compact*. We will discuss the use of compact and non-compact variables in detail in chapters 3–5.

Local analysis

The equilibrium points $\mathbf{y}_0$ of the system each satisfy the condition $\mathbf{f}(\mathbf{y}_0) = 0$. We can study the local stability properties of an equilibrium points, by looking at small perturbations around the equilibrium point, defined by:

$$\delta = \mathbf{y} - \mathbf{y}_0. \tag{1.45}$$

Taylor-expanding the non-linear functions around the equilibrium points, yield

$$\mathbf{f}(\mathbf{y}) = \mathbf{J} \cdot (\mathbf{y} - \mathbf{y}_0) + \mathbf{h}(\mathbf{y} - \mathbf{y}_0), \tag{1.46}$$

where

$$\mathbf{J}_{ij} \equiv \left. \frac{\partial f_i}{\partial y^j} \right|_{\mathbf{y}=\mathbf{y}_0} \tag{1.47}$$

is the Jacobian of $\mathbf{f}$ and $\mathbf{h}(\mathbf{y} - \mathbf{y}_0)$ is the set of functions which are at least of second order in $(\mathbf{y} - \mathbf{y}_0)$. Thus the nonlinear system (1.43) in the vicinity of the equilibrium point $\mathbf{y}_0$ can be approximated by the linearised system of equations

$$\delta' = \mathbf{J}\delta. \tag{1.48}$$

According to the Hartman-Grossman theorem [119], if the equilibrium point is *hyperbolic*, then the orbits of the linear system (1.48) can locally be continuously deformed into the orbits of the full non-linear system (1.43). The behaviour around the equilibrium points in the full non-linear system can thus be studied by analysing the linear system (1.48), as long as the equilibrium point is hyperbolic, that is the real parts of all the eigenvalues are non-zero.

We can then classify the equilibrium points of the non-linear system by using the eigenvalues of the Jacobian $\mathbf{J}$. The real parts of the eigenvalues determine the stability

of an equilibrium point. For the purpose of this thesis, we will classify hyperbolic equilibrium points as follows. If the real parts of the eigenvalues are:

- all positive, then the equilibrium point is called a *repeller* or source,
- all negative, then the equilibrium point is called an *attractor* or sink, and
- some negative and some positive, then the equilibrium point is called a *saddle* point.

In the case of non-hyperbolic points, i.e. when one (or $k \leq n$) of the eigenvalues has a vanishing real part, then we have a *line (or k-dimensional set) of equilibrium points*, which can be classified similarly to the hyperbolic equilibrium point. If the real parts of the non-zero eigenvalues are:

- all positive, then the set is called a repeller,
- all negative, then the set is called an attractor, and
- some negative and some positive, then the set is called a saddle.

Invariant sets

Invariant sets form an important part of the theory of dynamical systems and is especially useful in the study of cosmological models. These sets are subsets (S) of the whole state space, with the property that each element in S can only evolve to another state $\mathbf{x} \in S$. In other words, invariant subsets of the state space are similar to subspaces of vector spaces.

For example, in chapter 4 we consider the *orthogonal spatially homogeneous* Bianchi cosmologies. For these models the invariant sets or *submanifolds* are the following; the LRS Bianchi I and III models, the Kantowski-Sachs models and the open, closed and flat FLRW models. Each of these invariant sets further contains a vacuum and non-vacuum invariant subset.

Equilibrium points and cosmological solutions

The deceleration parameter q for an equilibrium point $\mathbf{y}_0$ is constant, i.e. $q(\mathbf{y}_0) = q_0$. The behaviour of the scale factor can then be obtained straightforwardly from (1.40), which now reads

$$\dot{\Theta} = -\tfrac{1}{3}(1 + q_0)\Theta^2. \tag{1.49}$$

The value of q_0 will then determine the type of solution we obtain. For instance when $q_0 = -1$ we have *de Sitter* solutions ($\Theta = \Theta_0$, a constant) or static solutions ($\Theta = 0$). For $q_0 = 0$ we have a *Milne* evolution and when $-1 < q_0 < 0$ or $q_0 > 0$ we have accelerated- and decelerated power law behaviours, respectively.

One may similarly obtain solutions for the behaviour of the remaining physical quantities $\mathbf{x}$ from their respective evolution equations.

1.5 Thesis outline

This thesis has been organised as follows:

In chapter 2 we give the actions and relevant field equations for general $f(R)$-theories of gravity and general STG. We also discuss the conformal relationships between these two theories.

In chapter 3 we consider the case of R^n-gravity and perform a detailed analysis of the dynamics in Bianchi I cosmologies which exhibit *local rotational symmetry*. We find exact solutions and study their behaviour and stability in terms of the values of the parameter n.

This analysis is extended in chapter 4 to the complete *orthogonal spatially homogeneous* Bianchi cosmologies in R^n-gravity. We construct a compact state space by dividing the state space into different sectors. We perform a detailed analysis of the cosmological behaviour in terms of the parameter n, determining all the equilibrium points, their stability and corresponding cosmological evolution. In particular, the appropriately compactified state space allows us to investigate static and bouncing solutions. We find no Einstein static solutions, but there do exist cosmologies with bounce behaviours. We also investigate the isotropisation of these models and find that all isotropic points are flat Friedmann like.

Chapter 5 is devoted to addressing important issues surrounding the choice of variables when performing a dynamical systems analysis of alternative theories of gravity. We discuss the advantages and disadvantages of compactifying the state space, and illustrate this using two examples. We first show how to define a compact state space for the class of LRS Bianchi type I models in R^n-gravity and compare to a non–compact expansion–normalised approach of chapter 3. In the second example we consider the flat Friedmann matter subspace of the previous example, and compare the compact analysis to studies where non-compact non–expansion–normalised

variables were used. In both examples we comment on the existence of bouncing or recollapsing orbits as well as the existence of static models.

In chapter 6 we study the state–space of FLRW models derived from STG where the non–minimal coupling is $F(\phi) = \xi\phi^2$ and the effective potential is $V(\phi) = \lambda\phi^n$. Our analysis allows to unfold many feature of the cosmology of this class of theories. For example, the evolution mechanism towards states indistinguishable from GR is recovered and proved to depend critically on the form of the potential $V(\phi)$. Also, transient almost–Friedmann phases evolving towards accelerated expansion and unstable inflationary phases evolving towards stable ones are found. Some of our results are shown to hold also for the String-Dilaton action.

In chapter 7 we set out a framework to analyse tensor anisotropies in the CMB that are generated by STG. As an example, we consider the class of STG's for which we found exact solution in chapter 6.

Chapter 8 contains some final remarks and a discussion on future work.

Chapter 2

Extended theories of gravity

In this chapter we will look at the actions and field equations of two general classes of extended theories of gravity. The first is a subclass of HOTG, namely $f(R)$-gravity. The second is a general class of STG, where the non-minimal coupling and the self interating potential are functions of a generic scalar field.

2.1 $f(R)$- theories

2.1.1 Action for generic scalar functions ($f(R)$)

We start with the general form for a non-linear Lagrangian that consists of a generic function of scalar curvature $f(R)$,

$$\mathcal{L} = \sqrt{-g} f(R). \tag{2.1}$$

The action describing the gravitational interactions then reads

$$\mathcal{A} = \int dx^4 \sqrt{-g} f(R). \tag{2.2}$$

By varying equation (2.2) we obtain the fourth order field equations

$$T_{ab} = f' R_{ab} - \tfrac{1}{2} f g_{ab} + S_{cd} \left(g^{cd} g_{ab} - g^{c}{}_{a}\, g^{d}{}_{b} \right). \tag{2.3}$$

where primes denote derivatives with respect to R and

$$\begin{aligned} S_{ab} &= \nabla_a\nabla_b f'(R) \\ &= f''\tilde{\nabla}_a\tilde{\nabla}_b R + f'''\tilde{\nabla}_a R\,\tilde{\nabla}_b R - f'''\dot{R}\left(\tilde{\nabla}_b R\,u_a + \tilde{\nabla}_a R\,u_b\right) - f''\left(\tilde{\nabla}_a\dot{R}\,u_b\right. \\ &\quad \left. + u^c\nabla_c(\tilde{\nabla}_b R)\,u_a\right) + f'''\dot{R}^2\,u_a u_b + f''\left(\ddot{R}\,u_a u_b - \dot{R}(\tilde{\nabla}_a u_b + u_a\dot{u}_b)\right). \quad (2.4) \end{aligned}$$

The d'Alembertian is then given by

$$\begin{aligned} S = \Box f'(R) &= g^{ab}\nabla_a\nabla_b f'(R) \\ &= f''\tilde{\nabla}^c D_c R + f'''\tilde{\nabla}^c R\,\tilde{\nabla}_c R + f''\dot{u}^c\tilde{\nabla}_c R - f''(\ddot{R} + \dot{R}\Theta) - f'''\dot{R}^2. \quad (2.5) \end{aligned}$$

The field equation (2.3) can be rewritten as

$$R_{ab} = f'^{-1}\left[T_{ab} + \tfrac{1}{2}f g_{ab} + S_{cd}\left(g^c{}_a\,g^d{}_b - g^{cd}g_{ab}\right)\right]. \quad (2.6)$$

The higher order field equations may be split as in the Einstein case (see Ellis [86]) to give the following terms:

$$\begin{aligned} R &= f'^{\,-1}\left[3p - \mu + 2f - 3\,S\right], & (2.7)\\ R_{ab}u^a u^b &= f'^{\,-1}\left[\mu - \tfrac{1}{2}f + h^{ab}S_{ab}\right], & (2.8)\\ R_{ab}u^a h^b{}_c &= f'^{\,-1}\left[-q_c + S_{ab}u^a h^b{}_c\right], & (2.9)\\ R_{ab}h^a{}_c\,h^b{}_d &= f'^{\,-1}\left[\pi_{cd} - \left(p + \tfrac{1}{2}f + S\right)h_{cd} + S_{ab}h^a{}_c\,h^b{}_d\right]. & (2.10) \end{aligned}$$

2.1.2 Decomposition of the stress energy tensor

The field equation (2.6) may be written as

$$R_{ab} - \tfrac{1}{2}Rg_{ab} = f'^{-1}T_{ab} + f'^{-1}\left[\tfrac{1}{2}(f - f'R)g_{ab} + S_{cd}\left(g^c{}_a\,g^d{}_b - g^{cd}g_{ab}\right)\right]. \quad (2.11)$$

The field equation can then be written in the standard form

$$G_{ab} = R_{ab} - \tfrac{1}{2}Rg_{ab} = \tilde{T}_{ab} = \frac{T_{ab}}{f'} + T^R_{ab},$$

where T_{ab} is the standard matter stress-energy tensor and

$$T^R_{ab} = \frac{1}{f'}\left[\tfrac{1}{2}(f - f'R)g_{ab} + S_{cd}\left(g^c{}_a\,g^d{}_b - g^{cd}g_{ab}\right)\right], \quad (2.12)$$

is the *curvature stress-energy momentum tensor*. We have thus moved from a model whose field equation have a complicated structure to one in which the gravitational

field takes on the standard GR form, but where the source is composed of two sources; a standard matter fluid and a curvature fluid which represents the non-Einsteinian contribution of the gravitational interaction. This transformation is not just restricted to $f(R)$-gravity. It can also be used for more general HOTG and STG.

In §1.3.1 we briefly mentioned that the twice contracted Bianchi identity for an ETG, is just the normal conservation equation for standard matter, that is equations (1.22) and (1.23). In the framework above, we can easily show why this is the case. Here the Bianchi identities can be written as

$$0 = \nabla^b \tilde{T}_{ab} = \nabla^c T^R_{ab} - \frac{f''}{f'^2}\,\partial^{\,b} R\, T_{ab} + \frac{1}{f'}\nabla^b T_{ab}. \tag{2.13}$$

By making use of the field equations and the definition of the Riemann tensor, it can be shown the first two terms on the right hand side cancel each other and so $\nabla^b \tilde{T}_{ab} \propto \nabla^b T_{ab}$. In fact, Eddington [73] and later others [120], showed that a first variation for the gravitational action is divergence free for any form of the invariant we choose for the Lagrangian. Thus, no matter how complicated the effective stress energy momentum tensor $\tilde{T}_{ab}$ for an extended theory of gravity, it is always divergence free if $\nabla^b T_{ab} = 0$.

It is useful to decompose the curvature stress-energy momentum tensor into its various components (see §1.3.1)

$$\begin{aligned}
\mu^R &= T^R_{ab} u^a u^b = f'^{-1}\left[-\tfrac{1}{2}(f - f'R) + S_{ab}h^{ab}\right], \\
p^R &= \tfrac{1}{3} T^R_{ab} h^{ab} = f'^{-1}\left[\tfrac{1}{2}(f - f'R) - S + \tfrac{1}{3} S_{ab}h^{ab}\right], \\
q^R_c &= -T^R_{ab} u^a h^b{}_c = -f'^{-1}\left[S_{ab}u^a h^b{}_c\right], \\
\pi^R_{ab} &= T^R_{cd} h^c{}_{\langle a}\, h^d{}_{b\rangle} = f'^{-1}\left[h^c{}_a\, h^d{}_b - \tfrac{1}{3} h_{ab}h^{cd}\right] S_{cd}.
\end{aligned} \tag{2.14}$$

Therefore, by redefining the kinematical quantities as follows:

$$\begin{aligned}
\tilde{\mu} &= \frac{\mu}{f'} + \mu^R, \\
\tilde{p} &= \frac{p}{f'} + p^R, \\
\tilde{q}_c &= \frac{q_c}{f'} + q^R_c, \\
\tilde{\pi}_{ab} &= \frac{\pi_{ab}}{f'} + \pi^R_{ab},
\end{aligned} \tag{2.15}$$

we may obtain the standard Einstein evolution and constraint equations (see Ellis *et al.* [85]). By substituting these identities into the equations given in §1.3, we can obtain the full set of propagation and constraint equations for a $f(R)$ theory of

gravity. It is easy to show that the equations obtained in this way are identical to ones derived from the field equations given by Rippl *et al.* [121].

2.1.3 Dynamics in $f(R)$-gravity

In this section we specialise the general propagation and constraint equations which are stated in the previous chapter, to the cases of general $f(R)$ theories as was shown by Rippl *et al.* [121]. We will only state the equations which will be used in the following chapters. The remaining equations can be found straightforwardly, by substituting the identities (2.15) into the relevant equation.

The propagation equations are given by the following:

Raychaudhuri equation:

$$\dot{\Theta} - \tilde{\nabla}_a \dot{u}^a + \tfrac{1}{3}\Theta^2 - (\dot{u}_a \dot{u}^a) + 2\,\sigma^2 - 2\,\omega^2 + f'^{\,-1}\left[\mu - \tfrac{1}{2}f + h^{ab}S_{ab}\right] = 0. \tag{2.16}$$

Shear propagation equation:

$$\begin{aligned}\dot{\sigma}_{\langle ab\rangle} - \tilde{\nabla}_{\langle a}\dot{u}_{b\rangle} + \tfrac{2}{3}\,\Theta\,\sigma_{ab} - \dot{u}_{\langle a}\,\dot{u}_{b\rangle} + \sigma^{c}{}_{\langle a}\,\sigma_{b\rangle c} + \omega_{\langle a}\,\omega_{b\rangle} + E_{ab} \\ -\tfrac{1}{2}f'^{\,-1}\pi_{ab} - \tfrac{1}{2}f'^{\,-1}\left[h^{c}{}_{a}\,h^{d}{}_{b} - \tfrac{1}{3}h_{ab}h^{cd}\right]S_{cd} = 0\ .\end{aligned} \tag{2.17}$$

When we have zero rotation, we also have the following equations:

3-*Ricci tensor:*

$$\begin{aligned}{}^3R_{ab} \;=\; & -\dot{\sigma}_{\langle ab\rangle} - \Theta\,\sigma_{ab} + \tilde{\nabla}_{\langle a}\dot{u}_{b\rangle} + \dot{u}_{\langle a}\,\dot{u}_{b\rangle} + \tfrac{1}{3}h_{ab}\left[2\sigma^2 - \tfrac{2}{3}\Theta^2\right] + f'^{\,-1}\pi_{ab} \\ & +\tfrac{1}{3}f'^{\,-1}\left[2\mu - f + f'\,R + S\right]h_{ab} + f'^{\,-1}\left[h^{c}{}_{a}\,h^{d}{}_{b} + \tfrac{1}{3}h_{ab}u^{c}u^{d}\right]S_{cd}.\end{aligned} \tag{2.18}$$

3-*Ricci scalar:*

$${}^3R = 2\sigma^2 - \tfrac{2}{3}\Theta^2 + f'^{\,-1}\left[\mu + 3p + f - 3S + 2h^{cd}S_{cd}\right]. \tag{2.19}$$

Gauss-Codazzi equations:

$$\begin{aligned}{}^3R_{ab} - \tfrac{1}{3}({}^3R)h_{ab} \;=\; & -\dot{\sigma}_{\langle ab\rangle} - \Theta\,\sigma_{ab} + \tilde{\nabla}_{\langle a}\dot{u}_{b\rangle} + \dot{u}_{\langle a}\,\dot{u}_{b\rangle} + f'^{\,-1}\pi_{ab} \\ & +f'^{\,-1}\left[h^{c}{}_{a}\,h^{d}{}_{b} - \tfrac{1}{3}h_{ab}h^{cd}\right]S_{cd}.\end{aligned} \tag{2.20}$$

2.2 Scalar-tensor gravity

2.2.1 Action for a general STG

We start with the general form for a non-linear Lagrangian that consists of a generic function of scalar field $F(\phi)$ coupled to the Ricci scalar,

$$\mathcal{L} = \sqrt{-g}\left[F(\phi)R - \tfrac{1}{2}g^{ab}\nabla_a\phi\,\nabla_b\phi - V(\phi) + \mathcal{L}_M\right]. \tag{2.21}$$

The action describing the gravitational interactions then reads

$$\mathcal{A} = \int dx^4\sqrt{-g}\left[F(\phi)R - \tfrac{1}{2}g^{ab}\nabla_a\phi\,\nabla_b\phi - V(\phi) + \mathcal{L}_M\right], \tag{2.22}$$

where $F(\phi)$ is a generic coupling, $V(\phi)$ is the self–interaction potential and $\mathcal{L}_M$ is the matter Lagrangian.

By varying the action (2.22) with respect to the metric g_{ab}, we obtain the field equations

$$\begin{aligned} R_{ab} = \quad F(\phi)^{-1} \quad & \left[T_{ab} + \tfrac{1}{2}F(\phi)Rg_{ab} + \tfrac{1}{2}\left(\tfrac{1}{2}\nabla^c\phi\,\nabla_c\phi - V(\phi)\right)g_{ab}\right. \\ & \left. + \left(g^c{}_a g^d{}_b - g^{cd}g_{ab}\right)\{\nabla_c\nabla_d F(\phi) + \tfrac{1}{2}\nabla_c\phi\,\nabla_d\phi\}\right], \end{aligned} \tag{2.23}$$

and the variation with respect to ϕ gives the Klein-Gordon equation

$$\Box\phi + RF'(\phi) - V'(\phi) = 0, \tag{2.24}$$

where primes denote differentiation with respect to ϕ.

The higher order field equations may be split as in the Einstein case (see Ellis [86]) to give the following terms:

$$R = F(\phi)^{-1}\left[\mu - 3p + \tfrac{1}{2}\nabla^c\phi\,\nabla_c\phi + 2V(\phi) + 3\Box F(\phi)\right], \tag{2.25}$$

$$\begin{aligned} R_{ab}u^a u^b = {} & F(\phi)^{-1}\left[\tfrac{1}{2}(\mu + 3p) - \tfrac{1}{2}V(\phi) - \tfrac{1}{2}\Box F(\phi)\right. \\ & \left. + \{\nabla_a\nabla_b F(\phi) + \tfrac{1}{2}\nabla_a\phi\,\nabla_b\phi\}u^a u^b\right], \end{aligned} \tag{2.26}$$

$$R_{ab}u^a h^b{}_c = F(\phi)^{-1}\left[-q_c + \{\nabla_a\nabla_b F(\phi) + \tfrac{1}{2}\nabla_a\phi\,\nabla_b\phi\}u^a h^b{}_c\right], \tag{2.27}$$

$$\begin{aligned} R_{ab}h^a{}_c\,h^b{}_d = {} & F(\phi)^{-1}\left[\pi_{cd} - \tfrac{1}{2}\{(\mu - p) + V(\phi) + \Box F(\phi)\}h_{cd}\right. \\ & \left. + \{\nabla_a\nabla_b F(\phi) + \tfrac{1}{2}\nabla_a\phi\,\nabla_b\phi\}h^a{}_c\,h^b{}_d\right]. \end{aligned} \tag{2.28}$$

The Bianchi identities $\nabla^a G_{ab} = 0$ give the conservation laws for both the matter and the scalar field. As a general result [122], it is possible to show that the conservation law for the scalar field is the Klein-Gordon equation.

The action (2.22) is very general and contains several interesting physical cases. For example, considering the transformation

$$\phi \rightarrow \exp[-\psi], \quad F(\phi) \rightarrow \frac{1}{2}\exp[-2\psi], \quad V(\phi) \rightarrow \frac{1}{2}\Lambda \exp[-2\psi], \tag{2.29}$$

which specifies a particular form of coupling and potential, leads to the 4D-String-Dilaton Effective Action

$$\mathcal{A} = \int dx^4 \sqrt{-g} e^{-\psi} \left[R - g^{ab} \nabla_a \psi \, \nabla_b \psi - \Lambda \right], \tag{2.30}$$

where Λ is the string charge. In this context, such a theory is nothing else but a particular STG [123]. This means that the considerations and results for the action (2.22), and the related dynamics, also hold for string-dilaton cosmology. On the other hand, the set of transformations

$$F(\phi) \rightarrow \psi, \quad \frac{F(\phi)}{2F'(\phi)^2} \rightarrow \omega(\psi), \quad V(\phi) \rightarrow 0, \tag{2.31}$$

give rise to the action

$$\mathcal{A} = \int dx^4 \sqrt{-g} \left[\psi R - \frac{\omega(\psi)}{\psi} g^{ab} \nabla_a \psi \, \nabla_b \psi \right], \tag{2.32}$$

which is nothing else but the BD action[1] [54]. In addition to the ones above other interesting kind of transformations are possible [124, 125].

2.2.2 Decomposition of the stress energy tensor

The field equation (2.23) may be written as

$$\begin{aligned} R_{ab} - \tfrac{1}{2} R g_{ab} &= F(\phi)^{-1} \, T_{ab} + F(\phi)^{-1} \left[\tfrac{1}{2} \left(\tfrac{1}{2} \nabla^c \phi \, \nabla_c \phi - V(\phi) \right) g_{ab} \right. \\ &\quad \left. + \left(g^c{}_a g^d{}_b - g^{cd} g_{ab} \right) \left\{ \nabla_c \nabla_d F(\phi) + \tfrac{1}{2} \nabla_c \phi \, \nabla_d \phi \right\} \right]. \end{aligned} \tag{2.33}$$

The field equation can then be written in the standard form

$$G_{ab} = R_{ab} - \tfrac{1}{2} R g_{ab} = \tilde{T}_{ab} = \frac{T_{ab}}{F(\phi)} + T^{\phi}_{ab}, \tag{2.34}$$

[1] To be precise, the proper BD action is exactly recovered only for $\omega =$ constant.

where

$$T^{\phi}_{ab} = \frac{1}{F(\phi)}\left[\tfrac{1}{2}\left(\tfrac{1}{2}\nabla^c\phi\,\nabla_c\phi - V(\phi)\right)g_{ab} + \left(g^c{}_a g^d{}_b - g^{cd}g_{ab}\right)\left\{\nabla_c\nabla_d F(\phi) + \tfrac{1}{2}\nabla_c\phi\,\nabla_d\phi\right\}\right], \tag{2.35}$$

is the *scalar field stress-energy momentum tensor*. This form of the equations shows clearly one of the most interesting features of STG: the Newtonian gravitational constant G_N, intended as the coupling of gravity with standard matter, has to be replaced by an effective gravitational "constant" $\tilde{G}$ that depends on the non–minimal coupling F (and, as a consequence, on ϕ) and *varies* in time.

We may decompose the curvature stress-energy momentum tensor into its various components (see §1.3.1)

$$\begin{aligned}
\mu^{\phi} &= \frac{1}{F(\phi)}\left[\tfrac{1}{2}\left(V(\phi) - \tfrac{1}{2}\nabla^c\phi\,\nabla_c\phi\right) + \left\{\nabla_a\nabla_b F(\phi) + \tfrac{1}{2}\nabla_a\phi\,\nabla_b\phi\right\}h^{ab}\right],\\
p^{\phi} &= \frac{1}{F(\phi)}\left[-\tfrac{1}{2}\left(V(\phi) + \tfrac{1}{2}\nabla^c\phi\,\nabla_c\phi\right) + \tfrac{1}{3}h^{ab}\left\{\nabla_a\nabla_b F(\phi) + \tfrac{1}{2}\nabla_a\phi\,\nabla_b\phi\right\} - \Box F(\phi)\right],\\
q^{\phi}_c &= -\frac{1}{F(\phi)}\left[u^a h^b{}_c\left\{\nabla_a\nabla_b F(\phi) + \tfrac{1}{2}\nabla_a\phi\,\nabla_b\phi\right\}\right],\\
\pi^{\phi}_{ab} &= \frac{1}{F(\phi)}\left(h^c{}_a\,h^d{}_b - \tfrac{1}{3}h_{ab}h^{cd}\right)\left[\nabla_c\nabla_d F(\phi) + \tfrac{1}{2}\nabla_c\phi\,\nabla_d\phi\right].
\end{aligned} \tag{2.36}$$

Again we may redefine the kinematical quantities as follows:

$$\begin{aligned}
\tilde{\mu} &= \frac{\mu}{F(\phi)} + \mu^{\phi},\\
\tilde{p} &= \frac{p}{F(\phi)} + p^{\phi},\\
\tilde{q}_c &= \frac{q_c}{F(\phi)} + q^{\phi}_c,\\
\tilde{\pi}_{ab} &= \frac{\pi_{ab}}{F(\phi)} + \pi^{\phi}_{ab},
\end{aligned} \tag{2.37}$$

from which we may obtain the standard Einstein evolution and constraint equations given in §1.3.

2.2.3 Dynamics in scalar-tensor gravity

In this section we specialise the general propagation and constraint equations which are stated in the previous chapter, to the cases of general $F(\phi)$ theories. As in the case of $f(R)$-gravity, we will only state the equation which we will use in the next chapters. The remaining equations can be found straightforwardly, by substituting

the identities (2.37) into the relevant equations.

The Raychaudhuri equation is given by

$$\begin{aligned}&\dot{\Theta}-\tilde{\nabla}_a\dot{u}^a+\tfrac{1}{3}\,\Theta^2-(\dot{u}_a\dot{u}^a)+2\,\sigma^2-2\,\omega^2+\tfrac{1}{2}F(\phi)^{\,-1}\,(\mu+3p)\\&=\tfrac{1}{2}F(\phi)^{\,-1}\left[V(\phi)+\Box F(\phi)-\{2\nabla_a\nabla_b F(\phi)+\nabla_a\phi\;\nabla_b\phi\}u^a u^b\right],\end{aligned}\tag{2.38}$$

and the generalised Friedmann equations is

$${}^3R=2\sigma^2-\tfrac{2}{3}\Theta^2+F(\phi)^{\,-1}\left[\mu+V(\phi)+\tfrac{1}{2}\nabla^c\phi\;\nabla_c\phi+2\left[\nabla_c\nabla_d F(\phi)+\tfrac{1}{2}\nabla_c\phi\;\nabla_d\phi\right]h^{cd}\right].\tag{2.39}$$

2.3 Conformal transformations

In alternative theories of gravity, such as STG and $f(R)$-gravity, we face the problem of *conformal transformations*. For STG this transformation allows us to transform the non-minimal coupling into a constant which amounts to moving from one *conformal frame* to another. These frames are not necessarily equivalent, and the question of which frame is physical arises. The two most frequently discussed are the Jordan- and the Einstein frames. In the Jordan frame the energy momentum tensor is covariantly conserved and test particle follow geodesics. In the Einstein frame this is not necessarily the case since the energy momentum tensor is not always covariantly conserved. The field equations in the Einstein frame take on the form of Einstein's equations. This frame is useful for studying vacuum solutions but less helpful when matter is present.

The debate over which of these two frames is the correct physical frame is still going on (see for example [126] and references therein). This question is particularly important for the analysis of experimental tests of gravitational theories. Some authors believe both frames to be equivalent [127] while others argue that this is not the case [128] (also see [126]). For some STG's (including the BD action (2.32)), Kaluza-Klein theories and $f(R)$-theories, selecting the Jordan frame as physical seems untenable, because of the negative definite or indefinite kinetic energy of the scalar field. This implies that these theories do not have stable ground states, which is a requirement for a viable classical theory of gravity. However, it should be noted that a stable ground state is not a necessary requirement for cosmological solutions [129]. We note that the action given by (2.22), does not have this problem and is therefore physical in both the Einstein and Jordan frames, although these frames are not physically equivalent for this class of STG [126].

We will now proceed to give a formal definition of a conformal transformation. A *Weyl* or conformal transformation of the metric g_{ab} into $\bar{g}_{ab}$ is given by

$$g_{ab} = \Omega^2(x)\, \bar{g}_{ab} \tag{2.40}$$

where $\Omega(x)$ is a non-degenerate arbitrary function of the space-time coordinates x. An equivalent transformation can be applied to a line-element,

$$ds^2 = \Omega^2(x)\, d\bar{s}^2 \tag{2.41}$$

and thus the square root of the determinant of the metric g_{ab} is

$$\sqrt{-g} = \Omega^4(x)\, \sqrt{-\bar{g}} \tag{2.42}$$

in four dimensions. As can be seen from the line element (2.41), conformal transformations of this kind changes distance or the standard size defined by the line element. These transformations are local and isotropic, that is it leaves the angle between two vectors invariant and hence the name 'conformal'.

It is useful to introduce the notation $\Gamma \equiv \ln \Omega$. The Ricci tensor and scalar can then be shown (see e.g. [130]) to transform under (2.40) according to

$$R_{ab} = \bar{R}_{ab} - 2\bar{\nabla}_{ab}\Gamma + 2\partial_a\Gamma\, \partial_b\Gamma - 2\bar{g}_{ab}\bar{g}^{cd}\partial_c\Gamma\, \partial_d\Gamma - \bar{g}_{ab}\bar{\Box}\Gamma \tag{2.43}$$

$$e^{2\Gamma} R = \bar{R} - 6\bar{g}^{ab}\partial_a\Gamma\, \partial_b\Gamma - 6\bar{\Box}\Gamma \tag{2.44}$$

and the d'Alembertian transforms as

$$e^{2\Gamma}\Box\phi = \bar{\Box}\phi + 2\bar{g}^{ab}\partial_a\Gamma\, \partial_b\phi \tag{2.45}$$

where the bars over operators indicate that they are defined using the metric $\bar{g}_{ab}$. These transformations can be used to show how the scalar-tensor and $f(R)$-theories can be transformed from the Jordan- to the Einstein frame.

2.3.1 $f(R)$-gravity

We first show the conformal transformation between the Jordan frame and the Einstein frame for $f(R)$-theories of gravity [131, 132].

We define

$$\phi \equiv \sqrt{3} \ln f',$$

then under the conformal transformation

$$\bar{g}_{ab} = f' g_{ab},$$

the field equations (2.11) take the form

$$\bar{R}_{ab} - \frac{1}{2}\bar{g}_{ab}\bar{R} = \frac{1}{2}\left(\nabla_a\phi\nabla_b\phi - \frac{1}{2}\bar{g}_{ab}\bar{g}^{cd}\nabla_c\phi\nabla_d\phi - \bar{g}_{ab}V\right) + \frac{T_{ab}}{f'} \tag{2.46}$$

where

$$V = \frac{(Rf' - f)}{2f'^2}. \tag{2.47}$$

From this we can see that in the absence of matter fields, $f(R)$-theories are conformally equivalent to GR in the presence of a scalar field with a potential V.

2.3.2 Scalar-tensor gravity

Scalar-tensor theories, like the one defined by the Lagrangian (2.22), which is in the Jordan frame, can be transformed to an equivalent in the Einstein frame. Because of the number of terms in (2.22), we will consider each term separately.

We first consider the term containing the Ricci scalar

$$\mathcal{L}_1 = \frac{1}{2}\sqrt{-g}F(\phi)R.$$

Applying the conformal transformation (2.40) and using (2.42), the expression above becomes

$$\mathcal{L}_1 = \frac{1}{2}\sqrt{-\bar{g}}F(\phi)\Omega^{-2}(\bar{R} + 6\bar{\Box}\Gamma - 6\bar{g}^{ab}\partial_a\Gamma\,\partial_b\Gamma). \tag{2.48}$$

The non-minimal coupling to the Ricci scalar can now be removed by making the choice of conformal factor

$$\Omega^2 = F(\phi), \tag{2.49}$$

so that

$$\partial_a\Gamma = \frac{1}{2}\frac{F'}{F}\partial_a\phi.$$

Thus (2.48) can be written as

$$\mathcal{L}_1 = \sqrt{-\bar{g}}\left(\frac{1}{2}\bar{R} - \frac{3}{4}\left(\frac{F'}{F}\right)^2\bar{g}^{ab}\partial_a\phi\,\partial_b\phi\right), \tag{2.50}$$

where the second term in (2.48) disappears on integrating by parts.

A similar procedure can be applied to the second term in (2.22). We get

$$\mathcal{L}_2 = -\tfrac{1}{2}\sqrt{-g}F^{-1}\bar{g}^{ab}\partial_a\phi\,\partial_b\phi, \tag{2.51}$$

which has the same appearance as the second term in (2.50). Collecting these terms we have

$$\mathcal{L}_1 + \mathcal{L}_2 = \frac{1}{2}\sqrt{-\bar{g}}\left(\bar{R} - \Delta\bar{g}^{ab}\partial_a\phi\,\partial_b\phi\right), \tag{2.52}$$

where

$$\Delta = \frac{3}{2}\left(\frac{F'}{F}\right)^2 + \frac{1}{F}.$$

Redefining of the scalar field via

$$d\psi = \sqrt{\Delta}\,d\phi \tag{2.53}$$

allow us to rewrite (2.52) as

$$\mathcal{L}_1 + \mathcal{L}_2 = \frac{1}{2}\sqrt{-\bar{g}}\left(\bar{R} - \bar{g}^{ab}\partial_a\psi\,\partial_b\psi\right). \tag{2.54}$$

The scalar field is now minimally coupled and the Klein-Gordon equation (2.24) is

$$\bar{\Box}\psi - \frac{d\bar{V}}{d\psi} = 0. \tag{2.55}$$

The new scalar field potential is then given by

$$\bar{V}(\psi) = \frac{V(\phi)}{F(\phi)^2}, \tag{2.56}$$

which is the conformal transformation of the third term in (2.22).

The completely transformed Lagrangian can then be written as

$$\mathcal{L} = \sqrt{-\bar{g}}\left(\tfrac{1}{2}\bar{R} - \tfrac{1}{2}\bar{g}^{ab}\partial_a\psi\,\partial_b\psi - \bar{V}(\psi) + \bar{\mathcal{L}}_M\right), \tag{2.57}$$

where $\bar{\mathcal{L}}_M$ is the conformally transformed matter Lagrangian.

Chapter 3

Shear dynamics in Bianchi I cosmologies with R^n-gravity

In GR the vacuum Kasner solutions [133] and their fluid filled counterparts, the Type I Bianchi models, proved useful as a starting point for the investigation of the structure of anisotropic models. Barrow and Clifton [134, 135] have recently shown that it is also possible to find solutions of the Kasner type for R^n-gravity models. In [134] they showed that exact Kasner-like solutions do exist in the range of parameter n for $n \in (1/2, 5/4)$ but with different Kasner-index relations to the ones in GR.

The dynamics of anisotropic models with $f(R)$-gravity have not been studied as intensively as their FLRW counterparts and it is therefore not known how the behaviour of the shear is modified in these theories of gravity. Bianchi spacetimes with isotropic 3-surfaces have been investigated for the quadratic theory [136] and it was found that in Bianchi I cosmologies the universe isotropises slower than in the Einstein case. The equations governing the evolution of shear in Bianchi spacetimes for general $f(R)$-theories can be found from the trace-free Gauss-Codazzi equations (see for example [85, 86]). However, it is not easy to solve these equations since the shear depends non-linearly on the Ricci scalar. Consequently the dynamical systems approach provides us with the best means of understanding the dynamics of these models.

In this chapter we extend the dynamical systems analysis of R^n–gravity [87] to Bianchi I cosmological models that exhibit *local rotational symmetry* (LRS) [137–139]. LRS spacetimes geometries are subgroups within anisotropic spacetimes in which isotropies can occur around a point within the spacetime in 1- or 3–dimensions. Thus there exists a unique preferred spatial direction at each point which constitutes a

local axis of symmetry. All observations are identical under rotation about the axis and are the same in all spatial directions perpendicular to that direction [137, 138].

3.1 Shear dynamics in $f(R)$-gravity

We consider a Bianchi spacetimes whose homogeneous hypersurfaces have isotropic 3-curvature ${}^3R_{ab} = \frac{1}{3}({}^3R)h_{ab}$. These spacetimes include the Bianchi models which, via the dissipation of the shear anisotropy σ_{ab}, can reach a FLRW limit. Spatial homogeneity implies that the spatial gradients will vanish and that $\dot{u}_a = 0 = \omega$. Thus the trace free Gauss-Codazzi equation (2.20) becomes

$$\dot{\sigma}_{\langle ab\rangle} + \Theta\,\sigma_{ab} = f'^{-1}\left[\pi_{ab} + \left(h^c_a h^d_b - \tfrac{1}{3}h_{ab}h^{cd}\right)S_{cd}\right], \tag{3.1}$$

and S_{ab} can be split as follows

$$\begin{aligned} S_{ab} &= f''\left(\ddot{R}u_a u_b - \dot{R}\nabla_b u_a\right) + f'''\dot{R}^2 u_a u_b, && (3.2)\\ S_{ab}u^a u^b &= f''\ddot{R} + f'''\dot{R}^2, && (3.3)\\ S_{ab}h^{ab} &= -f''\dot{R}\Theta, && (3.4)\\ S &= -f''(\ddot{R} + \dot{R}\Theta) - f'''\dot{R}^2. && (3.5) \end{aligned}$$

Substituting these components into the Gauss-Codazzi equation (3.1) gives

$$\dot{\sigma}_{\langle ab\rangle} + \Theta\,\sigma_{ab} = f'^{\,-1}\left[\pi_{ab} - f''\dot{R}\sigma_{\langle ab\rangle}\right]. \tag{3.6}$$

In the case of a perfect matter fluid, $\pi_{ab} = 0$, so that the equation above becomes

$$\dot{\sigma}_{\langle ab\rangle} + \Theta\,\sigma_{ab} = a^{-3}\frac{d}{d\tau}\left(a^3\,\sigma_{ab}\right) = -\frac{f''\dot{R}}{f'}\sigma_{ab}. \tag{3.7}$$

On integration this yields

$$\sigma_{ab} = f'^{\,-1}\Psi_{ab}a^{-3}, \qquad \dot{\Psi}_{ab} = 0, \tag{3.8}$$

which in turn implies

$$\sigma^2 = f'^{\,-2}\Psi^2 a^{-6}, \qquad \dot{\Psi}^2 = 0. \tag{3.9}$$

In the case of $f(R) = R$, equation (3.9) gives the standard GR solution (see [85] and references there in) whose behaviour can be summarised as follows:

$$\sigma^2 \to \infty \ \text{ as } \ a \to 0, \qquad \sigma^2 \to 0 \ \text{ as } \ a \to \infty.$$

This behaviour is modified in $f(R)$-theories of gravity (see [78,136]), because R (and therefore f') is a function of σ^2 (see (3.13) below) and therefore (3.9) is implicit. In particular, the dissipation of the shear in Bianchi I spacetimes is slower in quadratic gravity than in GR [136]. However, this result was obtained by solving the evolution equations under the assumption that the scale factor also has a power-law evolution. Although this is desirable it may not necessarily be true since no analytical cosmological solution could be obtained in [136]. A more general approach to this problem is to make use of the theory of dynamical systems (see [88] and references therein). In the following we will apply this technique to R^n gravity in order to investigate further the behaviour of the shear in this framework.

3.2 Cosmological equations for R^n-gravity

We begin by specialising all the evolution equations above to the case of $f(R) = R^n$ for a LRS Bianchi I spacetimes. The Raychaudhuri equation (2.16) is now

$$\dot{\Theta} + \tfrac{1}{3}\Theta^2 + 2\sigma^2 - \frac{1}{2n}R - (n-1)\frac{\dot{R}}{R}\Theta + \frac{\mu}{nR^{n-1}} = 0, \tag{3.10}$$

and the trace free Gauss-Codazzi equation (3.6) for LRS spacetimes is given by

$$\dot{\sigma} = -\left(\Theta + (n-1)\frac{\dot{R}}{R}\right)\sigma. \tag{3.11}$$

The Friedmann equation can be found from (2.19)

$$\tfrac{1}{3}\Theta^2 - \sigma^2 + (n-1)\frac{\dot{R}}{R}\Theta - \frac{(n-1)}{2n}R - \frac{\mu}{nR^{n-1}} = 0. \tag{3.12}$$

In general, the substitution of the Friedmann equation (3.12) into the Raychaudhuri equation (3.10) yields

$$R = 2\dot{\Theta} + \tfrac{4}{3}\Theta^2 + 2\sigma^2. \tag{3.13}$$

Note that, in this relation the energy density does not appear explicitly, but is however still contained implicitly in the variables on the right hand side.

In this chapter we will assume standard matter behaves like a perfect fluid with barotropic pressure $p = w\mu$. The conservation equation (1.22) in this case is

$$\dot{\mu} = -(1+w)\mu\Theta. \tag{3.14}$$

In order to convert the equations above into a system of autonomous first order

differential equations, we define the following set of expansion normalised variables [1];

$$\Sigma = \frac{3\sigma^2}{\Theta^2}\,, \qquad x = \frac{3\dot{R}}{R\Theta}(n-1)\,, \qquad (3.15)$$
$$y = \frac{3R}{2n\Theta^2}(n-1)\,, \qquad z = \frac{3\mu}{nR^{n-1}\Theta^2}\,,$$

whose equations are

$$\begin{aligned}
\Sigma' &= 2\left(-2+2\Sigma-\frac{y}{n-1}-2x+z\right)\Sigma,\\
x' &= y(2+x)-\frac{y}{n-1}(2+nx)-2x-2x^2+xz+(1-3w)z+2x\Sigma,\\
y' &= \frac{y}{n-1}\left[(3-2n)x-2y+2(n-1)z+4(n-1)\Sigma+2(n-1)\right], \qquad (3.16)\\
z' &= z\left[2z-(1+3w)-3x-\frac{2y}{n-1}+4\Sigma\right],
\end{aligned}$$

where primes denote derivatives with respect to a new time variable $\tau = \ln a$ and the dynamical variables are constrained by

$$1-\Sigma+x-y-z=0. \qquad (3.17)$$

3.3 Dynamics of the vacuum case

We first consider the vacuum case ($\mu = 0$). In this case the set of dynamical equations (3.16) are given by

$$\begin{aligned}
\Sigma' &= 2\left(-2+2\Sigma-\frac{y}{n-1}-2x\right)\Sigma,\\
x' &= y(2+x)-\frac{y}{n-1}(2+nx)-2x-2x^2+2x\Sigma, \qquad (3.18)\\
y' &= \frac{y}{n-1}\left[(3-2n)x-2y+4(n-1)\Sigma+2(n-1)\right],
\end{aligned}$$

together with the constraint equation

$$1-\Sigma+x-y=0. \qquad (3.19)$$

3.3.1 Equilibrium points and solutions

The two most useful variables are Σ and y since they respectively represent a measure of the expansion normalised shear and the expansion normalised Ricci curvature and

[1] It is important to note that this choice of variables will exclude GR, i.e the case of $n = 1$. See [88] for the dynamical systems analysis of the corresponding cosmologies in GR.

hence allow us to investigate how the shear is modified by the curvature. We can therefore simplify the system (3.18), by making use of the constraint (3.19), which allow us to write the equation for x as a combination of the two variables Σ and y:

$$\begin{aligned} \Sigma' &= -2\left(\frac{2n-1}{n-1}\right) y\,\Sigma, \\ y' &= \frac{y}{n-1}\left[(2n-1)\Sigma - (2n-1)y + (4n-5)\right], \end{aligned} \tag{3.20}$$

which together with the constraint (3.19) represents our new system. Setting $\Sigma' = 0$ and $y' = 0$ we obtain one isotropic equilibrium point $\mathcal{A}$: $\left(0, \frac{4n-5}{2n-1}\right)$ and a line of equilibrium points $\mathcal{L}_1$: $(\Sigma_*, 0)$ where $\Sigma_* \geq 0$ ($\Sigma_* < 0$ would imply imaginary shear) [2]. The point $\Sigma_* = 0$ on $\mathcal{L}_1$ represents another isotropic equilibrium point that merges with $\mathcal{A}$ when $n = 5/4$.

The equilibrium points may be used to find exact solutions for the Bianchi I models. We substitute the definitions (3.15) into (3.13) to obtain

$$\dot{\Theta} = \left(\frac{n}{n-1} y_i - \Sigma_i - 2\right)\frac{\Theta^2}{3}, \tag{3.21}$$

where (Σ_i, y_i) represents the coordinates of the fixed points. Given that $n \neq 1$ and $y_i - (n-1)(\Sigma_i + 2) \neq 0$, this equation can be integrated to give

$$a = a_0 (t - t_0)^{\alpha}, \quad \text{where} \quad \alpha = \left(2 + \Sigma_{\mathrm{i}} - \tfrac{\mathrm{n}}{\mathrm{n}-1}\mathrm{y}_{\mathrm{i}}\right)^{-1}. \tag{3.22}$$

In the case of the equilibrium point $\mathcal{A}$ we have

$$a = a_0 (t - t_0)^{\frac{(1-n)(2n-1)}{(n-2)}}, \tag{3.23}$$

which is the same as the solution found in [87].

For the fixed line $\mathcal{L}_1$ we have

$$a = a_0 (t - t_0)^{\frac{1}{2+\Sigma_*}}, \tag{3.24}$$

but direct substitution into the cosmological equations reveals that this solution is only valid for $n > 1$. For $n < 1$ the equilibrium points on $\mathcal{L}_1$ are non physical because the field equations do not hold there.

The analysis above would be incomplete without determining the equilibrium points at infinity. In order for us to compactify the phase space, we transform our

[2] Σ_* are the coordinates on the Σ-axis.

Table 3.1: The equilibrium points and eigenvalues for R^n-gravity in a LRS Bianchi I vacuum model.

	Coordinates (Σ, y)	Eigenvalues
Point $\mathcal{A}$	$\left(0, \frac{4n-5}{2n-1}\right)$	$\left[\frac{2(5-4n)}{n-1}, \frac{(5-4n)}{n-1}\right]$
Line $\mathcal{L}_1$	$(\Sigma_*, 0)$	$\left[0, \frac{(4n-5)}{n-1} + \frac{(2n-1)}{n-1}\Sigma_*\right]$

Table 3.2: The solutions of the scale factor and shear evolution for R^n-gravity in a LRS Bianchi I vacuum model.

	Scale factor	Shear
Point $\mathcal{A}$	$a = a_0 (t - t_0)^{\frac{(1-n)(2n-1)}{(n-2)}}$	$\sigma = 0$
Line $\mathcal{L}_1$	$a = a_0 (t - t_0)^{\frac{1}{2+\Sigma_*}}$, (only valid for $n > 1$)	$\sigma = \sigma_0 a^{-(2+\Sigma_*)}$

coordinates (Σ, y) to polar coordinates

$$\Sigma = \bar{r}\cos\phi, \qquad y = \bar{r}\sin\phi \tag{3.25}$$

and set $\bar{r} = \frac{r}{1-r}$. Now since $\Sigma \geq 0$, we will only consider half of the phase space, i.e. $-\pi/2 \leq \phi \leq \pi/2$. In the limit $r \to 1$ ($\bar{r} \to \infty$), equations (3.20) take on the form

$$r' = \frac{(2n-1)}{4(n-1)}\left[\cos\phi - \cos 3\phi - 5\sin\phi - \sin 3\phi\right], \tag{3.26}$$

$$\phi' = \frac{(2n-1)\left[\cos\phi - \cos 3\phi + \sin\phi + \sin 3\phi\right]}{(n-1)(1-r)}. \tag{3.27}$$

Since (3.26) does not depend on r we can find the equilibrium points by making use of (3.27) only. Setting $\phi' = 0$ we obtain four equilibrium points which are listed in Table 3.4. We note that the solutions corresponding to these points given in [82] do not satisfy the definition of variables (3.15) (see chapter 5 for a detailed discussion).

3.3.2 Stability of the equilibrium points

The stability of the equilibrium points may be determined by linearising the system of equation (3.20). This can be done by perturbing Σ and y around the equilibrium points (Σ_i, y_i) via $\Sigma = \Sigma_i + \delta\Sigma$ and $y = y_i + \delta y$. The corresponding eigenvalues of the linearised system are given in Table 3.1. The equilibrium point $\mathcal{A}$ is an unstable node (repeller) for values of n in the range $n \in (1, 5/4)$. For all other values of n it is a stable node (attractor).

The equilibrium points on line $\mathcal{L}_1$ all contain at least one zero eigenvalue and therefore we will have to study the effect of small perturbations around the line. We find that they have the following solutions

$$\delta\Sigma = \frac{\kappa}{\eta} e^{\eta\tau}, \qquad \delta y = C\, e^{\eta\tau}, \tag{3.28}$$

where C is a constant of integration and

$$\eta = \frac{(2n-1)}{(n-1)}\Sigma_* + \frac{(4n-5)}{(n-1)}, \qquad \kappa = -\frac{2(2n-1)}{(n-1)}. \tag{3.29}$$

In order for the equilibrium points on line $\mathcal{L}_1$ to be stable nodes, we must have $\eta < 0$. The equilibrium point is an unstable node when $\eta > 0$. Over the interval $0 \leq \Sigma_* < \frac{5-4n}{2n-1}$, we will have stable nodes for $n \in (1, 5/4)$ and unstable nodes for $n \in (1/2, 1)$. The remainder of the points $\Sigma_* > \frac{5-4n}{2n-1}$, will be stable nodes for $n \in (1/2, 1)$ and unstable nodes for $n \in (1, 5/4)$. When $n < 1/2$ and $n > 5/4$, the equilibrium points are always unstable nodes. We also note that for $\Sigma_* = 1$, $\eta = 6$ and is therefore always an unstable node. The stability of all the equilibrium points is given in Table 3.3.

A similar analysis may be performed for the equilibrium points at infinity. We only need to perturb the angular variable ϕ around the equilibrium points ϕ_i via $\phi = \phi_i + \delta\phi$. The equilibrium points will be stable if $r' > 0$ and the eigenvalue $\lambda < 0$ for the linearised equation $\delta\phi' = \lambda\, \delta\phi$, in the limit of $\bar{r} \to \infty$. When both conditions are satisfied the point is an stable node, if only one is satisfied it is a saddle and when neither holds it is an unstable node. Substituting the expression above into (3.27) and linearising as before, yields

$$\delta\phi' \approx \frac{(2n-1)}{4(n-1)(1-r)} \left[-\sin\phi_i + 3\sin 3\phi_i + \cos\phi_i + 3\cos 3\phi_i \right]\, \delta\phi. \tag{3.30}$$

The stability of the equilibrium points are summarised in Table 3.4. We see that only point $\mathcal{D}_\infty$ have stable nodes for $n < 1/2$ and $n > 1$. Points $\mathcal{B}_\infty$ and $\mathcal{C}_\infty$ are always

Table 3.3: Stability of the equilibrium points for R^n-gravity in a LRS Bianchi I vacuum model.

	Range of n			
	$(-\infty, 1/2)$	$(1/2, 1)$	$(1, 5/4)$	$(5/4, \infty)$
Point $\mathcal{A}$	attractor	attractor	repeller	attractor
Line $\mathcal{L}_1$				
$\Sigma_* = 1$	repeller	repeller	repeller	repeller
$0 \leq \Sigma_* < \frac{5-4n}{2n-1}$	repeller	repeller	attractor	repeller
$\Sigma_* > \frac{5-4n}{2n-1}$	repeller	attractor	repeller	repeller

Table 3.4: Coordinates and stability of the asymptotic equilibrium points for R^n-gravity in a LRS Bianchi I vacuum model.

		Range of n		
Point	ϕ	$(-\infty, 1/2)$	$(1/2, 1)$	$(1, \infty)$
$\mathcal{A}_\infty$	0	repeller	saddle	repeller
$\mathcal{B}_\infty$	$\frac{\pi}{2}$	saddle	saddle	saddle
$\mathcal{C}_\infty$	$\frac{3\pi}{2}$	saddle	saddle	saddle
$\mathcal{D}_\infty$	$\frac{7\pi}{4}$	attractor	repeller	attractor

saddle points and $\mathcal{A}_\infty$ is a saddle when $n \in (1/2, 1)$ but is otherwise an unstable node.

3.3.3 Evolution of the shear

In the previous section we found two isotropic points; the fixed point $\mathcal{A}$ and one point on the fixed line at $\Sigma_* = 0$. The remaining equilibrium points all have non-vanishing shear.

The trace free Gauss Codazzi equation (3.11) can in general (i.e. for all points in the phase space) be represented in terms of the dynamical variables (3.15) as

$$\frac{\dot{\sigma}}{\sigma} = -\tfrac{1}{3}(2 + \Sigma + y)\Theta. \tag{3.31}$$

From the equation above it is clear that the shear evolution for all points in the phase space that lie on the line $y = 1 - \Sigma$, is the same as in the case of GR. The shear will dissipate faster than in GR when $\dot{\sigma}/\sigma < -\Theta$, that is all points that lie in the

region $y < 1 - \Sigma$. We will call this the *fast shear dissipation* (FSD) regime. When $\dot{\sigma}/\sigma > -\Theta$ and hence for all points in the region $y > 1 - \Sigma$, the shear will dissipate slower than in GR. This will be called the *slow shear dissipation* (SSD) regime.

The equilibrium points on $\mathcal{L}_1$ for which $\Sigma_* > 0$ all have non-vanishing shear. For these points (3.31) has the form

$$\frac{\dot{\sigma}}{\sigma} = -\tfrac{1}{3}(2 + \Sigma_*)\Theta = -(2 + \Sigma_*)\left(\frac{\dot{a}}{a}\right), \tag{3.32}$$

which may be integrated to give

$$\sigma = \sigma_0 a^{-(2+\Sigma_*)} = \sigma_0 a_0^{-(2+\Sigma_*)}(t - t_0)^{-1}, \tag{3.33}$$

where we made use of (3.24). We note that the final solution of the shear for these equilibrium points (3.33), does not depend on the parameter n. This is to be expected since both the coordinates of the points on $\mathcal{L}_1$ and equation (3.31) are independent of n.

The only other equilibrium point with non-vanishing shear is $\mathcal{D}_\infty$ which corresponds to $y \to -\infty$ as $\Sigma \to \infty$. In this limit (3.31) yields $\dot{\sigma}/\sigma = 0$ which implies that $\sigma = \sigma_0$ (i.e. constant shear).

We first consider values of the parameter for which $n < 1/2$ (see Figure 3.1). If the initial conditions of the universe lie in the region $y > 0$ (negative Ricci scalar), the orbits will always approach the isotropic equilibrium point $\mathcal{A}$. The shear will dissipate slower than in GR for almost all the orbits in this region, apart from the ones below the dotted line $y = 1 - \Sigma$, which make the transition from the SSD region to the FSD region. When the initial conditions lie in the region $y < 0$ (positive Ricci scalar), the orbits will approach the equilibrium point $\mathcal{D}_\infty$ which has constant shear.

The case $n \in (1/2, 1)$ is illustrated in Figures 3.2 and 3.3. If the initial conditions are such that they lie in the shaded area ($y < 1 - \Sigma$ and $y < 0$), then the evolution will always be in the FSD regime and will approach the isotropic solution of the point $\mathcal{A}$. Instead, the unshaded area $y < 0$ and $y > 1 - \Sigma$, is divided into two regions; the first one is located below the dash-dotted line and the second above the dash-dotted line. For initial conditions that lie in the first region, the orbits make a transition from the SSD region to the FSD region where they approach the point $\mathcal{A}$. When the initial conditions lie in the second region, the orbits will always lie in the SSD region and approach $\mathcal{L}_1$. When the initial conditions lie in $y < 1 - \Sigma$ and $y > 0$, the universe will evolve from the FSD regime to the SSD regime, in which the evolution will approach the stable solutions on $\mathcal{L}_1$. In the remaining area where $y > 1 - \Sigma$ and

$y > 0$, the shear will always dissipate slower than in GR.

We next consider $n \in (1, 5/4)$ which is illustrated in Figure 3.4. If the initial conditions of the universe are such that they lie in the shaded area, then the shear will always dissipate faster than in the case of GR. When the initial conditions lie in the region $y > 1 - \Sigma$ and $y > 0$, the universe will evolve from the SSD regime to the FSD regime and the evolution will approach the stable solutions on $\mathcal{L}_1$. If the initial conditions lie in the unshaded area of $y < 0$, the orbits will approach the equilibrium point $\mathcal{D}_\infty$. For initial conditions that lie in the region $y < 1 - \Sigma$, there will be a transition from the FSD region to the SSD region. For all initial conditions that lie in the region $y < 1 - \Sigma$, the orbits always lie in the SSD region. We can see that for this range of n, the equilibrium point $\mathcal{A}$ acts as a past attractor. This is an interesting feature since an isotropic past attractor implies that unlike GR, where the generic cosmological singularity is anisotropic, we have initial conditions which corresponds to a FLRW spacetime. This feature was also found in the braneworld scenarios where it was shown that homogeneous and anisotropic braneworld models (and some simple inhomogeneous models) have FLRW past attractors (see e.g. [115–118]). This means that although inflation is still required to produce the fluctuations observed in the cosmic microwave background (CMB), there is no need for special initial conditions for inflation to begin [140]. In the range $n \in (1, 5/4)$, we can obtain models whose evolution starts at the isotropic point $\mathcal{A}$ and then either evolves toward the equilibrium points $(\Sigma_*, 0)$ on line $\mathcal{L}_1$ or towards the point $\mathcal{D}_\infty$. The orbits that approach $\mathcal{L}_1$ will always lie in the FSD region. The orbits which approach $\mathcal{D}_\infty$ will make a transition from the FSD region to the SSD region. An interesting set of orbits are the ones that approach the equilibrium points on $\mathcal{L}_1$ for which $(\sigma/H)_* << 1$. These cosmic histories represent a universe that is initially isotropic and then develops shear anisotropies which approach a constant value that can be chosen to be comparable with the expansion normalised shear observed today ($(\sigma/H)_* < 10^{-9}$ [141–143]) [3]. Inflation is therefore not required to explain the low degree of anisotropy observed in the CMB. Furthermore, we still require all other observational constraints to be satisfied.

Finally, we consider values in the range $n > 5/4$ (see Figure 3.5). For all initial conditions that lie in the shaded region, the shear will always dissipate faster than in the case of GR; for $y > 0$ the orbits will approach $\mathcal{A}$ and for $y < 0$ approach the point $\mathcal{D}_\infty$. If initial conditions lie in the region $y > 1 - \Sigma$ and $y > 0$, the orbits will

[3] Strictly speaking these orbits do not satisfy the Collins and Hawking [144] definition for isotropisation, which require σ/H to asymptotically approach zero.

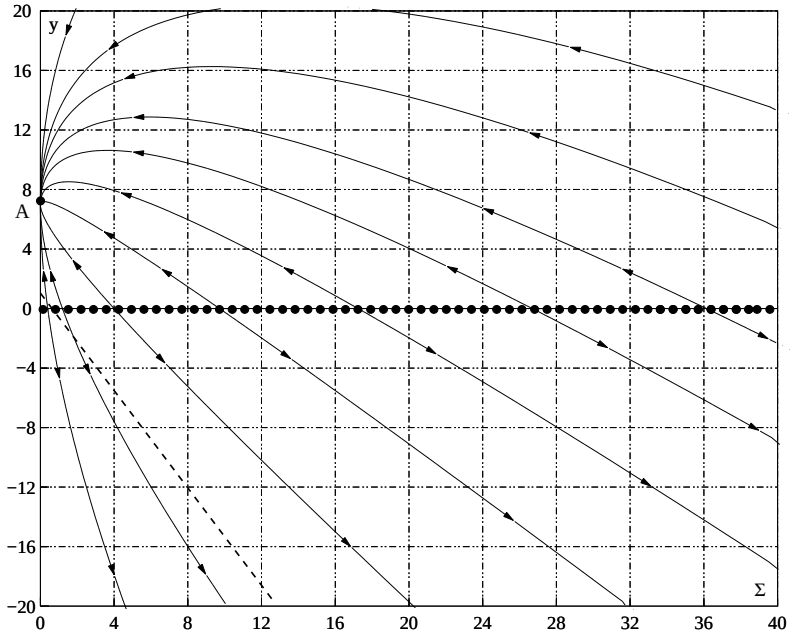

Figure 3.1: Phase space of the vacuum LRS Bianchi model with $n < 1/2$.

initially be in the SSD region, and then approach the isotropic solution $\mathcal{A}$, which is in the FSD region. For all orbits in the region $y > 1 - \Sigma$ and $y < 0$, the shear will always dissipate slower than in the case of GR.

3.4 Dynamics of the matter case

We will now consider the dynamics of LRS Bianchi I models in the presence of matter. As noted in [87], in HOTG there is a difference between vacuum and non-vacuum physics in the sense that not all higher order couplings are consistent in the presence of standard matter. This can be seen in the evolution equations (3.10) and (3.12) where the matter terms are coupled with a generic power of the curvature. Since the sign of the Ricci scalar is not fixed, these terms will not be defined for every real value of n. Thus, the inclusion of matter induces a natural constraint through the field equations on R^n- gravity and it is therefore necessary to express the results in terms of the allowed set of values of n. Following [87], we will work as if n is unconstrained, supposing that the intervals we devise are meant to represent the subset of allowed values within these intervals.

Similar to the vacuum case, we can reduce the system (3.16) to the three variables

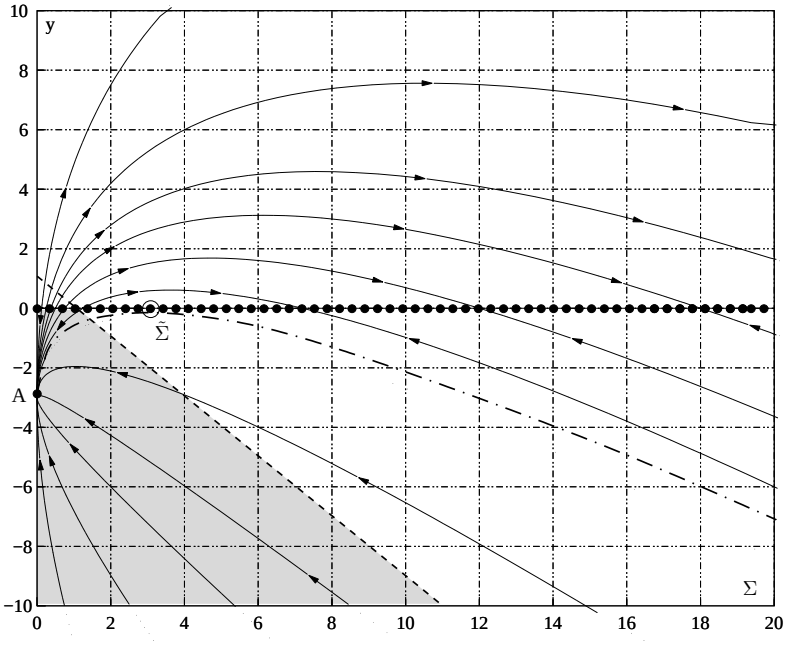

Figure 3.2: Phase space of the vacuum LRS Bianchi model with $n \in (1/2, 1)$ and where $\tilde{\Sigma} = \frac{5-4n}{2n-1}$. The shaded region represents the region of initial conditions for which the shear will always evolve faster than in GR.

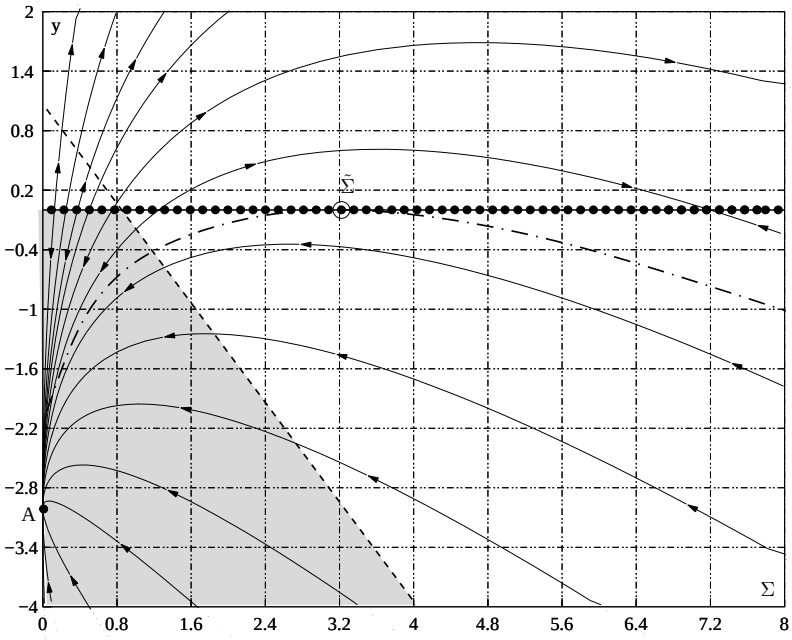

Figure 3.3: Close-up of the phase space of the vacuum LRS Bianchi model with $n \in (1/2, 1)$ around the line $y = 1 - \Sigma$.

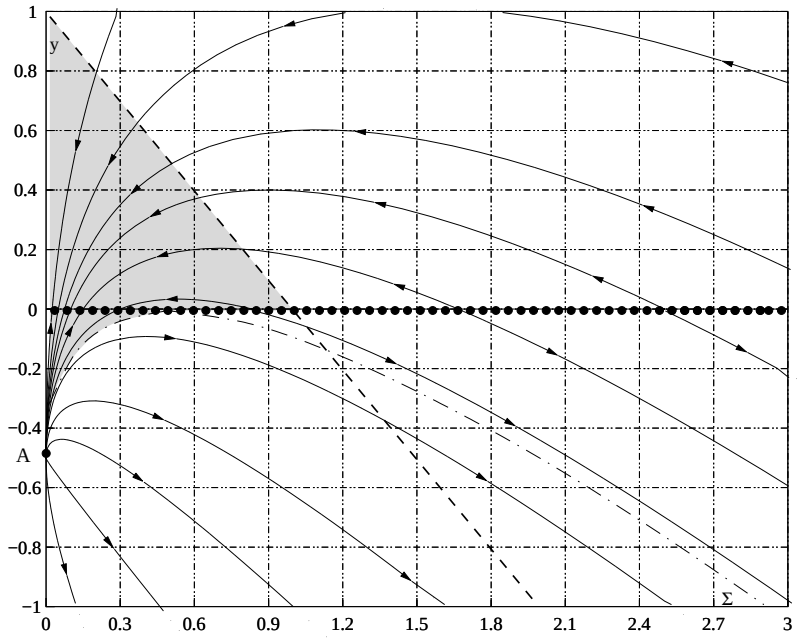

Figure 3.4: Phase space of the vacuum LRS Bianchi model with $n \in (1, 5/4)$.

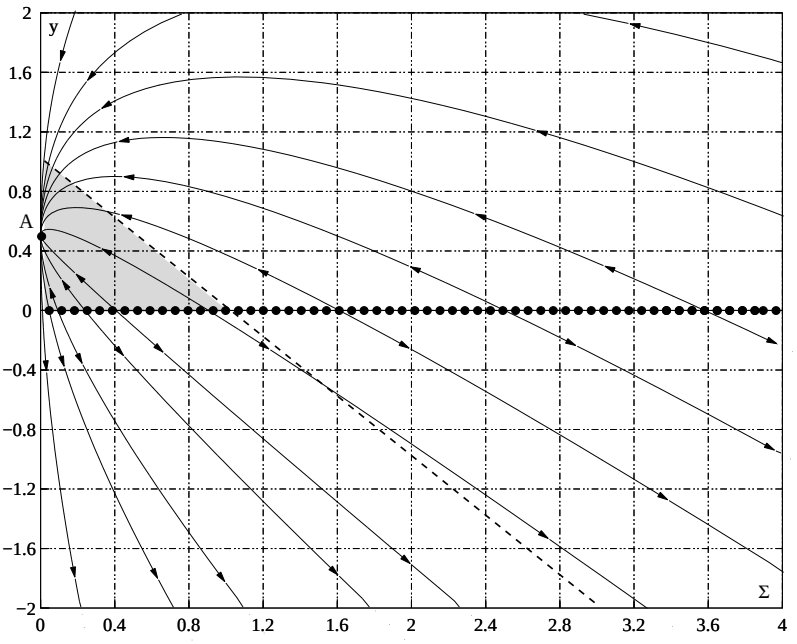

Figure 3.5: Phase space of the vacuum LRS Bianchi model with $n > 5/4$.

Σ, y and z by making use of the constraint (3.17);

$$\begin{aligned} \Sigma' &= -2\left[\left(\frac{2n-1}{n-1}\right)\, y + z\right]\Sigma, \\ y' &= \frac{y}{n-1}\left[(2n-1)\Sigma - (2n-1)y + z + (4n-5)\right], \\ z' &= z\left[(2-3w) - z + \Sigma - \left(\frac{3n-1}{n-1}\right)\, y\right]. \end{aligned} \tag{3.34}$$

We note that when $y = 0$ then $y' = 0$ and when $z = 0$, $z' = 0$. The two planes $y = 0$ and $z = 0$ therefore corresponds to two invariant submanifolds. When $z = 0$, the system (3.34) reduces to system (3.20) and one would be tempted to consider the plane $z = 0$ as the vacuum invariant submanifold of the phase space, which would not be entirely correct. To illustrate this point, we write the energy density in terms of our expansion normalised variables (3.15)

$$\mu \propto z y^{n-1} \Theta^{2n}. \tag{3.35}$$

From this relation it can be seen that when $z = 0$ and $y \neq 0$ the energy density is zero. However when $y = 0$ and $z \neq 0$ the behaviour of μ does depend on the value of n. In this case the energy density is zero when $n > 1$ but is divergent when $n < 1$. When both y and z are equal to zero and $n < 1$, one can only determine the behaviour of μ by direct substitution into the cosmological equations.

3.4.1 Equilibrium points and solutions

Setting $\Sigma' = 0$, $y' = 0$ and $z' = 0$ we obtain three isotropic equilibrium points $\mathcal{A}$, $\mathcal{B}$, $\mathcal{C}$ and a line of equilibrium points $\mathcal{L}_1 :\ (\Sigma_*,\ 0,\ 0)$, where $\Sigma_* \geq 0$ (see Table 3.5). When $\Sigma_* = 0$ we have another isotropic equilibrium point which merges with $\mathcal{A}$ when $n = 5/4$ and with $\mathcal{B}$ when $w = 2/3$. This point will merge with $\mathcal{C}$ when $n = 5/4$ and $w = 2/3$.

We again substitute the definitions (3.15) into (3.13) to obtain

$$\dot{\Theta} = \left(\frac{n}{n-1} y_i - \Sigma_i - 2\right)\frac{\Theta^2}{3}. \tag{3.36}$$

Under the condition that $n \neq 1$ and the terms inside the brackets are not equal to zero, this equation may be integrated to give the following solution

$$a = a_0\,(t - t_0)^{\alpha}, \quad \text{where} \quad \alpha = \left(2 + \Sigma_{\mathrm{i}} - \tfrac{\mathrm{n}}{\mathrm{n}-1}\mathrm{y_i}\right)^{-1}. \tag{3.37}$$

The point $\mathcal{A}$ and line $\mathcal{L}_1$ will all have the same solutions as in the vacuum case, since either $y = 0$ or $z = 0$ for these points.

The behaviour of the scale factor for point $\mathcal{B}$ is

$$a = a_0 \left(t - t_0\right)^{1/2}, \tag{3.38}$$

and since $y_2 = 0$ and $z_2 \neq 0$, the energy density is zero (only valid for $n > 1$). When $n < 1$, point $\mathcal{B}$ and the points on $\mathcal{L}_1$ are non physical since the energy density is divergent.

For point $\mathcal{C}$, the scale factor behaves as

$$a = a_0 \left(t - t_0\right)^{\frac{2n}{3(1+w)}}, \tag{3.39}$$

while the energy density is

$$\mu = \mu_0 t^{-2n}, \tag{3.40}$$

where

$$\begin{aligned} \mu_0 &= (-1)^n 3^{-n} 2^{2n-1} n^n (1+w)^{-2n} (4n - 3(1+w))^{n-1} \\ &\quad \times \left[2n^2(4+3w) - n(13+9w) + 3(1+w)\right]. \end{aligned}$$

This point thus represents a power-law regime which in the case of $n > 0$, yields an expanding solution with the energy density decreasing in time. In the case of $n < 0$ we obtain a contracting solution with μ increasing in time. In order for $\mathcal{C}$ to be a physical point, we require $\mu > 0$ and therefore $\mu_0 > 0$ (see [87] for detailed analysis). Note than when $n > \frac{3}{2}(1+w)$, this solution corresponds to accelerated expansion.

We next study the behaviour of the system (3.34) at infinity. The compactification of the phase space can be achieved by transforming to spherical coordinates

$$\Sigma = \bar{r} \sin\theta \cos\phi, \qquad y = \bar{r} \sin\theta \sin\phi, \qquad z = \bar{r} \cos\theta, \tag{3.41}$$

and setting $\bar{r} = \frac{r}{1-r}$, where $0 \leq \bar{r} \leq \infty$, $0 \leq \theta \leq \pi$ and since we are again only considering half of the phase space, $-\pi/2 \leq \phi \leq \pi/2$. In the limit $r \to 1$ ($\bar{r} \to \infty$),

Table 3.5: Equilibrium points, eigenvalues and scale factor solutions for LRS Bianchi I with matter.

Point	Coordinates (Σ, y, z)	Scale factor	Matter density
$\mathcal{A}$	$\left(0,\ \frac{4n-5}{2n-1},\ 0\right)$	$a = a_0\,(t-t_0)^{\frac{(1-n)(2n-1)}{(n-2)}}$	$\mu = 0$
$\mathcal{B}$	$(0,\ 0,\ 2-3w)$	$a = a_0\,(t-t_0)^{\frac{1}{2}}$	$\mu = 0 \quad (n>1)$
$\mathcal{C}$	$\left(0,\ \frac{(n-1)[4n-3(1+w)]}{2n^2},\ \frac{n(13+9w)-2n^2(4+3w)-3(1+w)}{2n^2}\right)$	$a = a_0\,(t-t_0)^{\frac{2n}{3(1+w)}}$	$\mu = \mu_0 t^{-2n}$
Line $\mathcal{L}_1$	$(\Sigma_*, 0, 0)$	$a = a_0\,(t-t_0)^{\frac{1}{2+\Sigma_*}}$	$\mu = 0 \quad (n>1)$

equations (3.34) take on the form

$$
\begin{aligned}
r' &= \frac{1}{4(n-1)}\big[\,2\cos\theta\{3-2n+(2n-1)\cos 2\phi\}+2\cos^3\theta\{(2n-1)\cos 2\phi-1\} \\
&\quad +2\sin\theta\,\cos^2\theta\{(2n-1)\cos 2\phi-1\}\{\cos\phi+\sin\phi\} \\
&\quad +(2n-1)\sin\theta\,\{\cos\phi-\cos 3\phi-5\sin\phi-\sin 3\phi\}\,\big], \qquad (3.42)\\
\theta' &= \frac{\sin 2\theta\{1-(2n-1)\cos 2\phi\}\,[\cos\theta+\sin\theta\{\cos\phi+\sin\phi\}\,]}{4(n-1)(1-r)} \qquad (3.43)\\
\phi' &= \frac{(2n-1)\sin 2\phi\,[\cos\theta+\sin\theta\{\cos\phi+\sin\phi\}\,]}{2(n-1)(1-r)}. \qquad (3.44)
\end{aligned}
$$

Now since (3.42) does not depend on r we can find the equilibrium points by just making use of (3.43) and (3.44). Setting $\theta' = 0$ and $\phi' = 0$ we obtain the equilibrium points which are listed in Table 3.11. As in the vacuum case, there are no solutions corresponding to these points (see chapter 5).

3.4.2 Stability of the equilibrium points

We next check the stability of the equilibrium point by linearising the system of equation (3.34). The eigenvalues of the linearised system are given in Table 3.6.

For the stability analysis, we consider three cases: dust $w = 0$, radiation $w = 1/3$ and stiff matter $w = 1$. The stability of the equilibrium points $\mathcal{A}$, $\mathcal{B}$ and $\mathcal{C}$ are summarised in Tables 3.7, 3.8 and 3.9 respectively. Their behaviour is similar to the flat ($k = 0$) points ($\mathcal{C}$, $\mathcal{F}$ and $\mathcal{G}$) considered in [87].

As in the vacuum case we find that the equilibrium points on the line $\mathcal{L}_1$ have

Table 3.6: Eigenvalues and shear solutions for LRS Bianchi I with matter.

Point	Eigenvalues	Shear
$\mathcal{A}$	$\left[\frac{2(5-4n)}{n-1},\ \frac{5-4n}{n-1},\ \frac{n(13+9w)-2n^2(4+3w)-3(1+w)}{1-3n+2n^2}\right]$	$\sigma = 0$
$\mathcal{B}$	$\left[-2+3w,\ -4+6w,\ \frac{4n-3(1+w)}{n-1}\right]$	$\sigma = 0$
$\mathcal{C}$	$\left[\frac{3((2n-1)w-1)}{n},\ \frac{P_1(n,w)-\sqrt{P_2(n,w)}}{4n(n-1)},\ \frac{P_1(n,w)+\sqrt{P_2(n,w)}}{4n(n-1)}\right]$ $P_1(n,w) = 3(1+w) + 3n\left((2n-3)w-1\right)$ $P_2(n,w) = (n-1)\left[4n^3(8+3w)^2 - 4n^2(152+3w(55+18w))\right.$ $\left.+3n(1+w)(139+87w) - 81(1+w)^2\right]$	$\sigma = 0$
Line $\mathcal{L}_1$	$\left[0,\ \frac{(4n-5)}{n-1} + \frac{(2n-1)}{n-1}\Sigma_*,\ 2-3w+\Sigma_*\right]$	$\sigma = \sigma_0 a^{-(2+\Sigma_*)}$

Table 3.7: Stability of the equilibrium point $\mathcal{A}$ for LRS Bianchi I with matter. The parameters are $N_\pm = \frac{1}{16}(13 \pm \sqrt{73})$, $P_\pm = \frac{1}{5}(4 \pm \sqrt{6})$ and $Q_\pm = \frac{1}{14}(11 \pm \sqrt{37})$.

	Range of n				
	$(-\infty, N_-)$	(N_-, P_-)	(P_-, Q_-)	$(Q_-, 1/2)$	$(1/2, 1)$
$w = 0$	attractor	saddle	saddle	saddle	attractor
$w = 1/3$	attractor	attractor	saddle	saddle	attractor
$w = 1$	attractor	attractor	attractor	saddle	attractor
	$(1, Q_+)$	$(Q_+, 5/4)$	$(5/4, P_+)$	(P_+, N_+)	$n > N_+$
$w = 0$	repeller	repeller	saddle	saddle	attractor
$w = 1/3$	repeller	repeller	saddle	attractor	attractor
$w = 1$	repeller	saddle	attractor	attractor	attractor

Table 3.8: Stability of the equilibrium point $\mathcal{B}$ for LRS Bianchi I with matter.

	Range of n			
	$(-\infty, 3/4)$	$(3/4, 1)$	$(1, 3/2)$	$(3/2, \infty)$
$w = 0$	saddle	attractor	saddle	saddle
$w = 1/3$	saddle	saddle	saddle	saddle
$w = 1$	repeller	repeller	saddle	repeller

Table 3.9: Stability of the equilibrium point $\mathcal{C}$ for LRS Bianchi I with matter. The parameters are given in Table 3.7.

	Range of n				
	$(-\infty, N_-)$	(N_-, P_-)	(P_-, Q_-)	$(Q_-, 3/4)$	$(3/4, 1)$
$w = 0$	saddle	attractor	attractor	attractor	saddle
$w = 1/3$	saddle	saddle	attractor	attractor	attractor
$w = 1$	saddle	saddle	saddle	attractor	attractor
	$(1, Q_+)$	(Q_+, P_+)	(P_+, N_+)	$(N_+, 3/2)$	$n > 3/2$
$w = 0$	attractor	attractor	attractor	saddle	saddle
$w = 1/3$	attractor	attractor	saddle	saddle	saddle
$w = 1$	saddle	repeller	repeller	repeller	saddle

zero eigenvalues. We therefore study the perturbations around the fixed line which lead to the following solutions

$$\delta\Sigma = -\tfrac{2(2n-1)}{(n-1)}\tfrac{C_0}{\eta}e^{\eta\tau} - 2\Sigma_*\,\tfrac{C_1}{\kappa}e^{\kappa\tau}, \qquad \delta y = \tfrac{C_0}{\eta}e^{\eta\tau}, \qquad \delta z = \tfrac{C_1}{\kappa}e^{\kappa\tau}, \tag{3.45}$$

where C_0 and C_1 are constants of integration and

$$\eta = \frac{(2n-1)}{(n-1)}\Sigma_* + \frac{(4n-5)}{(n-1)}\,, \qquad \kappa = 2 - 3w + \Sigma_*. \tag{3.46}$$

In order for the equilibrium points on line $\mathcal{L}_1$ to be stable nodes, we must have $\eta < 0$ and $\kappa < 0$. When $\eta > 0$ and $\kappa < 0$ or $\eta < 0$ and $\kappa > 0$ we have a saddle and when $\eta > 0$ and $\kappa > 0$ it is an unstable node. The results have been summarised in Table 3.7.

A similar analysis can be performed for the equilibrium points at infinity. We can check the stability of the equilibrium point by linearising the system of equation (3.42)-(3.44). The eigenvalues of the linearised system are given in Table 3.11. The stability of the equilibrium points $\mathcal{A}_\infty$, $\mathcal{B}_\infty$, $\mathcal{C}_\infty$, $\mathcal{D}_\infty$ and $\mathcal{E}_\infty$ can then be found straightforwardly as in the vacuum case (see Table 3.12). Points $\mathcal{A}_\infty$ and $\mathcal{B}_\infty$ are always saddle points. The point $\mathcal{C}_\infty$ lie on the fixed line $\mathcal{L}_1$ and is an unstable node for $n < 1/2$ and $n > 1$ and a saddle for $n \in (1/2, 1)$. Point $\mathcal{D}_\infty$ is an unstable node for $n < 0$ and $n > 1$, a saddle for $n \in (0, 1/2)$ and a stable node for $n \in (1/2, 1)$. Point $\mathcal{E}_\infty$ is a stable node for $n < 0$ and $n > 1$, a saddle for $n \in (0, 1/2)$ and an unstable node for $n \in (1/2, 1)$.

Table 3.10: Stability of the line of equilibrium points $\mathcal{L}_1$ for LRS Bianchi I with matter. Here $\Sigma_b(n) = \sqrt{\frac{5-4n}{2n-1}}$ is a bifurcation value depending on n.

	Range of Σ		
$w = 0, 1/3$	$[0, \Sigma_b(n))$	$(\Sigma_b(n), \infty)$	
$n < 1/2$	repeller	repeller	
$n \in (1/2, 1)$	repeller	saddle	
$n \in (1, 2)$	saddle	repeller	
$n > 2$	repeller	repeller	
$w = 1$	$[0, 1)$	$(1, \Sigma_b(n))$	$(\Sigma_b(n), \infty)$
$n < 1/2$	saddle	repeller	repeller
$n \in (1/2, 1)$	saddle	repeller	saddle
	$[0, \Sigma_b(n)))$	$(\Sigma_b(n), 1)$	$(1, \infty)$
$n \in (1, 5/4)$	attractor	saddle	repeller
$n > 5/4$	saddle	saddle	repeller

Table 3.11: Coordinates, eigenvalues and value of r' of the ordinary asymptotic equilibrium points for LRS Bianchi I with matter. The eigenvalues for the line of equilibrium points are given in the text and $\tilde{\theta} = \arctan[-1/(\cos\phi_i + \sin\phi_i)]$.

Point	(θ, ϕ)	Eigenvalues	r'
$\mathcal{A}_\infty$	$(0, 0)$	$\left[-1, \frac{2n-1}{n-1}\right]$	-1
$\mathcal{B}_\infty$	$(\pi, 0)$	$\left[1, -\frac{2n-1}{n-1}\right]$	1
$\mathcal{C}_\infty$	$(\frac{\pi}{2}, 0)$	$\left[1, \frac{2n-1}{n-1}\right]$	0
$\mathcal{D}_\infty$	$(\frac{\pi}{2}, \frac{\pi}{2})$	$\left[-\frac{n}{n-1}, \frac{2n-1}{n-1}\right]$	$-\frac{2n-1}{n-1}$
$\mathcal{E}_\infty$	$(\frac{\pi}{2}, \frac{3\pi}{2})$	$\left[-\frac{2n-1}{n-1}, \frac{n}{n-1}\right]$	$\frac{2n-1}{n-1}$
Line			
$\mathcal{L}_\infty$	$(\tilde{\theta}, \phi)$	$[\lambda_1, \lambda_2]$	-

Table 3.12: Stability of the ordinary asymptotic equilibrium points for LRS Bianchi I with matter. Results are independent of w.

	Range of n			
Point	$(-\infty, 0)$	$(0, 1/2)$	$(1/2, 1)$	$(1, \infty)$
$\mathcal{A}_\infty$	saddle	saddle	saddle	saddle
$\mathcal{B}_\infty$	saddle	saddle	saddle	saddle
$\mathcal{C}_\infty$	repeller	repeller	saddle	repeller
$\mathcal{D}_\infty$	attractor	saddle	repeller	attractor
$\mathcal{E}_\infty$	repeller	saddle	attractor	repeller

The eigenvalues of the fixed line $\mathcal{L}_\infty$ are given by

$$[\lambda_1, \lambda_2] = \left[\frac{P_1(n,\phi) - \sqrt{P_2(n,\phi)}}{4(n-1)(2+\sin 2\phi)^{3/2}}, \frac{P_1(n,\phi) + \sqrt{P_2(n,\phi)}}{4(n-1)(2+\sin 2\phi)^{3/2}} \right], \tag{3.47}$$

where

$$\begin{aligned} P_1(n,\phi) &= (3n-4)\cos\phi + n\cos 3\phi - (3n+1)\sin\phi + (n-1)\sin 3\phi, \\ P_2(n,\phi) &= 2(2+\sin 2\phi)^{3/2}\left[(2n^2-2n+1)(1+\sin 2\phi)\right. \\ &\quad \left. +(2n-1)(-\cos 2\phi - 2\sin 4\phi + (2n-1)\sin 6\phi)\right]. \end{aligned}$$

The stability can then be found in a similar fashion as the ordinary asymptotic equilibrium points. The eigenvalues in this case is dependent on two variables, n and ϕ, which makes it difficult to express the results in a table. We have therefore summarised these results in a diagram (see Figure 3.6) [4]. The stability of any equilibrium point on the line $\mathcal{L}_\infty$ for a given value of n can be read from this diagram. For example the black dot in Figure 3.6 represents the equilibrium point at $\phi = 0.4$ for a model with $n = 1.4$. It lies within a region that classify it as an attractor.

3.4.3 Evolution of the shear

The trace free Gauss Codazzi equation (3.11) can in general (i.e. for all points in the phase space) be represented in terms of the dynamical variables (3.15) as

$$\frac{\dot{\sigma}}{\sigma} = -\tfrac{1}{3}(2 + \Sigma + y + z)\Theta. \tag{3.48}$$

[4] This diagram was found by plotting $\tau = \lambda_1 + \lambda_2$, $\Delta = \lambda_1\lambda_2$ and $\tau^2 - 4\Delta$ and using the definitions for stability to classify the regions [145].

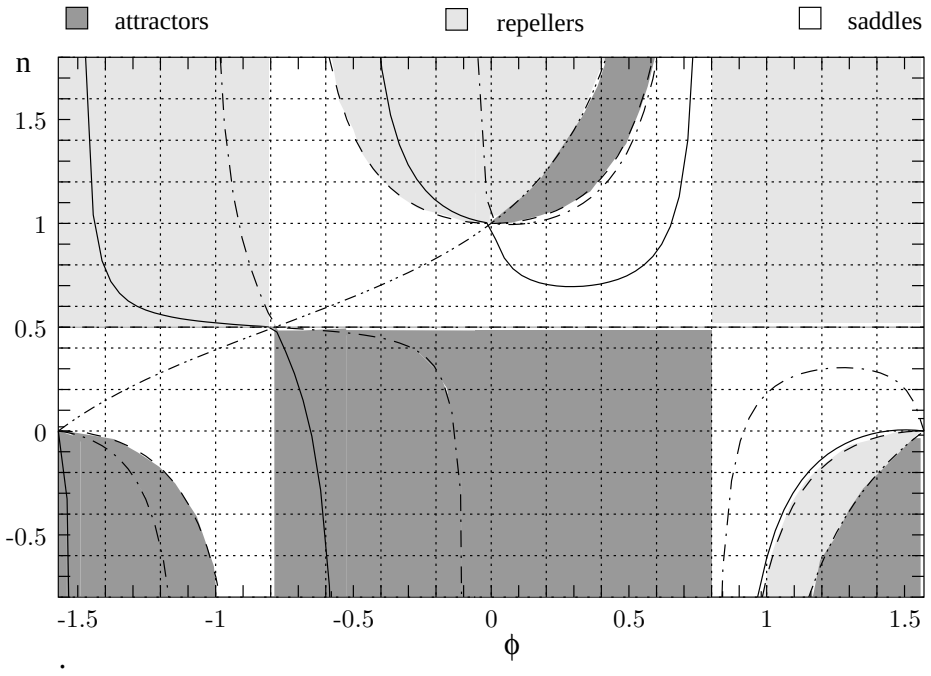

Figure 3.6: Stability of the line of equilibrium points $\mathcal{L}_\infty$ for LRS Bianchi I with matter. Results are independent of w. The black dot represents the equilibrium point at $\phi = 0.4$ for a model with $n = 1.4$.

The shear evolves at the same rate as in GR when $\dot{\sigma}/\sigma = -\Theta$, which holds for all values on the plane $1 = \Sigma + y + z$. The shear will dissipate faster than in GR when $\dot{\sigma}/\sigma < -\Theta$, that is all points that lie in the region $1 > \Sigma + y + z$. We may again call this the *fast shear dissipation* (FSD) regime. The shear will dissipate slower than in GR when $\dot{\sigma}/\sigma > -\Theta$ and hence all points in the region $1 < \Sigma + y + z$. This will be called the *slow shear dissipation* (SSD) regime. Analysing the three dimensional phase space for this system is more difficult than the two dimensional spaces considered in the vacuum case since it is harder to visualise.

All the finite equilibrium points ($\mathcal{A}$, $\mathcal{B}$ and $\mathcal{C}$) together with the point $\Sigma_* = 0$ on $\mathcal{L}_1$, lie on the plane $\Sigma = 0$ and are therefore isotropic.

The evolution of the shear for the anisotropic equilibrium points on $\mathcal{L}_1$ can be obtained as in the vacuum case. For these points (3.48) take the form

$$\frac{\dot{\sigma}}{\sigma} = -\tfrac{1}{3}(2 + \Sigma_*)\Theta = -(2 + \Sigma_*)\left(\frac{\dot{a}}{a}\right). \tag{3.49}$$

which may be integrated to give

$$\sigma = \sigma_0 a^{-(2+\Sigma_*)} = \sigma_0 a_0^{-(2+\Sigma_*)}(t-t_0)^{-1}, \tag{3.50}$$

where we made use of (3.22). This is the same solutions that where obtained in the vacuum case. This is to be expected since all these equilibrium points lie on the line $\mathcal{L}_1$ for which $z = 0$.

3.5 Discussion

We have derived the evolution equations of the shear for Bianchi I cosmologies with $f(R)$-gravity. This general expression, allows us to consider the shear evolution for any function of the scalar curvature. However, because the shear depend non-linearly on the Ricci scalar one can not determine how the dissipation of the shear anisotropy compares with the case in GR even if one chooses a specific form for $f(R)$ (such as $R+R^2$ or R^n). One way of dealing with this problem is to make certain assumptions (for example the form of the evolution of the scale factor a [136]) to obtain a solution. A more general approach is to make use of the dynamical systems approach to study HOTG in these cosmologies since it provides both exact solutions and the global behaviour of the system.

Our main aim in this chapter was to see how the shear behaves in LRS Bianchi I cosmologies with R^n- gravity and whether these models isotropises at early and late times. To achieve this goal we used the theory of dynamical systems to analyse the system of equations governing the evolution of this model with and without matter.

The phase space for these models have a number of interesting features, in particular it contains one isotropic equilibrium point and a line of equilibrium points with non-vanishing shear. The isotropic equilibrium point is an attractor (stable node) for values of the parameter n in the ranges $n < 1/2$, $n \in (1/2, 1)$ and $n > 5/4$. In the range $n \in (1, 5/4)$ this point is a repeller (unstable node) and therefore may be seen as a past attractor. An isotropic past attractor implies that inflation can start without requiring special initials conditions. However, since we have attractors for $(\sigma/H)_* << 1$ on $\mathcal{L}_1$, we may not need inflation since the shear anisotropy approaches a constant value which may be chosen as the expansion normalised shear observed today ($(\sigma/H)_* < 10^{-9}$ [141–143]), provided that other observational constraints such as nucleosynthesis are satisfied.

We also found that the line $y = 1-\Sigma$ separates the phase space into two part. For all points on this line, the shear dissipates at the same rate as in GR. In the region

above the line the shear dissipates faster (FSD) than GR and in the region below the line, slower (SSD) than in GR. From Figures $1-5$ we can see that there are a number of orbits which cross the dotted line. These are systems which initially lie in the FSD region and then make a transition to the SSD region and *vice versa*. An interesting feature of the vacuum case is that when the evolution of the universe reaches the stable solutions on $\mathcal{L}_1$, the shear will evolve according to $\sigma \propto t^{-1}$ irrespective of the value of n. For values that lie in the range $n \in (1/2, 1)$ and $y > 0$, one may have orbits that initially lie in the FSD region (see Figures 3.1 and 3.2) and then make a transition to the SSD region at late times. The opposite will happen for values that lie in the range $n \in (1, 5/4)$ and $y > 0$. Initially the orbits lie in the SSD region (see Figure 3) and then make a transition to the FSD region.

We observe the same kind of behaviour in the matter case where the phase space is however 3-dimensional, but is similarly divided into two regions, by the plane $1 = \Sigma + y + z$. The space above the plane is the SSD region and below the FSD region. Similar argument to the vacuum case can be used here to investigate the orbits. When matter is included we do however only have stable equilibrium points on $\mathcal{L}_1$ for values of n in the range $n \in (1, 5/4)$.

In conclusion we have shown that R^n- gravity modifies the dynamics of the shear in LRS Bianchi I cosmologies by altering the rate at which the shear dissipates. There are cases in which the shear always dissipate slower or faster than in GR, and there are ones which make transitions from first evolving faster and later slower (and *vice versa*) than in GR.

Chapter 4

Anisotropic cosmologies with R^n-gravity

A natural extension to the previous chapter is to investigate the effect of spatial curvature on the isotropisation in HOTG. In GR, it is well-known that spatial curvature can source anisotropies for Bianchi models [140, 146]. In this chapter we extend the analysis given in the previous chapter to the case of *orthogonal spatially homogeneous* (OSH) Bianchi models [139], in order to investigate the effect of spatial curvature on the isotropisation of R^n models. OSH Bianchi models exhibit local rotational symmetry (LRS), and include the LRS Bianchi types I (BI), III (BIII) and the Kantowski-Sachs (KS) models. For a review of this class of cosmologies see [137–139].

In GR, a cosmological constant or scalar field is required to obtain an Einstein static solution in a closed ($k = +1$) Friedmann-Lemaître-Robertson-Walker (FLRW) model [89, 147]. The existence of Gödel and Einstein static universes has been investigated for gravitational theories derived from functions of linear and quadratic contractions of the Riemann curvature tensor [148]. Recently, the stability of Einstein static models in some $f(R)$-theories of gravity was investigated [149]. It was shown that the modified Einstein static universe is stable under homogeneous perturbations, unlike its GR counterpart [150]. Static solutions are interesting in their own right, but are often an important first step in finding cosmologies that have a "bounce" during their evolution [151].

The existence conditions for a bounce to occur for FLRW universes in $f(R)$-gravity have been determined recently [152]. Bouncing cosmological models have been found for FLRW models in R^n-gravity [81, 153]. This should in principle be possible for anisotropic models as well, since the higher order corrections can mimic a cosmological constant, and so prevent the model from collapsing to a singularity. In [154], it was

shown that bounce conditions for OSH Bianchi models cannot be satisfied in GR with a scalar field, but can be satisfied for KS models in the Randall-Sundrum type Braneworld scenario.

As in chapter 3, we make use of the dynamical systems approach [88–90] in this analysis. This approach has been applied to study the dynamics of a range of extended theories of gravity [81–83, 87, 104, 105, 107–110, 155]. However, in these works, the dynamical variables were non-compact, i.e. their values did not have finite bounds. This non-compactness of the state space has certain disadvantages (see chapter 5 for detailed discussion of this issue).

While static solutions correspond to equilibrium points at infinity and can be analysed by performing a Poincaré projection [156, 157], bouncing or recollapsing behaviours on the other hand are very difficult to study in this framework. In both cases ambiguities at infinity can easily occur, since in general only the expanding copy of the state space is studied. A point at infinity may for example appear as an attractor in the expanding non–compact analysis, even though it corresponds to a bounce when also including the collapsing part of the state space.

In order to avoid these ambiguities, we will here construct compact variables that include both expanding and collapsing models, allowing us to study static solutions and bounce behaviour in R^n-theories of gravity. This approach is a generalisation of [147], which has been adapted to more complicated models in [113, 114, 117, 118].

4.1 Dynamics of OSH Bianchi cosmologies

We here consider the case $f(R) = R^n$ for OSH Bianchi spacetimes, where the Raychaudhuri equation (2.16) becomes

$$\dot{\Theta} + \tfrac{1}{3}\Theta^2 + 2\sigma^2 - \frac{1}{2n}R - (n-1)\frac{\dot{R}}{R}\Theta + \frac{\mu}{nR^{n-1}} = 0, \tag{4.1}$$

and the trace free Gauss-Codazzi equation (2.20) is given by

$$\dot{\sigma} = -\left(\Theta + (n-1)\frac{\dot{R}}{R}\right)\sigma + \frac{1}{2\sqrt{3}}{}^3R\,. \tag{4.2}$$

The Friedmann equation (2.19) is now given by

$$\tfrac{1}{3}\Theta^2 - \sigma^2 + (n-1)\frac{\dot{R}}{R}\Theta - \frac{(n-1)}{2n}R - \frac{\mu}{nR^{n-1}} + \tfrac{1}{2}\,{}^3R = 0. \tag{4.3}$$

Combining the Friedmann and Raychaudhuri equations yields

$$R = 2\dot{\Theta} + \tfrac{4}{3}\Theta^2 + 2\sigma^2 + {}^3R. \tag{4.4}$$

We will assume standard matter to behave like a perfect fluid with barotropic index w, so that the conservation equation gives

$$\dot{\mu} = -(1+w)\mu\Theta. \tag{4.5}$$

In the following, we assume $n > 0$ and $n \neq 1$.

4.1.1 Construction of the compact state space

The overall goal here is to define compact dimensionless expansion–normalised variables and a time variable τ such that the system of propagation equations above (4.1)-(4.5) can be converted into a system of autonomous first order differential equations. We choose the expansion normalised time derivative

$$' \equiv \frac{d}{d\tau} \equiv \frac{1}{D}\frac{d}{dt} \tag{4.6}$$

and make the following ansatz for our set of expansion normalised variables [1]:

$$\Sigma = \frac{\sqrt{3}\sigma}{D}\,, \qquad x = \frac{3\dot{R}\Theta}{RD^2}(1-n)\,, \quad y = \frac{3R}{2nD^2}(n-1)\,, \tag{4.7}$$
$$z = \frac{3\mu}{nR^{n-1}D^2}\,, \qquad K = \frac{{}^3R}{2D^2}\,, \qquad Q = \frac{\Theta}{D}\,.$$

Here D is a normalisation of the form

$$D = \sqrt{\Theta^2 - \Delta}\,, \tag{4.8}$$

where Δ is a linear combination of the terms appearing on the right hand side of the Friedmann equation (4.3) as discussed below. In order to maintain a monotonically increasing time variable, Δ must be chosen such that the normalisation D is real–valued and strictly positive.

Note that we have chosen to define x with an opposite sign to that in [82] in order to have a simple form of the Friedmann equation (see below), and σ can be both positive and negative [139]. We emphasise that the coordinates (4.7) are strictly speaking only defined for $R \neq 0$, which means for $y \neq 0$. Even though the case

[1] It is important to note that this choice of variables excludes GR, i.e., the case of $n = 1$. See [88,89] for the dynamical systems analysis of the corresponding cosmologies in GR.

$R = 0$ may not be of physical interest, the limiting case is interesting in the context of the stability analysis, since we obtain equilibrium points with $y = 0$. This means that the system may evolve towards/away from that singular state if these points are attractors or repellers. In the analysis below we will investigate this by taking the limit $y \to 0$ (by letting $R \to 0$) and find that this puts a constraint on the relation between the coordinates.

We now turn to the issue of compactifying the state space. It is useful to re–write the Friedmann equation (4.3) as

$$\Theta^2 = \hat{\Sigma}^2 - \hat{K} + \hat{x} + \hat{y} + \hat{z} \equiv D^2 + \Delta \,, \tag{4.9}$$

where the quantities with a hat are just the variables defined in (4.7) without the normalisation D. If all the contributions ($\hat{\Sigma}^2$, $-\hat{K}$, $\hat{x}$, $\hat{y}$ and $\hat{z}$) to the central term in equation (4.9) are non–negative, we can simply normalise with Θ^2 (i.e. $\Delta = 0$), but we have to explicitly make the assumption $\Theta \neq 0$. We can then conclude that the state space is compact, since all the non–negative terms have to add up to 1 and are consequently bounded between 0 and 1.

However, while Σ^2 is always positive, $-\hat{K}$, $\hat{x}$, $\hat{y}$ and $\hat{z}$ may be positive or negative for the class of models considered here [2]. This means that the variables (4.7) do not in general define a compact state space.

In the following, we will study the class of LRS BIII models with ${}^3R < 0$ and the class of KS models with ${}^3R > 0$ separately, as in [147]. While we may in principle normalise with Θ^2 in the Bianchi III subspace, we have to absorb the curvature term into the normalisation D in the KS subspace.

For both classes of models, we can construct a compact state space by splitting up the state space into different sectors according to the sign of $\hat{x}\,, \hat{y}$ and $\hat{z}$. In both the open and the closed subspaces we will have to define $2^3 = 8$ sectors, corresponding to the possible signs of the three variables $\hat{x}\,, \hat{y}$, $\hat{z}$. In the following, we will refer to the spatially open BIII sectors as sector 1_o to sector 8_o, where the subscript 'o' stands for 'open'. Similarly, the spatially closed KS sectors will be labeled sectors 1_c - 8_c, where the 'c' stands for 'closed'.

After defining the appropriate normalisations for the various sectors, we derive the dynamical equations for the accordingly normalised variables in each sector. For each sector we then analyse the dynamical system in the standard way: we find the equilibrium points and their eigenvalues, which determine their nature for each sector.

[2] Note that the sign of K is preserved within the open and the closed sectors.

The overall state space is then obtained by matching the different sectors along their common boundaries.

4.1.2 The LRS BIII subspace

If ${}^3R \leq 0$, we obtain the class of spatially open LRS BIII cosmologies. This class of models contains the flat LRS BI models as a subclass. In this case K enters the Friedmann equation with a non–negative sign and does not have to be absorbed into the normalisation. As can be seen from the Friedmann equation in each sector (see Table 4.1), $K \in [-1,\, 0]$ and $\Sigma \in [-1,\, 1]$ holds in each sector.

Sector 1_o

The first open sector denoted 1_o is defined to be that part of the state space where $\hat{x}\,, \hat{y},\, \hat{z} \geq 0$. In this case all the contributions to the right-hand side of (4.9) are non–negative, and we can choose $\Delta = 0$. This means we can normalise with $D = |\Theta| = \epsilon\Theta$, where ϵ is the sign function of Θ and $\epsilon = \pm 1$ for expanding/collapsing phases of the evolution. Note that it is crucial to include ϵ in the normalisation: if we were to exclude this factor, time would decrease for the collapsing models, and any results about the dynamical behaviour of collapsing equilibrium points would be time-reversed.

It is important to note that we have to exclude $\Theta = 0$ in this sector, so we cannot consider static or bouncing solutions here. However, this assumption is not as strong as it first appears: we can see from the Friedmann equation (4.9) that the only static solution in *this* sector appears for $\hat{x} = \hat{y} = \hat{z} = \hat{\Sigma} = \hat{K} = 0$, because all the quantities enter (4.9) with a positive sign in this sector by construction. This means that we only have to exclude the static flat isotropic vacuum cosmologies [3]. Under this restriction, the normalisation above is strictly positive and thus defines a monotonically increasing time variable via (4.6). Equation (4.9) now becomes

$$1 = \Sigma^2 - K + x + y + z\,. \tag{4.10}$$

We can directly see from (5.1) that the appropriately normalised variables (4.7) define a compact subsector of the total state space:

$$x,\, y,\, z \in [0, 1]\,, \quad K \in [-1, 0] \;\text{ and }\; \Sigma \in [-1, 1]\,. \tag{4.11}$$

Here $Q = \epsilon$ is constant and not a dynamical variable.

[3] The same restriction appears in GR, see [147]

This sector is different from all the other sectors in both the open BIII and the closed KS subspaces for the following reasons. When gluing together the different sectors to obtain the total state space, we will actually use two copies of 1_o: one copy with $\epsilon = 1$ corresponding to expanding cosmologies and one copy with $\epsilon = -1$ corresponding to collapsing cosmologies. The two copies are in fact disconnected: The closed sector 1_c from the KS subspace separates the expanding and collapsing copies of open sector 1_o. Again, this reflects the fact that we cannot study static solutions in sector 1_o. In all the other sectors we allow $\Theta = 0$, and the expanding and collapsing sets are connected via the non–invariant subset $Q = 0$.

We can now derive the propagation equations for the dynamical systems variables in this sector by using the definitions (4.6) and (4.7) and substituting them into the original propagation equations (4.1)-(4.5). We obtain five equations, one for each of the dynamical variables defined in (4.7). These variables are constrained by the Friedmann equation (4.9), which we use to eliminate x, resulting in a 4–dimensional state space. Note that we have to verify that the constraint is propagated using all five (unconstrained) propagation equations, which we have done for each sector. The effective system[4] is given by

$$\begin{aligned} K' &= 2\,\epsilon\,K\left[1+\Sigma^2-\tfrac{n}{n-1}\,y+\epsilon\Sigma+K\right]\,, \\ \Sigma' &= -\epsilon\,\left[\epsilon\Sigma\left(\tfrac{2n-1}{n-1}\,y+z-2K\right)-K\right]\,, \\ y' &= \frac{\epsilon\,y}{n-1}\left[z+(2n-3)K-(2n-1)y+(2n-1)\Sigma^2+4n-5\right]\,, \\ z' &= -\epsilon\,z\left[z-\Sigma^2+\tfrac{3n-1}{n-1}\,y-3K+3w-2\right]\,. \end{aligned} \tag{4.12}$$

Only in this sector does the sign of the expansion–rate appears directly in the dynamical equations, and we can see directly that the stability of the collapsing equilibrium points is given by simple time-reversal of the stability of the expanding points and vice versa.

The subset $K = 0$ (Bianchi I) is a two dimensional invariant sub–manifold, so it is justified to discuss the Bianchi I subspace on its own. This is done in detail in [158]. The vacuum subset $z = 0$ and the submanifold $y = 0$ are also invariant subspaces. On the other hand, the isotropic subset $\Sigma = 0$ is not invariant unless $K = 0$. This agrees with GR, where it was found that the spatial curvature can source anisotropies for Bianchi models [140, 146].

[4]If we used the unconstrained 5–dimensional system, we would not constrain the allowed ranges of n and w for the different equilibrium points correctly. We would also get a fifth zero–valued eigenvalue for all equilibrium points.

We can find the equilibrium points and the corresponding eigenvalues of the dynamical system (4.12), and classify the equilibrium points according to the sign of their eigenvalues as attractors, repellers and saddle points (see [157]). Because of the large number of sectors that need to be studied, we do not show the results for each sector. Instead we combine the results from the various sectors in Table 4.2.

Sectors $2_o - 8_o$

Sectors $2_o - 8_o$ are defined according to the possible signs of $\hat{x}$, $\hat{y}$, $\hat{z}$ as summarised in Table 4.1. In each sector Δ is defined as the sum of the strictly negative contributions to (4.9), so that $-\Delta$ is strictly positive, making D strictly positive even for $\Theta = 0$. This means that D is a well–defined (non-zero) normalisation, and (4.6) defines a well-defined *monotonously increasing* time variable for each sector, even for static or bouncing solutions. With this choice of normalisation, only positive contributions

Table 4.1: Choice of normalisation in the different LRS Bianchi III sectors, where the subscripts in the sector labels stand for open, differentiating the labels for the open sectors from the ones defined in the closed KS subspace below. We abbreviate $\hat{x} \equiv (1-n)\dot{R}\Theta/R$, $\hat{y} \equiv (1-n)R/n$ and $\hat{z} \equiv \mu/(nR^{n-1})$.

sector	$\hat{x}$	$\hat{y}$	$\hat{z}$	normalisation	Friedmann equation	range of (x, y, z)
1_o	≥ 0	≥ 0	≥ 0	$\Delta = 0$	$1 = x + y + z + \Sigma^2 - K$	$[\,0,\,1] \times [\,0,\,1] \times [\,0,\,1]$
2_o	< 0	> 0	> 0	$\Delta = \hat{x}$	$1 = y + z + \Sigma^2 - K$	$[-1, 0] \times [\,0,\,1] \times [\,0,\,1]$
3_o	> 0	< 0	> 0	$\Delta = \hat{y}$	$1 = x + z + \Sigma^2 - K$	$[\,0,\,1] \times [-1, 0] \times [\,0,\,1]$
4_o	> 0	> 0	< 0	$\Delta = \hat{z}$	$1 = x + y + \Sigma^2 - K$	$[\,0,\,1] \times [\,0,\,1] \times [-1, 0]$
5_o	< 0	< 0	> 0	$\Delta = \hat{x} + \hat{y}$	$1 = z + \Sigma^2 - K$	$[-1, 0] \times [-1, 0] \times [\,0,\,1]$
6_o	< 0	> 0	< 0	$\Delta = \hat{x} + \hat{z}$	$1 = y + \Sigma^2 - K$	$[-1, 0] \times [\,0,\,1] \times [-1, 0]$
7_o	> 0	< 0	< 0	$\Delta = \hat{y} + \hat{z}$	$1 = x + \Sigma^2 - K$	$[\,0,\,1] \times [-1, 0] \times [-1, 0]$
8_o	< 0	< 0	< 0	$\Delta = \hat{x} + \hat{y} + \hat{z}$	$1 = \Sigma^2 - K$	$[-1, 0] \times [-1, 0] \times [-1, 0]$

remain in the Friedmann equation, and the appropriately normalised variables define a compact sub–sector of the total state- space, as can be seen from the respective versions of the Friedmann equation in Table 4.1. Note that the Friedmann equation looks different in each sector, which is of course due to the different normalisation for each sector. We also gain a second constraint equation which arises from the definition of Q:

$$1 = Q^2 - \frac{\Delta}{D^2}\,, \tag{4.13}$$

which can be written in terms of the variables (4.7) in each sector.

It is straightforward to derive the dynamical equations for each sector, and again

we analyse them as outlined in the previous subsection. We confirm in each sector that the flat LRS BI subset is indeed an invariant submanifold.

Equilibrium points of the full LRS BIII state space

The equilibrium points of the entire BIII state space are obtained by combining the equilibrium points in each sector. We summarise them in Table 4.2. Note that not all the points occur in all of the sectors, and some points only occur in a given sector for certain ranges of n or a specific equation of state w. For this reason, we cannot express all the equilibrium points in terms of the same variables. When possible we state the coordinates in terms of the dimensionless variables defined for sector 1_o, i.e if the given point occurs in this sector. This is true for all the points except the line $\mathcal{L}_2$, whose coordinates are described in terms of the variables defined in sector 2_o (see below for more details on the relation between $\mathcal{L}_1$ and $\mathcal{L}_2$).

We emphasise that if the same point occurs in different sectors, it will have different coordinates in each of these sectors. In particular, Q can be a function of n or w in sectors $2_o - 8_o$ even if $Q = \epsilon$ is a constant in sector 1_o. This simply reflects the fact that we have to exclude the static solutions in sector 1_o but not in the other sectors. This issue will be of importance when looking for static solutions in section 4.1.4. In order to ensure that equilibrium points obtained in different sectors correspond to the same solution, we have to look at the exact solution at these points. This is outlined in section 4.1.4.

Note that each of the isolated equilibrium points has an expanding ($\epsilon = 1$) and a collapsing ($\epsilon = -1$) version as indicated in the labeling of the points via the subscript ϵ in Table 4.2. Similarly, the lines each have an expanding and a contracting branch (see below). We will however drop the subscript in the following unless we explicitly address an expanding or contracting solution.

We find the three equilibrium points $\mathcal{A}$, $\mathcal{B}$ and $\mathcal{C}$ corresponding to spatially flat Friedmann cosmologies. The expanding versions of these points correspond to the equally labeled points in the BI analysis [82] (see [158] for detailed comparison). These points were also found in the Friedmann analysis [87]. $\mathcal{A}$ and $\mathcal{B}$ are vacuum Friedmann points, while $\mathcal{C}$ represents a non-vacuum Friedmann point whose scale factor evolution resembles the well known Friedmann-GR perfect fluid solution with $a \propto t^{\frac{2}{3(1+w)}}$.

We now address the two lines of equilibrium points denoted by $\mathcal{L}_1$ and $\mathcal{L}_2$. Both these lines correspond to the spatially flat anisotropic BI cosmologies. The ratio of shear Σ and curvature component x changes as we move along both lines. We note

that in [82] a single line of equilibrium points denoted $\mathcal{L}_1^*$ was found. In section 4.1.6 we will discuss in more detail how $\mathcal{L}_1$ and $\mathcal{L}_2$ are related to $\mathcal{L}_1^*$.

We emphasise that for $\mathcal{L}_1$ the two expanding and contracting branches are disconnected and appear as two copies $\mathcal{L}_{1,\epsilon}$ of the line labeled by ϵ in Table 4.2. Each of these two branches range from purely shear dominated ($\Sigma = 1$) to isotropic ($\Sigma = 0$), to purely shear dominated with opposite orientation ($\Sigma = -1$). For $\mathcal{L}_2$ on the other hand the expanding and contracting branches are connected: each $\mathcal{L}_{2,+}$ and $\mathcal{L}_{2,-}$ ranges from expanding ($Q_* > 0$) and static ($Q_* = 0$) to collapsing ($Q_* < 0$). The two disconnected copies $\mathcal{L}_{2,+}$ and $\mathcal{L}_{2,-}$ correspond to positive and negative values of the shear respectively. Note that there is no isotropic subset of $\mathcal{L}_2$ in analogy to the fact that there is no static subset of $\mathcal{L}_1$.

A closer look shows that $\mathcal{L}_1$ and $\mathcal{L}_2$ are actually the same object in different sectors: $\mathcal{L}_1$ has $\hat{x} \geq 0$ hence occurs in sectors 1_o, 3_o, 4_o and 7_o, while $\mathcal{L}_2$ is the analog with $\hat{x} < 0$ occurring in sectors 2_o, 5_o, 6_o and 8_o. This statement is confirmed by looking at the exact solutions corresponding to the points on both lines; we find that both these lines have the same parametric solution of scale factor and shear (see section below). For this reason, we could in fact give the two lines the same label. However, it is useful to treat them separately, since we obtain different bifurcations in the sectors with $\hat{x} > 0$ and $\hat{x} < 0$ respectively. Furthermore, the subset of the line denoted by $\mathcal{L}_2$ allows for static solutions unlike the subset labeled $\mathcal{L}_1$. This is due to the fact that a negative curvature contribution $\hat{x}$ can effectively act as a cosmological constant by counter–balancing other contributions in the Friedmann equation. This is explored in section 4.1.4 below.

Finally, we find the equilibrium points $\mathcal{D}$ and $\mathcal{E}$ corresponding to spatially open models. Point $\mathcal{D}$ is independent of n and w, while $\mathcal{E}$ depends on the value of w. The points $\mathcal{F}$ and $\mathcal{G}$ can be spatially open, flat or closed depending on the value of n and/or w, i.e. they move through the different sectors of the total state space as n, w are varied. This is reflected in Tables 4.9 and 4.10, where we summarise the stability properties of the equilibrium points of the closed and open subspaces separately, and observe that these two points occur in each subspace for certain ranges of n only.

4.1.3 The Kantowski-Sachs subspace

When ${}^3R > 0$, we obtain the class of spatially closed KS cosmologies. Here $\hat{K}$ is positive and needs to be absorbed into the normalisation in all sectors. This means that in this subspace, $-\Delta$ is strictly positive in all closed subsectors 1_c - 8_c, hence D^2 is strictly positive even for $\Theta = 0$. We can therefore consider static and bouncing

Table 4.2: Equilibrium points of the full OSH Bianchi state space in terms of the coordinates defined for sector 1_0, except for the line $\mathcal{L}_{2,\pm}$, where we have to use the coordinates defined for BIII sector 2_o (see text). Here $\epsilon = \pm 1$ labels the expanding/contracting solutions. We have abbreviated $f(w) = \frac{-3(3w^2-3w+1)}{(3w-2)^2}$, $P_1(n) = 2n^2 - 2n - 1$ and $P_2(n) = 2n^2 - 5n + 5$. We will not explicitly state the expressions for $R_1(n,w), ..., R_4(n,w)$, which are rational functions of n and w. The constants $Q_*,\ \Sigma_*$ take real values in $[-1,\ 1]$. We have denoted the coordinates Q that can become non-constant in sectors other than the first sector with the superscript †.

Point	(Q, K, Σ, x, y, z)	Description
$\mathcal{A}_\epsilon$	$\left(\epsilon^\dagger,\ 0,\ 0,\ \frac{2(2-n)}{2n-1},\ \frac{4n-5}{2n-1},\ 0\right)$	Friedmann flat
$\mathcal{B}_\epsilon$	$\left(\epsilon^\dagger,\ 0,\ 0,\ 3w-1,\ 0,\ 2-3w\right)$	Friedmann flat
$\mathcal{C}_\epsilon$	$\left(\epsilon^\dagger,\ 0,\ 0,\ \frac{3(n-1)(1+w)}{n},\ \frac{(n-1)[4n-3(1+w)]}{2n^2}\right.$ $\left., \frac{n(13+9w)-2n^2(4+3w)-3(1+w)}{2n^2}\right)$	Friedmann flat
Line $\mathcal{L}_{1,\epsilon}$	$\left(\epsilon,\ 0,\ \Sigma_*,\ 1-\Sigma_*^2, 0, 0\right)$	flat LRS Bianchi I
Line $\mathcal{L}_{2,\pm}$	$\left(Q_*,\ 0,\ \pm 1,\ Q_*^2-1, 0, 0\right)$	flat LRS Bianchi I
$\mathcal{D}_\epsilon$	$(\epsilon,\ -3/4,\ -\epsilon/2,\ 0,\ 0,\ 0)$	open LRS BIII
$\mathcal{E}_\epsilon$	$\left(\epsilon^\dagger,\ f(w),\ \frac{\epsilon}{3w-2},\ 3w\frac{3w-1}{3w-2},\ 0,\ 3w\, f(w)\right)$	open LRS BIII
$\mathcal{F}_\epsilon$	$\left(\epsilon^\dagger,\ \frac{3(4n^2-10n+7)P_1(n)}{P_2(n)^2}, \epsilon\frac{P_1(n)}{P_2(n)},\ \frac{6(n^2-3n+2)}{P_2(n)}\right.$ $\left., \frac{9(4n^4-18n^3+31n^2-24n+7)}{P_2(n)^2},\ 0\right)$	vacuum BI, BIII or KS
$\mathcal{G}_\epsilon$	$\left(\epsilon^\dagger,\ R_1(n,w),\ \epsilon R_2(n,w),\ \frac{3(n-1)(1+w)}{n},\ R_3(n,w)\right.$ $\left.,\ R_4(n,w)\right)$	BI, BIII or KS

solutions in all sectors that make up the closed subspace. The flat subspace is obtained in the limit ${}^3R \to 0$. As explained in the previous subsection, we have to exclude static flat isotropic vacuum cosmologies in this limit.

The closed sectors can be defined as in the BIII case, except that K no longer appears in the Friedmann equation (see Table 4.3). Similar to the BIII case, the first sector labeled 1_c is defined as the subset of the state space where $\hat{x}\,, \hat{y},\, \hat{z} \geq 0$. In this case we choose $\Delta = -\hat{K}(< 0)$, so that equation (4.9) becomes

$$1 = \Sigma^2 + x + y + z\,. \tag{4.14}$$

The curvature can be obtained from (4.13), which in this sector becomes

$$1 = Q^2 + K. \tag{4.15}$$

From (4.14) and (4.15) it is clear that the appropriately normalised variables (4.7) define a compact subsector of the total state space with

$$x,\, y,\, z \in [0,1]\,, \quad K \in [0,1] \;\text{ and }\; Q,\, \Sigma \in [-1,1]\,. \tag{4.16}$$

Note that the variable K will not be used explicitly in any of the closed sectors.

As in the BIII case, we derive the propagation equations for the dynamical systems variables in this sector and reduce the dimensionality of the state space to four by eliminating x via the Friedmann constraint (4.14). Again we have verified that the constraint is preserved using all five propagation equations. We obtain the following dynamical system:

$$\begin{aligned}
Q' &= \frac{1}{3}(Q^2-1)\left[1 + Q\Sigma + \Sigma^2 - \frac{ny}{n-1}\right], \\
\Sigma' &= \frac{\Sigma}{3Q}\left[Q^2\left(\Sigma^2 - 1 - \frac{ny}{n-1}\right) + 1 - \Sigma^2 - y - z\right] + \frac{1}{3}(\Sigma^2-1)(Q^2-1)\,, \\
y' &= \frac{y}{3Q}\left[2\Sigma Q(Q^2-1) - \frac{1}{n-1}(1-\Sigma^2-y-z) + 2Q^2\left(2 + \Sigma^2 - \frac{ny}{n-1}\right)\right], \\
z' &= \frac{z}{3Q}\left[2\Sigma Q(Q^2-1) + 1 - \Sigma^2 - y - z + Q^2\left(1 - 3w + 2\Sigma^2\frac{-2ny}{n-1}\right)\right].
\end{aligned} \tag{4.17}$$

We recover the following features from the BIII subspace: The flat subset $K = 0$ (here corresponding to $Q^2 = 1$) is invariant, as can be seen from the Q'-equation together with the Friedmann equation (4.14). Other invariant subspaces are the hyper-surfaces $y = 0$ and $z = 0$. The isotropic subset $\Sigma = 0$ is not invariant unless $K = 0$.

The sectors 2_c-8_c are defined according to the possible signs of $\hat{x}$, $\hat{y}$, $\hat{z}$ as sum-

Table 4.3: Choice of normalisation in different KS sectors, where the subscripts in the sector labels stand for closed. See text and caption of Table 4.1 for details on the notation used here.

sector	$\hat{x}$	$\hat{y}$	$\hat{z}$	normalisation	Friedmann equation	range of (x, y, z)
1_c	≥ 0	≥ 0	≥ 0	$\Delta = -\hat{K}$	$1 = x + y + z + \Sigma^2$	$[\,0,\,1] \times [\,0,\,1] \times [\,0,\,1]$
2_c	< 0	> 0	> 0	$\Delta = \hat{x} - \hat{K}$	$1 = y + z + \Sigma^2$	$[-1, 0] \times [\,0,\,1] \times [\,0,\,1]$
3_c	> 0	< 0	> 0	$\Delta = \hat{y} - \hat{K}$	$1 = x + z + \Sigma^2$	$[\,0,\,1] \times [-1, 0] \times [\,0,\,1]$
4_c	> 0	> 0	< 0	$\Delta = \hat{z} - \hat{K}$	$1 = x + y + \Sigma^2$	$[\,0,\,1] \times [\,0,\,1] \times [-1, 0]$
5_c	< 0	< 0	> 0	$\Delta = \hat{x} + \hat{y} - \hat{K}$	$1 = z + \Sigma^2$	$[-1, 0] \times [-1, 0] \times [\,0,\,1]$
6_c	< 0	> 0	< 0	$\Delta = \hat{x} + \hat{z} - \hat{K}$	$1 = y + \Sigma^2$	$[-1, 0] \times [\,0,\,1] \times [-1, 0]$
7_c	> 0	< 0	< 0	$\Delta = \hat{y} + \hat{z} - \hat{K}$	$1 = x + \Sigma^2$	$[\,0,\,1] \times [-1, 0] \times [-1, 0]$
8_c	< 0	< 0	< 0	$\Delta = \hat{x} + \hat{y} + \hat{z} - \hat{K}$	$1 = \Sigma^2$	$[-1, 0] \times [-1, 0] \times [-1, 0]$

marised in Table 4.3: In each sector Δ is defined as the sum of the strictly negative contributions to (4.9). The dynamical equations analogous to (4.17) can be derived straightforwardly for each sector. We then solve these equations in each sector for their respective equilibrium points and the corresponding eigenvalues, and classify the equilibrium points according to their dynamical properties. The results are combined with the results from the open sectors and summarised in Tables 4.6–4.10.

4.1.4 Exact solutions corresponding to the equilibrium points

We now derive the solutions corresponding to the various equilibrium points. Special attention has to be paid to the points with $y = 0$, since these correspond to the limit $R \to 0$, which may make the coordinate x singular. We will study this issue in detail below. Note that it is legitimate to take the limit $R \to 0$ in the original field equations as long as $n > 1$, which results in the constraint $T^M_{ab} \to 0$. Consequently it is only possible to study the limit $R \to 0$ for $\mu \to 0$ and $n > 1$ when solving for the solutions corresponding to the equilibrium points with $y = 0$.

It is important to emphasise that the dynamical system by itself is well-defined for $y = 0$; only when going back to the original equations to solve for the exact solutions corresponding to the equilibrium points with $y = 0$ do we notice that there may not be an exact solution corresponding to these coordinates.

We now proceed to find the exact solutions corresponding to the non–static ($\Theta\,, Q \neq 0$) equilibrium points. As usual, we can solve the energy conservation equation (4.5) for the non–vacuum solutions to obtain

$$\mu = \mu_0\, a^{-3(1+w)}\,, \tag{4.18}$$

where μ_0 is determined by the z-coordinate of the given equilibrium point. We require $\mu_0 \geq 0$, which constrains the allowed range of n or w for a given equilibrium point (see below).

In order to determine the scale factor evolution at each equilibrium point, we rewrite the Raychaudhuri equation (4.1) as

$$\dot{\Theta} = -\left(1 + q_i\right) \frac{\Theta^2}{3}\,, \tag{4.19}$$

where we express the deceleration parameter q_i at each point in terms of the dimensionless variables (4.7):

$$q_i = 2\frac{\Sigma_i^2}{Q_i^2} + \frac{x_i}{Q_i^2} - \frac{y_i}{(n-1)Q_i^2} + \frac{z_i}{Q_i^2}\,. \tag{4.20}$$

Note that this equation is invariant in different sectors: for a given equilibrium point, each coordinate divided by Q^2 is the same in all sectors. This ensures that the corresponding solution is invariant, no matter with which coordinates we describe the equilibrium point.

Similarly, we re–write the trace free Gauss Codazzi equation (4.2) as

$$\dot{\sigma} = -\frac{1}{\sqrt{3}Q_i^2}\left[\left(Q_i - \frac{x_i}{3Q_i}\right)\Sigma_i - \frac{K_i}{3}\right]\,\Theta^2, \tag{4.21}$$

and the curvature constraint (4.4) as

$$R = \frac{2}{3}\Theta^2\left[1 - q_i + \frac{\Sigma_i^2}{Q_i^2} - \frac{K_i}{Q_i^2}\right] \tag{4.22}$$

for a given equilibrium point with coordinates $(Q_i, K_i, \Sigma_i, x_i, y_i, z_i)$ and deceleration parameter q_i.

Power-law solutions

We first study the non–stationary ($q \neq -1$) cosmologies, for which (4.19) has the solution

$$\Theta = \frac{3}{\left(1 + q_i\right) t}\,. \tag{4.23}$$

We have set the Big Bang time $t_0 = 0$. Given Θ, we can solve for all the other dynamical quantities for a given equilibrium point to obtain the scale factor evolution

$$a = a_0\,|t|^{\alpha}, \quad \text{where} \quad \alpha = \left(1 + q_i\right)^{-1}\,, \tag{4.24}$$

the shear

$$\sigma = \frac{\beta}{t} + const\,, \quad \text{where} \;\; \beta = \frac{\sqrt{3}}{(1+q_i)^2}\left[\frac{\Sigma_i}{Q_i}\left(3 - \frac{x_i}{Q_i^2}\right) - \frac{K_i}{Q_i^2}\right]\,, \tag{4.25}$$

and the curvature scalar

$$R = \frac{\gamma}{t^2}\,, \quad \text{where} \;\; \gamma = \frac{6}{(1+q_i)^2}\left[1 - q_i + \frac{\Sigma_i^2}{Q_i^2} + \frac{K_i}{Q_i^2}\right]\,. \tag{4.26}$$

Again, we point out that even though a given equilibrium point formally has different coordinates in the different sectors, the exact solutions corresponding to the point are invariant, since the coordinates only enter the solutions (4.24)–(4.26) with a factor $1/Q_i^2$. The solutions for each point are summarised in Table 4.4, where constants of integration were obtained by substituting the solutions into the original equations.

When substituting the points with $y = 0$ into the original field equations, we find that these are only satisfied for special values of n. This is reflected in Table 4.4. Point $\mathcal{B}$ only has a solution for $n = 5/4$ and $w = 2/3$. The solutions for points $\mathcal{D}$ and $\mathcal{E}$ only satisfy the original equations for $n = 1$, which has been excluded from the start. These points therefore do not have any physical power–law solutions. The points on the lines $\mathcal{L}_{1,2}$ only have corresponding solutions for special coordinate values, making only two points on each line physical (see below).

Excluding these non-physical points, we find that the only non–vacuum solutions are given by $\mathcal{C}$ and $\mathcal{G}$. Substituting the solution (4.18) into the definition of z, we find that the constant μ_0 must satisfy

$$\mu_0 \;\; = \;\; z_i y_i^{n-1}\left(\frac{\alpha}{Q_i}\right)^{2n}(3n)^n\left(\frac{2}{n-1}\right)^{n-1}\,.$$

In order for these solutions to be physical, we require that $\mu > 0$ and therefore $\mu_0^i > 0$. For $\mathcal{C}$ we find that this condition is satisfied for

$$1 < n < \frac{1}{4(4+3w)}\left(13 + 9w + \sqrt{9w^2 + 66w + 73}\right)\,, \quad w > -1, \tag{4.27}$$

while for $\mathcal{G}$ it is only valid for

$$\begin{cases} 1 < n < N_+\,, & -1 < w \leq 0\;\,, \\ N_- < n < N_+\,, & 0 < w < \frac{1}{15}(-15 + 4\sqrt{15})\;\,, \end{cases} \tag{4.28}$$

where $N_\pm = \frac{1}{4(2+w)}\left(9 + 5w \pm \sqrt{1 - 30w - 15w^2}\right)$.

For points $\mathcal{A}$ and $\mathcal{F}$ the solutions only depend on n, while the solutions at $\mathcal{C}$ and $\mathcal{G}$ depend on both n and w. We can see from these solutions that points $\mathcal{A}$ and $\mathcal{C}$ are the isotropic analogs of points $\mathcal{F}$ and $\mathcal{G}$ respectively.

The lines $\mathcal{L}_1$ and $\mathcal{L}_2$ have the same solutions for shear and energy density. As noted above, they are the same line but for different ranges of $\hat{x}$ and hence α. $\mathcal{L}_1$ contains the isotropic subset of solutions ($\Sigma_* = 0$) while $\mathcal{L}_2$ contains the static subset ($\alpha = Q_* = 0$).

In Table 4.5 we summarise the behaviour of the deceleration parameter q. By studying the deceleration parameter, we can determine whether the power law solutions above correspond to accelerated ($-1 < q < 0$) or decelerated ($q > 0$) expansion or contraction. The expansion (or contraction) of point $\mathcal{A}$ is decelerating for $n \in (0, 1/2)$ or $n \in (1, \frac{1}{2}(1+\sqrt{3}))$ and accelerating for $n \in (\frac{1}{2}(1+\sqrt{3}), 2)$. Point $\mathcal{B}$ and lines $\mathcal{L}_{1,2}$ only admit decelerating behaviours. Point $\mathcal{F}$ has a decelerated behaviour for $n \in (0, \frac{1}{2}(1+\sqrt{3}))$ and an accelerated behaviour for $n \in (\frac{1}{2}(1+\sqrt{3}), 2)$. The equilibrium points $\mathcal{C}$ and $\mathcal{G}$ for $w \in [0, 1]$, have decelerated behaviours when $n \in (0, \frac{3}{2}(1+w))$ and accelerated behaviours when $n \in (\frac{3}{2}(1+w), \infty)$.

Stationary solutions

If $q = -1$, we obtain stationary solutions ($\dot{\Theta} = 0$), which have an exponentially increasing scale factor. As reflected in Table 4.5, the vacuum points $\mathcal{A}$ and $\mathcal{F}$ correspond to de Sitter solutions for the bifurcation value $n = 2$ for all equations of state, while the matter points $\mathcal{C}$ and $\mathcal{G}$ are de Sitter–like for all $n > 0$ but $w = -1$ only, and $\mathcal{E}$ appears to be de Sitter–like for $w = 1$ for all values of $n > 0$. Since $\mathcal{E}$ has $y = 0$, we will have to study this case in more detail below.

For a constant expansion rate

$$\Theta = \Theta_0 \,, \tag{4.29}$$

the scale factor has the following solution

$$a = a_0 \; e^{\frac{1}{3}\Theta_0 t}. \tag{4.30}$$

The energy conservation equation becomes

$$\dot{\mu} = 0 \Rightarrow \mu = \mu_0 \,. \tag{4.31}$$

The trace free Gauss Codazzi equation (4.2) can be rewritten as

$$\dot{\sigma} = \beta_0, \quad \text{where} \quad \beta_0 = \frac{\Theta_0^2}{3\sqrt{3}Q_i^2}\left[K_i - \left(3Q_i - \frac{x_i}{Q_i}\right)\Sigma_i\right], \tag{4.32}$$

which on integration yields

$$\sigma = \beta_0 t + \sigma_0 \ , \tag{4.33}$$

where σ_0 is an integration constant. The evolution of the Ricci scalar can be obtained by substituting the solutions above into (4.4), to find

$$R = \frac{2}{3}\left(2 + \frac{K_i}{Q_i^2}\right)\Theta_0^2 + 2(\beta_0 t + \sigma_0)^2. \tag{4.34}$$

As before, we substitute the solutions at each equilibrium point into the definition of the coordinates, which constrains the constants of integration for each point. In particular, $\beta_0 = 0$ holds for all stationary equilibrium points, which means that we only have constant or vanishing shear.

As in the power–law case, we see that all the equilibrium points except for $\mathcal{C}$ and $\mathcal{G}$ correspond to vacuum solutions $\mu = 0$. For point $\mathcal{C}$ the energy density is given by

$$\mu = \mu_1^{\mathcal{C}} = 4^{n-1}3^{-n}(2-n)\Theta_0^{2n}, \tag{4.35}$$

and for $\mathcal{G}$ the energy density is given by

$$\mu = \mu_1^{\mathcal{G}} = 4^{n-1}(2-n)\Theta_0^{2n}. \tag{4.36}$$

Both of these solutions only hold for $1 < n \leq 2$ with $w = -1$.

Again, we substitute the generic solutions into the original field equations for each point, and find that the original equations are satisfied for all points with $y \neq 0$. It is however not possible to find a stationary solution at point $\mathcal{E}$ (which has $y = 0$), even after carefully considering the limit $y \to 0$.

Static solutions

The static equilibrium points are characterised by $\Theta = \dot{\Theta} = 0$. These points satisfy $Q = x = 0$, where the second identity comes from the fact that if $Q = 0$, then we require that $x = 0$ from the definition of the variables, as discussed below. [5]

We will now explore which of the equilibrium points obtained above correspond to static solutions. As indicated above, even though $Q = \pm\epsilon$ holds in the first sector as stated in Table 4.2, Q can be a function of n and/or w in the other sectors. In order to find the static equilibrium points, we have to look at the coordinates that

[5] Note that unlike in the bouncing or recollapsing case below, we do not consider $Q = y = 0,\ x \neq 0$ here, since this corresponds to the limit $R \to 0$. While we may want to study a bounce where the Ricci scalar approaches zero and then grows again, we are not interested in static solutions that have vanishing Ricci curvature at *all* times.

each equilibrium point takes in each sector, and find the values of n and/or w for which $Q = 0$ in the given sector.

An obvious static solution appears to be the subset $Q = 0$ on line $\mathcal{L}_{2,\pm}$ for all values of n and w. We can however not find a solution corresponding to this limit, since $Q_* = 0$ implies $\sigma = 0$, which contradicts the value of the shear coordinate of this equilibrium point. We can study the eigenvalues associated with the line $\mathcal{L}_2$ in the limit $Q \to 0^{\pm}$ and find that the static subset is an unstable saddle point for all values of n for both $\mathcal{L}_{2,+}$ and $\mathcal{L}_{2,-}$.

The point $\mathcal{A}$ appears to admit a static solution for the bifurcation value $n = 1/2$. This bifurcation only occurs in sectors 2, 3, 6 and 7 of the open and the closed sectors. However, it is not possible to find a solution satisfying the coordinates of the static equilibrium point that satisfies the original field equations. For this reason, this static equilibrium point is unphysical. We explore the stability of the static solution in the limit $n \to 1/2$ from the appropriate sides: for example, point $\mathcal{A}$ only lies in the open sector 2 for $n \in [0,\, 1/2]$ or $n \in [2,\, \infty]$, making only the limit $n \to 1/2^{-}$ well-defined. We find that this bifurcation represents a saddle point in the state space since two of the eigenvalues approach ∞ from the left and $-\infty$ from the right, making the point unstable.

Even though the Q–coordinate of point $\mathcal{B}$ is a function of w in sectors 2, 4, 5 and 7, Q cannot be zero for any values of w. This means point $\mathcal{B}$ does not admit any static solutions.

Point $\mathcal{C}$ can only be static in the limit $n \to 0$ in sector 6 for $w = 0,\, 1/3,\, 1$ and in sector 3 and 5 for $w = -1$. Again, we cannot find a solution for this special case, but this case is physically not interesting either way.

The Q–coordinate of point $\mathcal{E}$ is zero in sectors 6-8 for $w = 2/3$, but again there is no solution corresponding to this limit.

Even though point $\mathcal{F}$ has Q as a function of n in open sectors 2 and 6, $Q(n)$ is non–zero for the allowed ranges of n.

Point $\mathcal{G}$ becomes static in the limit $n \to 0$ in sectors 4, 6 and 8, which again is not physically relevant.

4.1.5 The full state space

The full state space is obtained by matching the various sectors along their common boundaries. Because the full state space is 4–dimensional it is not easily visualised, so we refer to [158] for an illustration of the 2–dimensional Bianchi I vacuum subspace and the 2–dimensional flat FLRW subspace with matter. We emphasise that we have

Table 4.4: Solutions for scale factor, shear, curvature and energy density corresponding to the equilibrium points.

Point		Scale factor (a)	Shear (σ)	Ricci Scalar (R)	μ
$\mathcal{A}$	$\begin{cases} n \neq 2 \\ n = 2 \end{cases}$	$\begin{cases} a_0\lvert t\rvert^{\frac{(1-n)(2n-1)}{(n-2)}} \\ a_0 e^{\frac{1}{3}\Theta_0 t} \end{cases}$	0	$\begin{cases} \frac{6n(1-n)(2n-1)(4n-5)}{(n-2)^2t^2} \\ \frac{4}{3}\Theta_0^2 \end{cases}$	0
$\mathcal{B}$	$n=\frac{5}{4},\ w=\frac{2}{3}$	$a_0\lvert t\rvert^{\frac{1}{2}}$	0	0	0
$\mathcal{C}$	$\begin{cases} w \neq -1 \\ w = -1 \end{cases}$	$\begin{cases} a_0\lvert t\rvert^{\frac{2n}{3(1+w)}} \\ a_0 e^{\frac{1}{3}\Theta_0 t} \end{cases}$	0	$\begin{cases} \frac{4n(4n-3(1+w))}{3(1+w)^2t^2} \\ \frac{4}{3}\Theta_0^2 \end{cases}$	$\begin{cases} \mu_0^{\mathcal{C}}\ t^{-2n} \\ \mu_1^{\mathcal{C}} \end{cases}$
$\mathcal{F}$	$\begin{cases} n \neq 2 \\ n = 2 \end{cases}$	$\begin{cases} a_0\lvert t\rvert^{\frac{(2n^2-5n+5)}{3(2-n)}} \\ a_0 e^{\frac{1}{3}\Theta_0 t} \end{cases}$	$\begin{cases} \frac{(1+2n-2n^2)}{\sqrt{3}(n-2)t} \\ \frac{1}{\sqrt{3}}\Theta_0 \end{cases}$	$\begin{cases} \frac{6n(1-n)(4n^2-10n+7)}{(n-2)^2t^2} \\ \frac{10}{3}\Theta_0^2 \end{cases}$	0
$\mathcal{G}$	$\begin{cases} w \neq -1 \\ w = -1 \end{cases}$	$\begin{cases} a_0\lvert t\rvert^{\frac{2n}{3(1+w)}} \\ a_0 e^{\frac{1}{3}\Theta_0 t} \end{cases}$	$\begin{cases} \frac{(3(1+w)-2n)}{\sqrt{3}(1+w)t} \\ \frac{1}{\sqrt{3}}\Theta_0 \end{cases}$	$\begin{cases} \frac{4n(2(n-1)+w(1+3w-2n))}{(1+w)^2t^2} \\ \frac{10}{3}\Theta_0^2 \end{cases}$	$\begin{cases} \mu_0^{\mathcal{G}}\ t^{-2n} \\ \mu_1^{\mathcal{G}} \end{cases}$
Line					
$\mathcal{L}_1$	$\begin{cases} \Sigma_*^2 = \frac{5-4n}{2n-1} \\ n \in (1, \frac{5}{4}) \end{cases}$	$a_0\lvert t\rvert^{\frac{1}{2+\Sigma_*^2}}$	$\frac{\sqrt{3}\lvert\Sigma_*\rvert}{(2+\Sigma_*^2)t}$	0	0
$\mathcal{L}_2$	$\begin{cases} Q_*^2 = \frac{2n-1}{5-4n} \\ n \in (\frac{1}{2}, 1) \end{cases}$	$a_0\lvert t\rvert^{\frac{Q_*^2}{1+2Q_*^2}}$	$\frac{\sqrt{3}\lvert Q_*\rvert}{(1+2Q_*^2)t}$	0	0

Table 4.5: Deceleration parameter for the equilibrium points. In the last three columns we state explicitly for which values of n the deceleration parameter q (stated in the second column) is less, equal to or larger than 0, i.e. whether the have accelerated, de–Sitter–like or decelerated behaviours. The parameters are $P_+ = \frac{1}{2}(1+\sqrt{3})$ and $S_w = \frac{3}{2}(1+w)$.

			$q=-1$	$-1<q<0$	$q>0$
Point	q	w	Range of n		
$\mathcal{A}$	$\frac{1+2n-2n^2}{1-3n+2n^2}$	all	2	$(P_+, 2)$	$\begin{cases} (0, \frac{1}{2}) \\ (1, P_+) \end{cases}$
$\mathcal{B}$	1	all	-	-	$(0, \infty)$
$\mathcal{C}$	$\frac{3(1+w)-2n}{2n}$	-1	$(0, \infty)$	-	-
		$[0, 1]$	-	(S_w, ∞)	$(0, S_w)$
$\mathcal{F}$	$\frac{1+2n-2n^2}{5-5n+2n^2}$	all	-	$(P_+, 2)$	$(0, P_+)$
$\mathcal{G}$	$\frac{3(1+w)-2n}{2n}$	-1	$(0, \infty)$	-	-
		$[0, 1]$	-	(S_w, ∞)	$(0, S_w)$
Line					
$\mathcal{L}_1$	$1+\Sigma_*^2$	all	-	$(0, \infty)$	-
$\mathcal{L}_2$	$1+\frac{1}{Q_*^2}$	all	-	$(0, \infty)$	-

to formally exclude the subset with $Q = 0$ and $x \neq 0$ from the state space unless $y \to 0$. This is an artifact of the definition of the variable x, and reflected by the fact that there are no orbits crossing this subset – the only trajectories crossing the plane $Q = 0$ pass through the points with $x = 0$ or $y = 0$.

4.1.6 Qualitative Analysis

We summarise the dynamical behaviour of the equilibrium points and lines of equilibrium points in Tables 4.6, 4.9 and 4.10 and Tables 4.7 and 4.8 respectively. For the stability analysis, we only consider the four cases: cosmological constant $w = -1$, dust $w = 0$, radiation $w = 1/3$ and stiff matter $w = 1$. We only state the results for the equilibrium points corresponding to expanding solutions. The collapsing points are obtained by time–reversal – in other words their dynamical stability properties are simply reversed: If $\mathcal{A}_+$ is a repeller for a given range of n, then $\mathcal{A}_-$ is an attractor for the same range of n.

Table 4.6 consists of all the BI subspace equilibrium points (excluding the lines); their behaviour is similar to the flat Friedmann points which were found previously [82, 87]. We note that some of the solutions corresponding to the Friedmann and BI equilibrium points, have been found in [134, 135].

The lines of equilibrium points have to be treated more carefully. We summarise their dynamical behaviour in Tables 4.7 and 4.8. As noted above, the two lines include the same parametric solutions, but $\mathcal{L}_1$ corresponds to $x \geq 0$, while $\mathcal{L}_2$ has $x \leq 0$.

Since these lines correspond to flat solutions they should have been found in [82]. In fact, the authors of [82] found a line of equilibrium points denoted by $\mathcal{L}_1^*$, extending over $\Sigma_{**} \in [0, \infty)$, where Σ_{**} measures the shear contribution to the Friedmann equation. The range $0 \leq \Sigma_{**} \leq 1$ corresponds to our $\mathcal{L}_{1,+}$, while $\Sigma_{**} > 1$ corresponds to $\mathcal{L}_{2,+}$ as can be seen from the solutions of the scale factor in [82]. In [82] the isotropic solution was at $\Sigma_{**} = 0$ and the static one occured for $\Sigma_{**} \to \infty$. Note that [82] did not address the collapsing solutions $\mathcal{L}_{1,-}$ or opposite orientation of the shear $\mathcal{L}_{2,-}$ because the phase space for BI is symmetric about the plane $\Sigma = 0$. The stability for $\Sigma < 0$ can be obtained by time reversal from the corresponding points in the $\Sigma > 0$ subspace.

As stated above, $\mathcal{L}_{1,2}$ are only physical for certain special coordinates. These are

$$\Sigma_* = \pm\sqrt{\frac{5-4n}{2n-1}}, \quad n \in (1, 5/4), \quad \text{and} \quad Q_* = \pm\sqrt{\frac{2n-1}{5-4n}}, \quad n \in (1/2, 1),$$

for $\mathcal{L}_1$ and $\mathcal{L}_2$ respectively. These equilibrium points are always saddles in nature.

Table 4.6: Nature of the expanding ($\epsilon = +1$) spatially flat BI equilibrium points. The collapsing analogs are simply time reversed. The parameters are $P_+ = \frac{1}{2}(1+\sqrt{3})$ and $V_+ = \frac{1}{14}(11+\sqrt{37})$.

Point	w	Range of n							
		$(0,1/2)$	$(1/2,1)$	$(1,V_+)$	$(V_+,5/4)$	$(5/4,P_+)$	$(P_+,3/2)$	$(3/2,2)$	$(2,\infty)$
$\mathcal{A}_+$	-1	saddle	attractor	repeller	repeller	saddle	saddle	saddle	attractor
	0	saddle	attractor	repeller	repeller	saddle	attractor	attractor	attractor
	1/3	saddle	attractor	repeller	repeller	saddle	attractor	attractor	attractor
	1	saddle	attractor	repeller	saddle	saddle	attractor	attractor	attractor
$\mathcal{B}_+$	-1	saddle	saddle	saddle	saddle	saddle	saddle	saddle	saddle
	0	saddle	saddle	saddle	saddle	saddle	saddle	saddle	saddle
	1/3	saddle	saddle	saddle	saddle	saddle	saddle	saddle	saddle
	1	repeller	repeller	saddle	saddle	saddle	saddle	repeller	repeller
$\mathcal{C}_+$	-1	saddle	saddle	attractor	attractor	attractor	attractor	attractor	saddle
	0	saddle	saddle	saddle	saddle	saddle	saddle	saddle	saddle
	1/3	saddle	saddle	saddle	saddle	saddle	saddle	saddle	saddle
	1	saddle	saddle	saddle	repeller	repeller	repeller	saddle	saddle

The nature of the BIII equilibrium points is stated in Table 4.9. For the sake of completeness we have included the stability of points $\mathcal{D}$ and $\mathcal{E}$, but will not discuss them any further since they are not physical. The point $\mathcal{F}$ lies in the BIII subspace for $n \in (0, \frac{1}{2}(1+\sqrt{3}))$. $\mathcal{F}_+$ is a saddle for $w = -1$ and for $n \in (1, 5/4)$ when $w = 0$, but an attractor otherwise. $\mathcal{G}$ lies in the BIII subspace for $n \in (0, 3/2)$ when $w = 0$, for all n when $w = 1/3$ and $n \in (0, 1)$ and $n \in (3, \infty)$ when $w = 1$. $\mathcal{G}_+$ is saddle except for $n \in (1, 5/4)$ when $w = 0$ where it becomes an attractor.

The nature of the KS equilibrium points is stated in Table 4.10. Point $\mathcal{F}$ lies in the KS subspace for $n > \frac{1}{2}(1+\sqrt{3})$ and $\mathcal{F}_+$ is always a saddle. Similarly, $\mathcal{G}$ lies in the KS subspace for all n when $w = -1$, for $n > 3/2$ when $w = 0$ and $n \in (1, 3)$ when $w = 1$. $\mathcal{G}_+$ is saddle except for $n \in (1, 1.13)$ when $w = 1$, where it is a repeller.

We can identify the following global attractors and repellers: $\mathcal{A}_+$ is a global attractor for $n \in (P_+, 2)$ when $w = 0$, 1/3 and 1, and for $n \in (2, \infty)$ (all w). When $w = -1$, $\mathcal{C}_+$ is a global attractor for $n \in (1, 2)$ and $\mathcal{E}_+$ for $n \in (0, 1/2)$. Point $\mathcal{F}_+$ is a global attractor for $n \in (0, 1/2)$ and $n \in (5/4, P_+)$ when $w = 0$, 1/3 and 1, and for $n \in (1, 5/4)$ when $w = 1/3$ and 1. $\mathcal{G}_+$ is only a global attractor for $n \in (1, 5/4)$ when $w = 0$. By time reversal the corresponding contracting solutions are global repellers. There are no global repellers in the expanding subspace since the lines $\mathcal{L}_{1,2}$ contain repellers and hence there are no global attractors in the collapsing subspace.

Table 4.7: Nature of the line of expanding spatially flat anisotropic equilibrium points $\mathcal{L}_{1+}$. Here $\Sigma_b(n) = \sqrt{\frac{5-4n}{2n-1}}$ is a bifurcation value depending on n.

w	n	$\Sigma \in [-1, -\Sigma_b(n))$	$\Sigma \in (-\Sigma_b(n), \Sigma_b(n))$	$\Sigma \in (\Sigma_b(n), 1)$
	$n \in (0,1)$	repeller	repeller	repeller
$-1, 0, 1/3$	$n \in (1, 5/4)$	repeller	saddle	repeller
	$n > 5/4$	repeller	repeller	repeller
1	All n	saddle	saddle	saddle

Table 4.8: Nature of the line of spatially flat anisotropic equilibrium points $\mathcal{L}_{2,\pm}$. Here $Q_b(n) = \sqrt{\frac{2n-1}{5-4n}}$ is a bifurcation value depending on n. We discuss the bifurcation $Q = 0$ in the section on static solutions below. Note that the dynamical behaviour of $\mathcal{L}_{2,+}$ and $\mathcal{L}_{2,-}$ is identical.

n	$Q \in [-1, -Q_b(n))$	$Q \in (-Q_b(n), 0)$	$Q \in (0, Q_b(n))$	$Q \in (Q_b(n), 1]$
$n \in [0, 1/2]$	attractor	attractor	repeller	repeller
$n \in (1/2, 1)$	attractor	saddle	saddle	repeller
$n > 1$	attractor	attractor	repeller	repeller

Table 4.9: Nature of the spatially open Bianchi III equilibrium points, where $P_+ = \frac{1}{2}(1 + \sqrt{3})$.

Point	w	range of n					
		$(0,1)$	$(1,5/4)$	$(5/4, P_+)$	$(P_+, 3/2)$	$(3/2, 3)$	$(3, \infty)$
$\mathcal{D}_+$	All	saddle	saddle	saddle	saddle	saddle	saddle
$\mathcal{E}_+$	-1	attractor	saddle	saddle	saddle	saddle	saddle
	0, 1/3, 1	saddle	saddle	saddle	saddle	saddle	saddle
$\mathcal{F}_+$	-1	saddle	saddle	saddle	-	-	-
	0	attractor	saddle	attractor	-	-	-
	1/3	attractor	attractor	attractor	-	-	-
	1	attractor	attractor	attractor	-	-	-
$\mathcal{G}_+$	-1	-	-	-	-	-	-
	0	saddle	attractor	saddle	saddle	-	-
	1/3	saddle	saddle	saddle	saddle	saddle	saddle
	1	saddle	-	-	-	-	saddle

Table 4.10: Nature of the spatially closed Kantowski-Sachs equilibrium points, where $P_+ = \frac{1}{2}(1+\sqrt{3})$ and $X \approx 1.13$.

Point	w	Range of n					
		$(0,1)$	$(1,X)$	(X,P_+)	$(P_+,3/2)$	$(3/2,3)$	$(3,\infty)$
$\mathcal{F}_+$	-1	-	-	-	saddle	saddle	saddle
	0	-	-	-	saddle	saddle	saddle
	1/3	-	-	-	saddle	saddle	saddle
	1	-	-	-	saddle	saddle	saddle
$\mathcal{G}_+$	-1	saddle	saddle	saddle	saddle	saddle	saddle
	0	-	-	-	-	saddle	saddle
	1/3	-	-	-	-	-	-
	1	-	repeller	saddle	saddle	saddle	-

4.1.7 Bouncing or recollapsing trajectories

As motivated above, any trajectory corresponding to a bouncing or recollapsing solution must pass through $x = Q = 0$ or $y = Q = 0$.

The existence of bouncing orbits for Bianchi I models has been studied in [158]. In the vacuum case it was found that there exist bouncing/recollapsing trajectories, but only for $y < 0$. If $n > 1$, R has to be negative and there can only be re-collapse ($\dot{\Theta} < 0$). For $n \in [0, 1/2]$ re-collapse may occur if $R > 0$, and for $n \in [0, 1/2]$ there may be a bounce ($\dot{\Theta} > 0$) for positive R. In all cases, the bouncing trajectories have to pass through the single point $x = Q = 0$ (denoted by $\tilde{\mathcal{M}}$ in [158]) in the 2-dimensional BI vacuum subspace. Note that it is not possible to achieve a bounce through $y = Q = 0$ here, since a line of equilibrium points passes through that point in this subspace.

When matter is added, we obtain another degree of freedom, and unlike in GR, the matter term may enhance bouncing or recollapsing behaviour due to the R^{n-1} term coupled to the energy density. The corresponding trajectories now have to pass through the 1-dimensional lines with $x = Q = 0$ or $y = Q = 0$ instead of the single point $\tilde{\mathcal{M}}$.

In the presence of spatial curvature, it is yet easier to achieve bouncing or recollapsing behaviour. If ${}^3R < 0$, the results from the flat Bianchi I case are qualitatively recovered. For ${}^3R > 0$ however, there are differences to the Bianchi I case. In particular, positive spatial curvature allows $\Theta = 0$ even for positive y.

4.2 Isotropisation of OSH Bianchi models

It is possible to study isotropisation by looking at the stability of the Friedmann points in the state space (see [90] and references therein). When such an isotropic point is an attractor, then we have asymptotic isotropisation in the future. If the point is a repeller we have an isotropic initial singularity, and when it is a saddle we have intermediate isotropisation. Because of the dimensionality and complexity of the state space, we will not study specific orbits to investigate viable models. We will therefore restrict the following discussion to the behaviour around the equilibrium points only.

In the previous sections we found two isotropic equilibrium points that admit cosmological solutions: a vacuum point $\mathcal{A}$ and a non-vacuum point $\mathcal{C}$. These points were also found in the BI case [82].

The expanding point $\mathcal{A}_+$ is an isotropic *past* attractor for $n \in (1, 5/4)$ when $w = -1$, 0 or $1/3$, and for $n \in (1, \frac{1}{14}(11 + \sqrt{37}))$ when $w = 1$. As pointed out in [82], this is an interesting feature, since the existence of an isotropic past attractor implies that we do not require special initial conditions for inflation to take place. The contracting analog $\mathcal{A}_-$ is an isotropic future attractor in these ranges. $\mathcal{A}_+$ is a *future* attractor for $n > 2$ when $w = -1$ and for $n > \frac{1}{2}(1 + \sqrt{3})$ when $w = 0$, $1/3$ or 1. By time reversal, $\mathcal{A}_-$ is a past attractor for these parameter values.

The equilibrium point $\mathcal{C}_+$ is an isotropic past attractor for $n \in (\frac{1}{14}(11 + \sqrt{37}, 3/2)$ when $w = 1$ and an isotropic future attractor for $n \in (1, 2)$ when $w = -1$. When $w = 0$ or $w = 1/3$ this point is a saddle for all values of n. This means that in this case we have a transient matter/ radiation dominated phase in which the model is highly isotropic and hence potentially compatible with observations.

We note that all isotropic equilibrium points found in this analysis are flat Friedmann like, unlike in [87], where the isotropic points $\mathcal{A}$ and $\mathcal{C}$ with non-zero spatial curvature were found. The reason for this discrepancy is that the plane $\Sigma = 0$ is no longer invariant when allowing for non–zero spatial curvature ($k \neq 0$); as in GR spatial curvature causes anisotropies to grow in models with R^n-gravity. For this reason the points $\mathcal{A}$ and $\mathcal{C}$ no longer remain equilibrium points in the full OSH Bianchi state space.

There are two equilibrium points of interest with non-zero shear: the vacuum point $\mathcal{F}$ and the non-vacuum point $\mathcal{G}$. These points are isotropic for certain bifurcation values of n and w: $\mathcal{F}$ is isotropic for $n = \frac{1}{2}(1 + \sqrt{3})$ for all w, and $\mathcal{G}$ is isotropic for $n = \frac{3}{2}(1 + w)$ if $w > -1$. The KS point $\mathcal{G}_+$ is a past attractor for $n \in (1, 1.13)$

when $w = 1$ and a saddle for $n > 3/2$ when $w = 0$. This means that we can have initial conditions which are anisotropic, or we can have intermediate anisotropic conditions which are conducive for structure formation, provided that the anisotropies are sufficiently small. When $w = 1/3$, the point $\mathcal{G}_+$ lies in the BIII state space and is a saddle for all values of n, and when $w = 0$ the same applies for $n \in (0, 1)$ or $n \in (5/4, 3/2)$.

4.3 Remarks and Conclusions

Our main aim in this chapter was to investigate the effects of spatial curvature on the isotropisation of OSH Bianchi models in R^n-gravity, and to possibly identify static solutions and bounce behaviours. To achieve this goal, we constructed a compact state space which allows one to obtain a complete picture of the cosmological behaviour for expanding, contracting and static as well as bouncing or recollapsing models. This is not possible with the non-compact variables used in chapter 3, since the equilibrium points with static solutions do not have finite coordinates in this framework. The Poincaré projection also does not allow one to patch together the expanding and contracting copies of the state space, so bounce behaviour cannot be investigated. This is discussed in detail in chapter 5 for the BI subspace, where the results obtained in this chapter are compared to the results obtained in chapter 3.

We do not find any exact Einstein static solutions in this analysis. However we do find orbits that exhibit cyclic behaviour, which was expected from previous work examining the conditions for bouncing solutions in $f(R)$ gravity [152]. We also recover all the isotropic equilibrium points that were found in [82]. The expanding vacuum point $\mathcal{A}_+$ is a past attractor for $n \in (1, 5/4)$ as in the BI case. We emphasise that we only find *flat* ($k = 0$) isotropic equilibrium points ($\mathcal{A}$, $\mathcal{B}$ and $\mathcal{C}$). Therefore for these types of theories, isotropisation also implies cosmological behaviours which evolve towards spatially flat spacetimes. Late time behaviour with non-zero spatial curvature will have a growth in anisotropies, as in GR.

In conclusion, we have shown that spatial curvature does indeed affect the isotropisation of cosmological models in R^n-gravity. While no exact static solutions could be found, we did find that bounces can occur in these cosmologies.

Chapter 5

Compactifying the state space for alternative theories of gravity

In this chapter, we consider the various frameworks in which dynamical systems theory can be applied to cosmology. In §5.1 we discuss the characteristics of non-compact and compact state spaces in general. We point out the advantages of compactifying the state space, emphasising the aspect of static and bounce type solutions. In §5.2, we proceed to give the specific example of LRS Bianchi I models in R^n–gravity and compare the results of [106] (chapter 4) and [82] (chapter 3), where compact and non–compact expansion–normalised variables were used respectively. In §5.3 we consider the flat Friedmann models in R^n–gravity and compare the compact formalism of [106] to that of Clifton *et al.* [81], where non-compact non–expansion–normalised variables were used.

5.1 Choice of the state space

In order to perform a dynamical systems analysis on homogeneous cosmologies, one has to construct variables corresponding to the kinematic and gravitational quantities as well as a time variable that together define an autonomous system of first-order differential equations. The choice of variables depends on several physical considerations: Firstly, one would like to study the cosmological behaviour close to the initial singularity and the late time behaviour of the model. Secondly, we want to study the effect of matter, shear and other physical influences on the cosmological dynamics. Finally, we would like to constrain the system by making use of observations such as the cosmic microwave background.

The so–called Hubble– or expansion–normalised variables together with a Hubble–normalised time variable [159] have been used successfully to study important issues such the isotropisation of cosmological models [144]. The state space defined by the Hubble–normalised variables is compact for simple classes of ever expanding models such as the open and flat FLRW models and the spatially homogeneous Bianchi type I models in GR. In these cases, the dynamical systems variables are bounded even close to the cosmological singularity [90]. This is due to the fact that these simple classes of cosmological models do not allow for bouncing, recollapsing or static models, since there are no contributions to the Friedmann equation that would allow for the Hubble–parameter to vanish.

As soon as there are additional degrees of freedom allowing Θ to pass through zero (e.g. the simple addition of positive spatial curvature), the state space obtained from expansion–normalised variables becomes non–compact. Note that even the time variable becomes ill-defined in this case and needs to be used carefully (see below). If the expansion normalised variables are unbounded, one has to perform an additional analysis to study the equilibrium points at infinity. This can be done using the well known Poincaré projection [156,157], where the points at infinity are projected onto a unit sphere. These projected equilibrium points can then be analysed in the standard way, i.e by considering small perturbations around the points. However, it may still be difficult to determine the stability of the equilibrium points at infinity.

Alternatively, one may break up the state space into compact subsectors, where the dynamical systems and time variables are normalised differently in each sector (see for e.g. [147]). The full state space is then obtained by pasting the compact subsectors together. We will discuss these two methods in the following subsections, highlighting the advantages and disadvantages in this context.

5.1.1 Non-compact state spaces and the Poincaré projection

In cosmology it is not always straightforward to construct variables defining a compact dynamical system associated with the class of cosmological models of interest. This is especially true if one considers more complicated theories such as modified theories of gravity. In many of the analyses of these types of theories, the dynamical systems variables are not expansion–normalised and define a non–compact state space [81,91–95,100–103]. These analyses make use of a conformal time, which places restrictions on the ranges of physical quantities, such as the energy density, Ricci scalar or scalar-field (see §5.3). The behaviour of the system at infinity can then be studied using a Poincaré projection. In this framework, the equilibrium points at infinity represent

the cosmological singularities such as initial singularities or other singularities where the scale factor, scalar field or other variables of the system tend to zero. Despite the non-compactness of the state space constructed in this way, one may in principle study bouncing or recollapsing behaviours as well as static solutions, since one does not normalise with Θ.

It is often useful to define expansion–normalised variables together with a dimensionless, expansion–normalised time variable in order to decouple the expansion rate from the remaining propagation equations. This approach only yields a well–defined time variable if we only study ever expanding or ever collapsing models; a sign change in the expansion rate would make this time variable non-monotonic. For the simple class of FLRW models in GR for example, there are no bouncing or recollapsing models, and the expanding or collapsing models can be studied separately in a well–defined compact framework. In a more general scenario however, static and recollapsing or bouncing solutions may occur, and one would have to introduce a modified normalisation in order to define a state space that includes these singularities.

In some cases it may be useful to employ expansion–normalised variables, but it may not feasible to compactify the state space. This is the case when e.g. only studying ever–expanding cosmological models. Non-compact expansion–normalised variables have been used successfully to study aspects of isotropisation in higher order gravity models [82,83]. As pointed out above, the non–compact expansion–normalised state space can only contain expanding (or, by time reversal, collapsing) solutions by construction. In particular, one cannot easily study bounce behaviours in this setup, since the expanding and collapsing subspaces would have to be pasted together at infinity, which is non-trivial. Furthermore, the time variable is ill-defined in this limit and needs careful treatment.

5.1.2 Compact state spaces

As mentioned above, expansion–normalised variables define a compact state space for certain simple classes of cosmologies such as the class of flat Friedmann models in GR [159]. When e.g. additionally allowing for positive spatial curvature however, this behaviour breaks down even in GR. Formally, we have a negative contribution to the Friedmann equation, allowing all the other variables to become unbounded. Physically, the reason for the non-compactness of the state space is that positive spatial curvature allows for static and bouncing solutions which have vanishing expansion rate at least at some point in time. At this point in time, the simple Hubble–normalisation is ill-defined, causing the expansion-normalised variables as well as the

expansion-normalised time to diverge.

In [147] a simple formalism has been established to compactify the state space: if any negative contribution to the Friedmann equation is absorbed into the normalisation, one can define compact expansion normalised variables. If there are any quantities that may be positive or negative, one has to study each option in a separate sector of the state space and obtain the full state space by matching the various sectors along their common boundaries. In particular, this choice of normalisation ensures that the accordingly normalised time variable is well-defined and monotonic, and the state space obtained in this way may include static, bouncing and recollapsing models. This approach has been successfully adapted to compactify the state space corresponding to more complicated classes of cosmologies (see for example [113, 114, 117, 118]).

5.2 Example 1: LRS Bianchi I cosmologies in R^n-gravity

In this section we outline how the method discussed in chapter 4 is used to construct a compact expansion–normalised state space for the simple class of LRS Bianchi I cosmologies. We then compare the results obtained in this framework to the results obtained using the non–compact expansion–normalised setup of [82] (chapter 3). We will express the equilibrium points and coordinates of the compact analysis (chapter 4) with a tilde to distinguish them from the corresponding points in the non-compact analysis (chapter 3). We end this section with a discussion of bouncing and recollapsing models based on the compact framework.

5.2.1 Construction of the compact state space

The LRS Bianchi I state space is compactified as discussed in detail in chapter 4. The dynamical variables are given by (4.7) (excluding K) together with the dimensionless time variable τ defined by (4.6)

The normalisation D will be chosen such that it is strictly positive at all times. As in GR, we have to explicitly exclude the static flat isotropic vacuum cosmologies [147]. We define eight different sectors according to the possible signs of $\tilde{x}$, $\tilde{y}$ and $\tilde{z}$[1]. The first sector is characterised by $\tilde{x},\ \tilde{y},\ \tilde{z} \geq 0$. In this sector, we can simply choose $D = |\Theta| = \epsilon\Theta$, where $\epsilon = \pm 1$ is defined to be the sign function of Θ: $\epsilon = |\Theta|/\Theta$. The

[1]Note that the sign of these quantities is independent of the exact choice of the normalisation, since D is real and enters quadratically.

Friedmann equation becomes

$$1 = \tilde{\Sigma}^2 + \tilde{x} + \tilde{y} + \tilde{z}\,. \tag{5.1}$$

By construction, all the contributions to the right hand side of (5.1) are positive, hence the variables $\tilde{x},\ \tilde{y}$ and $\tilde{z}$ have to take values in the interval $[0,1]$, while $\tilde{\Sigma}$ must lie in $[-1,1]$. Note that $\tilde{Q} = \epsilon = \pm 1$ is not a dynamical variable in this sector only, where we have excluded $\Theta = 0$ as motivated above. This means that we have to create two copies of this sector, one corresponding to the expanding models ($\tilde{Q} = \epsilon = 1$) and one to corresponding to the collapsing models ($\tilde{Q} = \epsilon = -1$). These two sectors are disconnected (see Figure 5.1).

In the other sectors, we absorb any negative contributions to the Friedmann equation into the normalisation. For example, if $\tilde{x},\ \tilde{y} > 0$ and $\tilde{z} < 0$ (as in sector 4 of [106]), we define $D = \sqrt{\Theta^2 - \frac{3\mu}{nR^{n-1}}}$. Note that we may now include the static and bouncing or recollapsing solutions with $\Theta = 0$ as long as there is matter present ($\mu \neq 0$). Again we can express the Friedmann equation in terms of the normalised variables (4.7) and observe that $\tilde{z}$ does not explicitly appear, but all the other contributions enter with a positive sign. This means that $\tilde{x},\ \tilde{y}$ and $\tilde{\Sigma}^2$ are positive and must take values in $[0,1]$. One can easily show that $\tilde{z}$ is bounded by the interval $[-1,0]$ in this sector, and $\tilde{Q}$ lies in $[-1,1]$. The other sectors are constructed by analogy (see [106] for details).

Note that in all the sectors other than the first one, $\tilde{Q}$ is a dynamical variable (taking values in $[-1,1]$) with the sign of $\tilde{Q}$ corresponding to the sign of the Hubble factor. This means that in these sectors, we naturally include both expanding and collapsing models and do not have to artificially create two copies of the sectors. Furthermore, we point out that in all sectors other than the sectors 1 and 2, we can principally include static solutions. The exclusion of static or bouncing/recollapsing models in sector 1 has been explained above. Sector 2 is similar to sector 1 in the limit $\Theta = 0$ because of the special way the variable x is defined: in this case the normalisation vanishes, and we therefore have to exclude this case.

The full state space is obtained by matching the various sectors along their common boundaries defined by $\tilde{x},\ \tilde{y},\ \tilde{z} = 0$. For simplicity, we will first address the vacuum subspace ($\tilde{z} = 0$). This space consists of four 2-dimensional compact sectors corresponding to the sign of the variables $\tilde{x}$ and $\tilde{y}$. As discussed above, we have to create the two copies of the first sector (labeled 1^+ and 1^-) corresponding to the disconnected expanding and collapsing parts respectively. The full state space is then composed of five different pieces as depicted schematically in Figure 5.1. Strictly speaking we have to exclude the points with $\tilde{Q} = 0$ and $\tilde{x},\ \tilde{y} \neq 0$, since $\tilde{Q} = 0$ implies

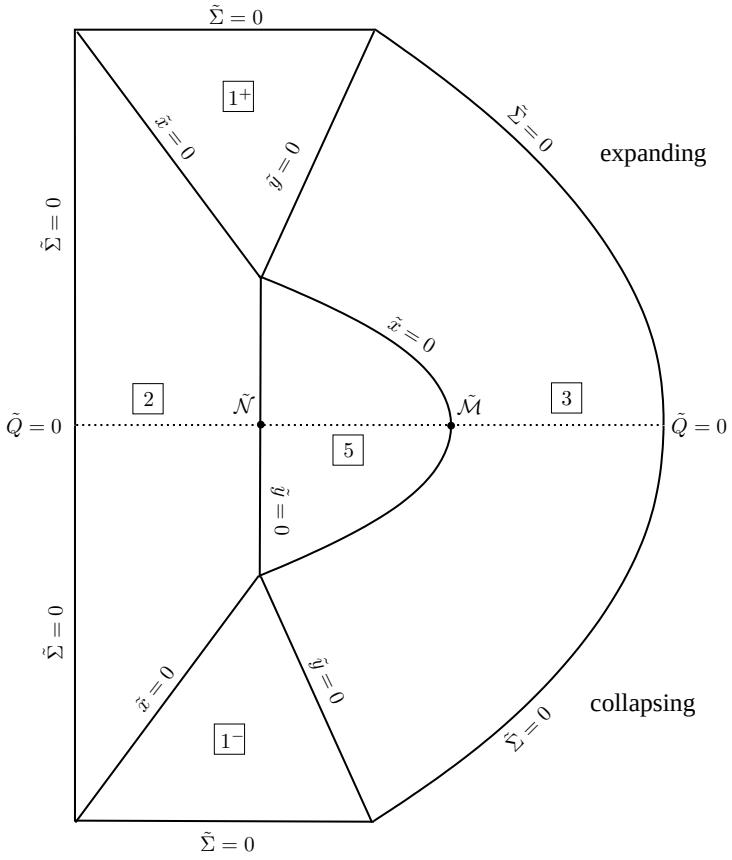

Figure 5.1: Schematic construction of the compact state space of the vacuum LRS Bianchi I models. The sectors have been labeled (numbers in square boxes) according to [106]. Note that the state space is symmetric around $\Sigma = 0$, so that this figure can represent $\Sigma \geq 0$ or $\Sigma \leq 0$.

$\Theta = 0$ which in turn implies $\tilde{x} = 0$ unless $R = 0$. This is indicated with a dotted line in Figures 5.1, 5.2, 5.3 and 5.4, showing that the $\tilde{Q} = 0$ plane may only be crossed at the points with $\tilde{x} = 0$ or $\tilde{y} = 0$. We will label these points $\tilde{\mathcal{M}}$ and $\tilde{\mathcal{N}}$ respectively.

The points with $\tilde{y} = 0$ have to be treated with caution: these points necessarily have vanishing Ricci scalar R and the corresponding cosmological solutions can only be discussed in the limit $R \to 0$. This issue is addressed in detail in chapter 4, where it was found that there only exist solutions corresponding to these points for very special values of n. The same issue applies to point $\tilde{\mathcal{N}}$, which is a degenerate point as discussed is §5.2.4 below.

The state space corresponding to the matter case is 3–dimensional and consists of eight separate sectors. It is straightforward to construct by analogy with the vacuum case, but harder to present in a graphic visualisation because of the higher

dimensionality of the state space. We therefore omit a graphic representation of the matter state space.

We point out that unlike in the vacuum case, where $\Theta = 0$ was only allowed at the single points $\tilde{\mathcal{M}}$ and $\tilde{\mathcal{N}}$, the matter case allows for one additional degree of freedom. In this case static or bouncing/recollapsing models must pass through the 1–dimensional lines extending $\tilde{\mathcal{M}}$ and $\tilde{\mathcal{N}}$ along the z–direction, and can therefore occur at for a wider range of variables. This is of course due to the fact that the curvature term coupled to the matter contribution can counterbalance the other terms in the Friedmann equation.

5.2.2 Comparison of equilibrium points

We first look at the vacuum equilibrium points found in [82] (chapter 3) and in the LRS Bianchi I state subspace of [106] (chapter 4). Since the former paper only considered expanding models, we restrict ourselves to the expanding subset of the compact LRS Bianchi I state subspace of chapter 4 in this comparison.

In the non-compact analysis (chapter 3), one Friedmann-like equilibrium point $\mathcal{A}$, a line of equilibrium points $\mathcal{L}_1$ corresponding to Bianchi I models, and four asymptotic equilibrium points $\mathcal{A}_\infty$, $\mathcal{B}_\infty$, $\mathcal{C}_\infty$ and $\mathcal{D}_\infty$ were found. The coordinates of $\mathcal{A}$ diverge as $n \to 1/2$. This means that for this bifurcation value the point moves to infinity, where it merges with the asymptotic equilibrium point $\mathcal{B}_\infty$ if $n \to 1/2^-$ and with $\mathcal{C}_\infty$ if $n \to 1/2^+$. The asymptotic point $\mathcal{A}_\infty$ is the "endpoint" of $\mathcal{L}_1$ at infinity. The four equilibrium points at infinity occur for all values of n. Note that for $n = 1/2$ a bifurcation occurs, where the isolated asymptotic equilibrium points turn into a ring of equilibrium points at infinity. This means that for this value of n, asymptotic equilibrium points occur at all angles. This bifurcation was not considered in chapter 3.

In the compact analysis (chapter 4), one Friedmann-like equilibrium point $\tilde{\mathcal{A}}$ and two Bianchi I lines of equilibrium points $\tilde{\mathcal{L}}_1$ and $\tilde{\mathcal{L}}_2$ were found in the flat vacuum subspace explored here. Note that the two lines are in fact the same but for different signs of the variable $\tilde{x}$ (see below).

Table 5.1 summarises the equilibrium points from the compact analysis and the corresponding counterparts in the non-compact analysis. We can see that the finite equilibrium points in chapter 3 correspond to the similarly labeled ones in chapter 4 for all values n, even for the bifurcation values of n for which the finite points in chapter 3 move to infinity. We note that the asymptotic points $\mathcal{B}_\infty$ and $\mathcal{C}_\infty$ only have analogs in the compact analysis for the bifurcation value $n = 1/2$. The line $\mathcal{L}_1$ in the

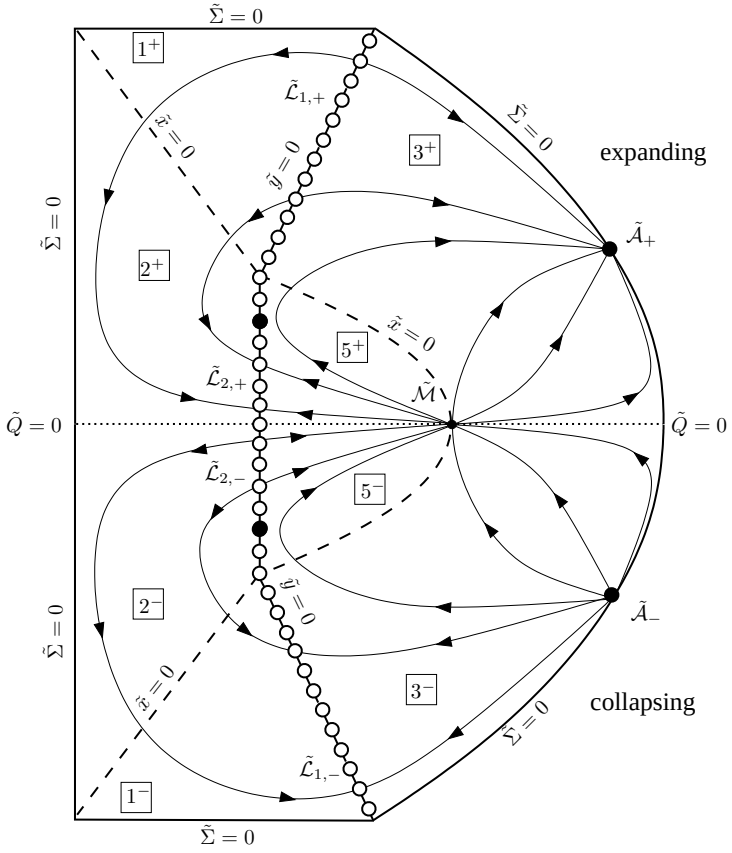

Figure 5.2: Compactified state space of the vacuum LRS Bianchi I models for $n \in (1/2, 1)$. The line of hollow circles corresponds to $\tilde{\mathcal{L}}_{1,2}$, where the only points with corresponding cosmological solutions are filled in solid. The dotted line represents the points with $\tilde{Q} = 0$, but only the point $\tilde{\mathcal{M}}$ with $\tilde{x} = \tilde{Q} = 0$ and the point on the line $\tilde{\mathcal{L}}_2$ with $\tilde{y} = \tilde{Q} = 0$ (referred to as $\tilde{\mathcal{N}}$ in the text) may have corresponding solutions to the underlying field equations. We emphasise that $\tilde{\mathcal{M}}$ is not an equilibrium point - it is highlighted because it represents the only point where orbits in this subspace can cross between the expanding and collapsing sectors. See text for more details.

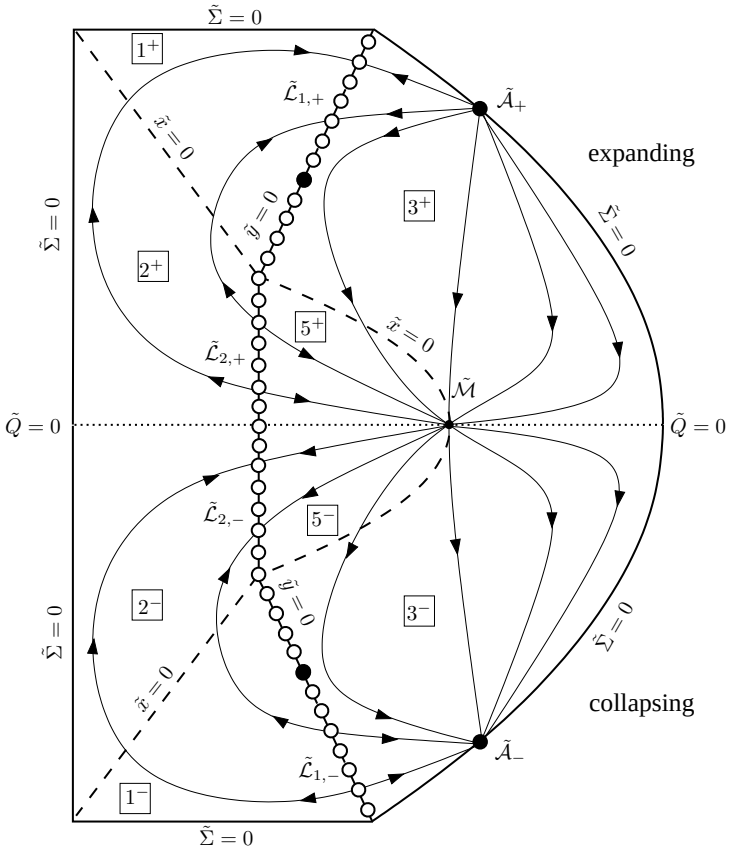

Figure 5.3: Compactified state space of the vacuum LRS Bianchi I models for $n \in (1, 5/4)$. See caption of Figure 5.2 for more details.

non-compact analysis corresponds to $\tilde{\mathcal{L}}_1$ in compact analysis for $\Sigma_* \in [0, 1]$ and to $\tilde{\mathcal{L}}_2$ for $\Sigma_* > 1$, where Σ_* parametrises the line $\mathcal{L}_1$. $\mathcal{A}_\infty$ corresponds to the single static ($\tilde{Q}_* = 0$) point on $\tilde{\mathcal{L}}_2$ in chapter 4, labeled $\tilde{\mathcal{N}}$ in this section.

The equilibrium point $\mathcal{D}_\infty$ in chapter 3 corresponds to the point $\tilde{\mathcal{M}}$ in the compact analysis as noted in Figures 5.2 and 5.3. Note that $\tilde{\mathcal{M}}$ is not an equilibrium point in the compact analysis; it only appears to be an equilibrium point in the non-compact analysis because in this case only the expanding half of the full state space was studied. When including the collapsing part of the state space as done in chapter 4, it becomes clear that $\tilde{\mathcal{M}}$ merely denotes the point at which orbits may cross between the expanding and contracting parts of the state space.

We now consider the matter equilibrium points. In the non-compact analysis, three finite isotropic points were found: the vacuum point $\mathcal{A}$ and two non-vacuum points $\mathcal{B}$ and $\mathcal{C}$. Furthermore, the vacuum Bianchi I line of points $\mathcal{L}_1$ was recovered. There were five asymptotic equilibrium points $\mathcal{A}_\infty$, $\mathcal{B}_\infty$, $\mathcal{C}_\infty$, $\mathcal{D}_\infty$ and $\mathcal{E}_\infty$, and a line

Table 5.1: Correspondence between the equilibrium points of the vacuum LRS Bianchi I state space in the compact (chapter 4) and non–compact (chapter 3) analysis. The last column states for which parameter values the correspondence occurs. Note that $\tilde{\mathcal{M}}$ is not an equilibrium point in the compact analysis; we have only included the last row for completeness.

Compact	Non-compact	parameter constraint
$\tilde{\mathcal{A}}_+$	$\mathcal{A}$	all n
	$\mathcal{B}_\infty$	$n \to \frac{1}{2}^-$
	$\mathcal{C}_\infty$	$n \to \frac{1}{2}^+$
$\tilde{\mathcal{L}}_{1,+}$	$\mathcal{L}_1$	all n, $\Sigma_* \in [0,1]$
$\tilde{\mathcal{L}}_{2,+}$	$\mathcal{L}_1$	all n, $\Sigma_* \in (1,\infty)$
	$\mathcal{A}_\infty$	all n, $\Sigma_* \to \infty$ $(\tilde{Q}_* = 0)$
$(\tilde{\mathcal{M}})$	$\mathcal{D}_\infty$	all n

of equilibrium points denoted $\mathcal{L}_\infty$. The coordinates of $\mathcal{A}$ diverge when $n \to 1/2$; in this case $\mathcal{A}$ merges with $\mathcal{D}_\infty$ when $n \to 1/2^-$ and with $\mathcal{E}_\infty$ when $n \to 1/2^+$. Similarly, the coordinates of equilibrium point $\mathcal{C}$ approach infinity when $n \to 0$: $\mathcal{C}$ merges with $\mathcal{A}_\infty$ when $n \to 0^-$ and with $\mathcal{B}_\infty$ when $n \to 0^+$. Point $\mathcal{B}$ on the other hand remains a finite equilibrium point for all values of n. As pointed out in the vacuum case, $\mathcal{C}_\infty$ is the "endpoint" of $\mathcal{L}_1$ at infinity with $\Sigma_* \to \infty$. As in the vacuum case, there is ring of asymptotic fixed points in the $z = 0$ plane at the bifurcation value $n = 1/2$. Furthermore, there is a ring of equilibrium points in the $\Sigma = 0$ plane at the bifurcation value $n = 0$. These bifurcations have not been noted in [82] (chapter 3).

In the compact analysis, the three isotropic points $\tilde{\mathcal{A}}$, $\tilde{\mathcal{B}}$ and $\tilde{\mathcal{C}}$ and the two vacuum Bianchi I lines of equilibrium points $\tilde{\mathcal{L}}_1$ and $\tilde{\mathcal{L}}_2$ were found. As in the vacuum case, we can see the correspondence between the equilibrium points in chapter 4 and the ones in chapter 3, where the finite equilibrium points may move to infinity for certain values of n. We have summarised these results in Table 5.2.

The line $\mathcal{L}_\infty$ is the higher dimensional matter analog of point $\mathcal{D}_\infty$ from the vacuum analysis: the counterpart of $\mathcal{L}_\infty$ in chapter 4 is not a line of equilibrium points. $\mathcal{L}_\infty$ only appears as a line of equilibrium points in the non compact analysis because the collapsing part of the state space is not included (see above).

Table 5.2: Correspondence between the equilibrium points of the LRS Bianchi I state space with matter in the compact (chapter 4) and non–compact (chapter 3) analysis. The last column states for which parameter values the correspondence occurs. Here the extension of $\tilde{\mathcal{M}}$ is the 1–dimensional generalisation of point $\tilde{\mathcal{M}}$ for the matter case (see text for details), which is not an equilibrium point in the compact analysis; we have only included the last row for completeness.

Compact	Non-compact	parameter constraints
$\tilde{\mathcal{A}}_+$	$\mathcal{A}$	all n
	$\mathcal{D}_\infty$	$n \to \frac{1}{2}^-$
	$\mathcal{E}_\infty$	$n \to \frac{1}{2}^+$
$\tilde{\mathcal{B}}_+$	$\mathcal{B}$	all n
$\tilde{\mathcal{C}}_+$	$\mathcal{C}$	all n
	$\mathcal{A}_\infty$	$n \to 0^-$
	$\mathcal{B}_\infty$	$n \to 0^+$
$\tilde{\mathcal{L}}_{1,+}$	$\mathcal{L}_1$	all n, $\Sigma_* \in [0,1]$
$\tilde{\mathcal{L}}_{2,+}$	$\mathcal{L}_1$	all n, $\Sigma_* \in (1,\infty)$
	$\mathcal{C}_\infty$	all n, $\Sigma_* \to \infty$ $(\tilde{Q}_* = 0)$
(extension of $\tilde{\mathcal{M}}$)	$\mathcal{L}_\infty$	all n

5.2.3 Solutions and stability

In both chapter 3 and 4, the exact solutions to the field equations (3.10)-(3.12) corresponding to each equilibrium point were derived.

The solutions to the finite points in the chapter 3 are the same as the ones obtained in chapter 4 for their counterparts in the compact analysis except for the points with $y = 0$, which are very special, since they necessarily have vanishing Ricci scalar R and their solutions can only be obtained in a careful limiting procedure. This is discussed in great detail in the previous chapter, where it was found that these points only have corresponding solutions for very special values of n. In the LRS Bianchi I state space discussed here, the point $\tilde{\mathcal{B}}$ and the lines $\tilde{\mathcal{L}}_{1,2}$ have vanishing Ricci scalar. As discussed in chapter 4, $\tilde{\mathcal{B}}$ only has a solution for the bifurcation value $n = 5/4$ and $w = 2/3$, and $\tilde{\mathcal{C}}_\pm$ only admits a solution for $n \in (1, N_+)$, where we abbreviate $N_\pm = \frac{1}{4(4+3w)}\left(13 + 9w \pm \sqrt{9w^2 + 66w + 73}\right)$. Only two points on $\tilde{\mathcal{L}}_{1,2}$ have corresponding cosmological solutions. These points are marked with solid circles

in Figures 5.2 and 5.3. This issue was not addressed in [82] (chapter 3), where the authors did not solve the full set of field equations to obtain the exact solutions. However, this is not a problem caused by the use of non-compact variables; the results of the previous chapter can be recovered using the setup of chapter 3 if one carefully solves for *all* cosmological variables (including R).

The solutions for the asymptotic equilibrium points in [82] differ from the ones obtained in [106] for the corresponding equilibrium points. In [82], the solutions corresponding to the asymptotic vacuum points $\mathcal{B}_\infty$, $\mathcal{C}_\infty$, $\mathcal{D}_\infty$ and the asymptotic matter points $\mathcal{A}_\infty$, $\mathcal{B}_\infty$, $\mathcal{D}_\infty$, $\mathcal{E}_\infty$ were all de Sitter like. In the compact analysis on the other hand, it was shown that there are no solutions to the corresponding equilibrium points.

A careful analysis shows that the stationary solutions in [82] are not valid, since they cannot simultaneously satisfy the evolution equations and the definitions of the dimensionless expansion normalised variables in this limit[2]. Note that these solutions can satisfy the coordinates of the asymptotic equilibrium points in the special static case. However, the static models do not satisfy all the original field equations for this class of models and therefore are not solutions as shown in the previous chapter. This was not investigated in [82] (chapter 3).

The solutions for the vacuum point $\mathcal{A}_\infty$ and the matter point $\mathcal{C}_\infty$ given in [82] were static in the appropriate limit $\Sigma_* \to \infty$. In chapter 4 however it is shown that the static models do not satisfy all the evolution equations and therefore do not present cosmological solutions. In this sense, we call all these equilibrium points 'unphysical'.

We conclude that while the non compact and compact analyses found the same solutions for the finite equilibrium points with $y \neq 0$ in chapter 3, there is disagreement with the solutions corresponding to the asymptotic points in chapter 3 and the points with $y = 0$. This discrepancy arises from the fact that the non–compact framework is much more complicated, so that it was not noticed that the given solutions indeed do not simultaneously satisfy the original equations and the coordinates of the (asymptotic) equilibrium points.

The nature of the equilibrium points remains unchanged in both formalisms, even though the time variable in chapter 3 is strictly speaking not well-defined at infinity. The reason for this agreement is that we study perturbations away from the equilibrium points, i.e. strictly speaking we never reach infinity when studying the eigenvalues. As long as the given point is actually an *equilibrium* point, the results

[2]Note that for this reason these solutions are not included in chapter 3. The asymptotic solutions given in [104] are also not included in chapter 6 for this reason.

from the expanding sector alone reflect the dynamical nature of the point in the entire state space correctly. However, we emphasise again that $\mathcal{D}_\infty$ and $\mathcal{L}_\infty$ in the non compact analysis are in fact not equilibrium points in the compact analysis. As explained in the previous subsection, they only appear to be fixed points in the non–compact dynamical system. The stability of $\mathcal{D}_\infty$ and $\mathcal{L}_\infty$ only indicates the direction of the orbits in the expanding part of the compact state space in the previous chapter.

5.2.4 Bounce behaviours

As motivated above, the non-compact expansion normalised variables are not suitable to study trajectories that correspond to recollapsing or bouncing cosmologies [3]. We therefore only discuss this issue in the context of the compact analysis (chapter 4).

We start with the vacuum case: from the Raychaudhuri and Friedmann equations, one can see that there can be bouncing solutions for $n \in (1/2, 1)$ and recollapsing solutions for $n \in (0, 1/2)$ or $n > 1$. This is reflected in Figures 5.2 and 5.3: we can see that there are trajectories corresponding to bouncing solutions for $n \in (1/2, 1)$ and to recollapsing solutions for $n \in (1, 5/4)$. In both cases, the bouncing or recollapsing trajectories have to go through the point $\tilde{\mathcal{M}}$, which is characterised by $\tilde{x} = \tilde{Q} = 0$. The existence of these bouncing or recollapsing solutions has been confirmed by a numerical analysis. For $n > 1$, the recollapsing models have a negative Ricci tensor R, while the bouncing or recollapsing models for $n < 1$ have a positive value of R.

In the matter case, there is one more degree of freedom. Any bouncing or recollapsing solution must now pass through the 1-dimensional extension of point $\tilde{\mathcal{M}}$ in the z–direction. This means it is easier to achieve bouncing or recollapsing behaviour in the matter case. In particular, there can be a bounce or recollapse even if $\tilde{y} > 0$ (if $\tilde{z} < -\tilde{y}$). Note that even though at first sight we also expect bouncing behaviours through the 1–dimensional extension of $\tilde{\mathcal{N}}$, this line in fact corresponds to degenerate cosmological models, and orbits approaching the line can never reach or cross it as explained in detail in the next example.

5.3 Example 2: Flat Friedmann cosmologies in R^n-gravity

In this section we consider the flat FLRW models with matter. We will compare the results of [106] (chapter 4) with the results of Clifton *et al.* [81], where non-compact

[3] Static models may be studied if one carefully takes into consideration that they have to be analysed separately in the two copies corresponding to expanding and collapsing models.

non–expansion–normalised variables were used.

We briefly summarise the approach used by [81] (which follows [91, 95]): A conformal time coordinate

$$d\tau = \sqrt{\frac{8\pi\mu}{3R^{n-1}}}\, dt, \tag{5.2}$$

and the dynamical variables

$$X = \frac{R'}{R} \quad \text{and} \quad Y = \frac{a'}{a}, \tag{5.3}$$

are introduced, where the primes here denote differentiation with respect to τ. Note that τ is only valid when R^{n-1} is a positive real root of R, which restricts the ranges of R and n.

Using the evolution equations (3.10) and (3.12) (with $\sigma = 0$), an autonomous set of first order differential equations for the variables X and Y is derived. This system is non–compact, and is then analysed using standard dynamical systems methods together with the Poincaré projection. Note that this approach does not exclude models with $\Theta = 0$, which allowed the authors of [81] to study static and bouncing or recollapsing models.

The class of flat FLRW cosmologies is the isotropic subspace of the class of LRS Bianchi I models studied in the previous section. We can therefore simply take over the framework from chapter 4 as outlined in §5.2. The equilibrium points for the FLRW state space are simply the isotropic equilibrium points from the previous example. Note that, unlike in the previous example, we now include both the expanding and collapsing sectors in order to compare to [81].

5.3.1 Comparison of equilibrium points

The analysis in [81] yielded the two pairs of finite equilibrium points $1, 2$ and $3, 4$. Furthermore, three pairs of equilibrium points at infinity were found: a pair of static points $5, 6$ and the two pairs $7, 8$ and $9, 10$ with power law solutions. The odd and even numbers in each pair correspond to expanding and collapsing models depending on the value of n. Note that points $1, 2$ only have real coordinates for $n > 0$ and $w < 2/3$, while $3, 4$ only have real coordinates for $n \in (N_-, N_+)$, where $N_\pm = \frac{1}{4(4+3w)}\left(13 + 9w \pm \sqrt{9w^2 + 66w + 73}\right)$. The pair $1, 2$ merges with $7, 8$ for $n = 0$ or $w = \frac{2}{3}$. Pair $3, 4$ merges with $5, 6$ for $n = 0$, and $9, 10$ merges with $5, 6$ for $n = \frac{1}{2}$.

The compact analysis (chapter 4) yields three flat Friedmann points (see §3): $\tilde{\mathcal{A}}_\pm$, $\tilde{\mathcal{B}}_\pm$ and $\tilde{\mathcal{C}}_\pm$, where the expanding solutions are indicated by a plus and collapsing ones by a minus subscript. As noted in the previous section, $\tilde{\mathcal{B}}_\pm$ only admits a solution at

the bifurcation $n = 5/4$ and $w = 2/3$, while $\tilde{\mathcal{C}}_\pm$ only has a cosmological solution for $n \in (1, N_+)$ and $w > -1$.

In Table 5.3 we summarise the equilibrium points from the previous chapter and the corresponding counterparts in the analysis of [81]. We note that the two matter solutions $\tilde{\mathcal{B}}_\pm$ and $\tilde{\mathcal{C}}_\pm$ in chapter 4 correspond to the finite equilibrium points $1, 2$ and $3, 4$ in [81], while the vacuum equilibrium point $\tilde{\mathcal{A}}_\pm$ in the compact analysis corresponds to the equilibrium points at infinity in [81]. This is due to the choice of coordinates (5.3), which diverge for $\mu \to 0$.

We now discuss in detail for which parameter values the correspondence between the equilibrium points occurs. We find that the expanding (collapsing) point $\tilde{\mathcal{A}}_+$ ($\tilde{\mathcal{A}}_-$) corresponds to 9 (10) for $n \in (1/2, 1)$ or $n > 2$, and to point 10 (9) for $n \in (0, 1/2)$ or $n \in (1, 2)$. There is no dependence on the equation of state parameter w in this case, since the point $\tilde{\mathcal{A}}_\pm$ corresponds to a vacuum solution. The matter point $\tilde{\mathcal{B}}_+$ ($\tilde{\mathcal{B}}_-$) corresponds to point 1 (2) for all $n > 0$ provided $w < \frac{2}{3}$, while for $w = 2/3$ point $\tilde{\mathcal{B}}_+$ ($\tilde{\mathcal{B}}_-$) corresponds to point 7 (8) when $n > 1$ and to point 8 (7) when $n \in (0, 1)$. Note that the matter point $\tilde{\mathcal{C}}_+$ ($\tilde{\mathcal{C}}_-$) corresponds to 3 (4) over the entire allowed range of n.

As in the previous example, an equilibrium point at infinity in the non–compact analysis (here $5, 6$ or $7, 8$) only has an analog in the compact framework for the specific bifurcation values (of n and in this case w) for which a finite equilibrium point moves to infinity and merges with the respective asymptotic point.

We now give special consideration to the points $5, 6$. We observe that the two points 5 and 6 have the single analog $\tilde{\mathcal{N}}$ in the compact analysis, which is not an equilibrium point in the compact analysis. The reason for this discrepancy is the following: the points $5, 6$ correspond to the limit $R \to 0$ (see equation (14) in [81]). As pointed out in [87], the plane $R = 0$ is invariant, so that orbits approaching this plane must turn around. Assuming R starts out positive and approaches zero, it is clear that the limit from the left corresponds to $R' < 0$ and $X \to -\infty$, while the limit from the right corresponds $R' > 0$ and $X \to \infty$. Thus $5, 6$ are not equilibrium points in the compact analysis: while they appear as sink and source respectively in [81], they merge into the single transitory point $\tilde{\mathcal{N}}$ in chapter 4, similar to the case of $\mathcal{D}_\infty$ above.

However, this point $\tilde{\mathcal{N}}$ represents a singular state: here $R = \Theta = \dot{\Theta} = 0$, that means the field equations break down and can only be studied in a careful limiting procedure (see chapter 4). In particular, orbits approaching $\tilde{\mathcal{N}}$ asymptotically slow down and never reach or pass through the point. In this sense we recover the results

Table 5.3: Correspondence between the equilibrium points in the state space of the flat FLRW models with matter in the compact (chapter 4) and non–compact [81] analysis. The plus-minus subscript indicates expanding and collapsing solutions respectively, and the last column states for which parameter values the correspondence occurs. We have abbreviated $N_{\pm} = \frac{1}{4(4+3w)}\left(13+9w \pm \sqrt{9w^2+66w+73}\right)$.

Compact	Non-compact	parameter constraints
$\tilde{\mathcal{A}}_{\pm}$	$5,6$	$n \to \frac{1}{2}$
	$9,10$	all n
$\tilde{\mathcal{B}}_{\pm}$	$1,2$	$w < \frac{2}{3}$
	$7,8$	$w = \frac{2}{3}$
$\tilde{\mathcal{C}}_{\pm}$	$3,4$	$n \in (N_-, N_+)$
	$5,6$	$n \to 0$
$(\tilde{\mathcal{N}})$	$5,6$	all n

of [81]: even though the two disconnected points $5,6$ have merged into the single point $\tilde{\mathcal{N}}$, no orbits can pass through $\tilde{\mathcal{N}}$ and therefore the qualitative result from [81] is maintained.

5.3.2 Solutions and stability

The solutions given in [81] have corresponding solutions in the compact analysis but only for specific values of the parameters (see section §5.2.3). The solutions for the points $7,8$ are the same as those found for $\tilde{\mathcal{B}}_{\pm}$ when $n = 5/4$ and $w = 2/3$. In [81], points $1,2$ have the same solutions as $7,8$ but they have no corresponding solutions in chapter 4. Points $3,4$ have the same solution as $\tilde{\mathcal{C}}_{\pm}$, and points $9,10$ have the same solutions as $\tilde{\mathcal{A}}_{\pm}$. The static solutions for points $5,6$ given in [81] do not satisfy all the evolution equations and therefore are strictly speaking no exact solutions. This result was also found in the previous chapter for the points $\tilde{\mathcal{A}}_{\pm}$ for $n \to 1/2$ and $\tilde{\mathcal{C}}_{\pm}$ for $n \to 0$, which again reflects the correspondence between the points in the respective limits.

The nature of the equilibrium points in the compact analysis agrees with the stability properties of the corresponding points in [81]. We note that the equilibrium points at infinity, $5,6$ and $7,8$, only have corresponding points in the compact analysis for specific values of n and w respectively. These parameter values correspond to the bifurcations where the stability of the equilibrium points changes and were not

analysed in detail in the previous chapter. We therefore do not compare the two formalisms in this case.

5.3.3 Bounce behaviours

Unlike in the expansion–normalised non–compact analysis [82] (chapter 3) studied in the previous example, bouncing or recollapsing solutions can be investigated in the non-compact formalism of [81], where specific examples were given: it was shown that for matter with $w = 0$ recollapsing solutions occur for $n = 1.1$ and bouncing solutions occur for $n = 0.9$.[4]

We confirm this in our compact analysis, where as in the LRS Bianchi I case, there are bouncing orbits through point $\tilde{\mathcal{M}}$ for $n \in (1/2, 1)$ and recollapsing orbits through $\tilde{\mathcal{M}}$ for $n > 1$. For $n \in (1/2, 1)$, only point $\tilde{\mathcal{A}}_{\pm}$ is physical, and so the physically relevant behaviour is restricted to sectors 3 and 5 (since $y = 0$ is invariant). The dynamics are the same as illustrated in Figure 5.2 for sectors 3 and 5, except that there is no line of equilibrium points. In the case of $n \in (1, N_+)$ and $w > -1$, point $\tilde{\mathcal{C}}_{\pm}$ is also physical so that we have both matter and vacuum solutions in the state space. This is the most interesting case and we will therefore concentrate the discussion below to this range of n for dust and radiation.

In Figure 5.4 we consider $w = 0$ and $n \in (1, N_+)$, and it can be seen that there are trajectories between the isotropic vacuum points $\tilde{\mathcal{A}}_+$ and $\tilde{\mathcal{A}}_-$ corresponding to recollapsing solutions. At a first glance there also appear to be bouncing solutions through point $\tilde{\mathcal{N}}$ in sectors 2 and 5. In sector 2 for example, orbits seem to move from the collapsing matter point $\tilde{\mathcal{C}}_-$ to its expanding counterpart $\tilde{\mathcal{C}}_+$. However, since $\tilde{\mathcal{N}}$ is a degenerate point (see §5.2.4) where $R = \Theta = \dot{\Theta} = 0$, orbits in the collapsing sector 2_- approach $\tilde{\mathcal{N}}$ asymptotically in the future while the orbits in the expanding sector 2_+ approach $\tilde{\mathcal{N}}$ asymptotically in the past. These orbit cannot move through point $\tilde{\mathcal{N}}$ and do therefore not represent bounce solutions.

We note that in sector 5 bounce cosmologies exist in which we first have expansion towards $\tilde{\mathcal{M}}$, and then asymptotic collapse towards $\tilde{\mathcal{N}}$. As noted above, these orbits cannot cross at $\tilde{\mathcal{N}}$, otherwise re-expansion to $\tilde{\mathcal{M}}$ with a final recollapse towards $\tilde{\mathcal{A}}_-$ could have been possible. Thus cyclic universes are not possible in this scenario, since it would require passing through a degenerate state represented by the point $\tilde{\mathcal{N}}$.

Comparing to [81], we observe that the orbits connecting points 4 and 6 in [81] correspond to the orbits between points $\tilde{\mathcal{C}}_-$ and $\tilde{\mathcal{N}}$ in the compact analysis for the case $n \in (1, N_+)$ considered here, while the orbits connecting points 3 and 5 correspond to

[4] Exact solutions corresponding to these bounces are given in [153].

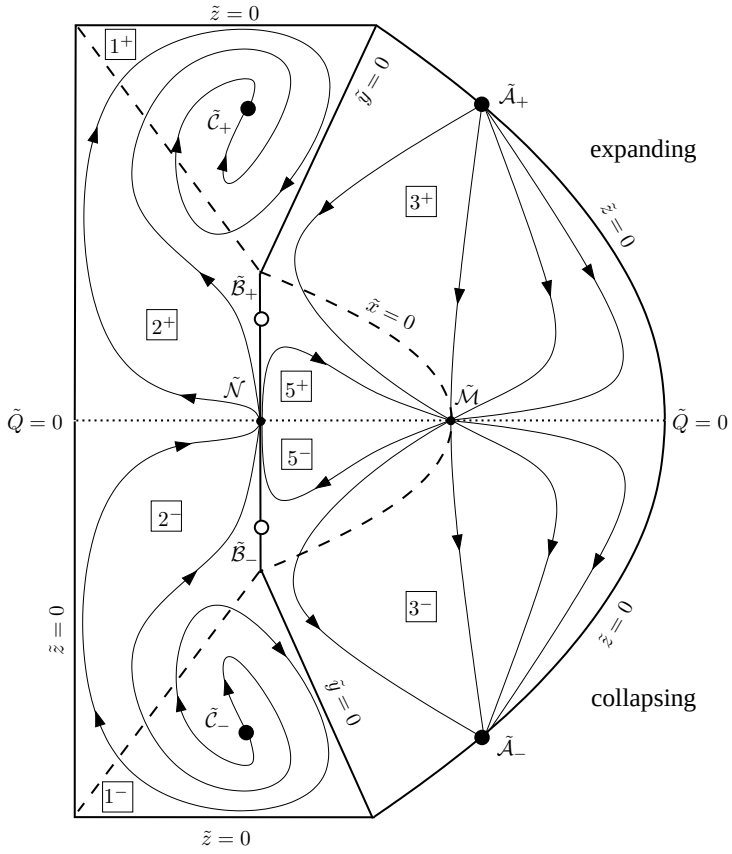

Figure 5.4: Compact state space of the flat ($k = 0$) Friedmann models with $n \in (1, N_+)$ and $w = 0$. The equilibrium point $\tilde{\mathcal{B}}_\pm$ is represented by a hollow circle because it only has a corresponding cosmological solution for the bifurcation value $w = 2/3$. The dotted line represents the points with $\tilde{Q} = 0$, but only the points $\tilde{\mathcal{M}}$ with $\tilde{x} = \tilde{Q} = 0$ and $\tilde{\mathcal{N}}$ with $\tilde{y} = \tilde{Q} = 0$ may have associated solutions to the underlying cosmological equations.

the orbits between points $\tilde{\mathcal{C}}_+$ and $\tilde{\mathcal{N}}$. We observe again that the bounce and recollapse behaviours found in [81] are recovered in this compact analysis.

The qualitative results remain unchanged when considering radiation dominated regimes with $w = 1/3$, the only difference being that point $\tilde{\mathcal{B}}_\pm$ moves closer towards the intersection of $\tilde{y} = 0$ and $\tilde{x} = 0$.

5.4 Remarks and Conclusions

In this work, we compared the use of compact and non-compact variables for a dynamical systems analysis of alternative theories of gravity. We first considered state spaces where expansion–normalised variables were used. These expansion–normalised

variables were first introduced in the context of flat FLRW models in GR [159], where they define a compact state space. This compactness is desirable for determining the global behaviour of cosmological models and was one of the original reasons for introducing expansion–normalised variables in dynamical systems theory applied to cosmology. In [147] a method to compactify the state space of more general cosmologies was introduced, which was successfully applied to a modified theory of gravity in the previous chapter.

We here showed that when non-compact expansion normalised–variables are used, we are restricted to expanding or contracting cosmological models only. Static solutions and bouncing or recollapsing type solutions lie at or approach infinity in this framework. This was illustrated in §5.2, where we compared the expansion–normalised compact (chapter 4) and non-compact (chapter 3) state spaces of LRS Bianchi I models in R^n-gravity. While the works agree for the finite points in the non–compact analysis with $y \neq 0$, discrepancies were found for the points with $y = 0$ and the points at infinity. For $y = 0$, which corresponds to the limit of vanishing Ricci curvature, differences with respect to the existence of solutions at the given points were observed. At infinity in the non–compact analysis, both the occurrence of equilibrium points and the exact solutions at the equilibrium points differs in places from the results obtained in the compact analysis. For example, we found that the asymptotic points in chapter 3 only have analogs in the compact analysis for specific values of the parameter n. The asymptotic equilibrium point $\mathcal{D}_\infty$ does not have a counterpart in the compact analysis at all - it only appears to be an equilibrium point in non compact analysis because the collapsing part of the state space is not included in this case.

We resolved these problems and found the approach used in the compact analysis (chapter 4) more straightforward to analyse: Since there are no infinities in this framework, the opportunity to miss relevant information is reduced.

In §5.3 we extended our comparison of formalisms by considering the non-compact non–expansion–normalised variables used in [81]. We compared the results of [81] with the compact analysis of chapter 4 for the flat Friedmann models. As in the first example, the points at infinity only have corresponding equilibrium points in the compact analysis for specific values of n and/or w. Unlike in chapter 3, bounce and recollapse behaviours could be investigated in the framework of [81], and we recover these results in the compact formalism.

We note that in both non-compact formalisms [82] (chapter 3) and [81], the equilibrium points at infinity are associated with a divergence in the respective dynamical

systems time variable τ. When expansion–normalised variables are used, τ diverges when $\Theta \to 0$, while in framework of [81] τ diverges when the matter density becomes negligible. This divergence however does not seem to effect the stability of the equilibrium points at infinity, since the same results were found in the compact analysis.

Finally, we observe that in both non-compact analyses considered here, there are more equilibrium points found than in the corresponding compact analysis. In the non-compact analysis of chapter 3 for example, five individual equilibrium points and a line of points were found for the expanding LRS Bianchi I vacuum models, while in the corresponding compact analysis only one equilibrium point and a line of equilibrium points were found in the expanding subset. Similarly, for the flat Friedmann model, five pairs of (expanding and collapsing) equilibrium points were found in [81], while only three pairs of points were found in the compact analysis. The detailed comparison in sections 5.2 and 5.3 of this chapter shows that there are two main reasons for the additional equilibrium points in the non-compact analyses [82] and [81]. The first is the duplication of equilibrium points at infinity: we find that in the non–compact analysis [81] two copies of same point in the finite analysis (here points $5, 6$) are created, and while static points exist only for special parameter values in the compact analysis, they have analogs at infinity in [82] (chapter 3) for all values of n (see Tables 5.1, 5.2 and 5.3). Secondly, some points which are classified as equilibrium points in the non-compact analysis, are not equilibrium points in the compact analysis. In the examples studied here, this applies to points $\mathcal{D}_\infty$ in chapter 3 and $5, 6$ in [81], which correspond to $\tilde{\mathcal{M}}$ and $\tilde{\mathcal{N}}$ respectively.

In conclusion, we have shown that it is advantageous to compactify the state space whenever possible. The use of appropriately constructed compact variables allows for a clear and complete analysis including static, bouncing and recollapsing solutions and avoids the complications caused by equilibrium points at infinity.

Chapter 6

Cosmological dynamics of Scalar Tensor Gravity

In this chapter, we consider the problem of determining the global dynamics of Friedmann—Lemaître–Robertson–Walker (FLRW) cosmologies of STG. We will study a generic class of STG theories, where quadratic non–minimal couplings to gravity and self–interaction power–law potentials are assumed. This class of models is strictly related to the String Dilaton action and naturally exhibit duality in the cosmological solutions [160]. Furthermore, they can be obtained from generic non–minimally coupled scalar–tensor Lagrangians if Noether symmetries are found in the dynamics [122, 161]. Several exact solutions of these models have been found, but the stability and global behaviour is still not well understood. Our aim is to give a full description of the global dynamics of this class of STG and determine if cosmic histories are possible that (i) present a transient matter–dominated Friedmann phase and then evolve towards an accelerated (dark energy–dominated or ΛCDM) regime or (ii) present a first unstable inflationary phase and a second inflationary attractor.

We will focus on models where the non–minimal coupling has the form $F(\phi) = \xi\phi^2$ and the self-interaction potential is taken to be an arbitrary power law of the form $V(\phi) = \lambda\phi^n$. This choice is general and motivated by several mathematical and physical reasons. In particular, beside the string-dilaton and BD actions, several effective quantum field theories, in low energy physics, can be related to such couplings and self–interacting potentials [16, 162]. Furthermore, this coupling and potential satisfy the requirement of Noether symmetries for the Lagrangian in (2.22), giving rise to general exact solutions of physical interest [161].

A final remark concerns the parameters of the theory. Very different models can be parameterised by the set (ξ, λ, n), but not all the combinations of these parameters are

necessarily physical. For example, attractive gravity is achieved for $\xi > 0$ and $\lambda > 0$, although physically interesting situation can also be achieved for $\xi < 0$, $\lambda < 0$ [163]. In this thesis, we will consider only the physical case $\xi > 0$, $\lambda > 0$.

6.1 The FLRW dynamical system

In order to analyse the phase-space of the Scalar Tensor FLRW cosmologies, the field equations need to be recast in a dynamical system form. In the FLRW metric and with our choice of coupling and potential the Einstein-Klein-Gordon equations given in §2.2, reduce to:

$$\dot{\Theta} + \frac{1}{3}\Theta^2 + \frac{\dot{\phi}}{\phi}\Theta + 3\frac{\ddot{\phi}}{\phi} + 3\left(1 + \frac{1}{6\xi}\right)\frac{\dot{\phi}^2}{\phi^2} - \frac{\lambda}{2\xi}\phi^{n-2} + \frac{\mu}{2\xi\phi^2}(1+3w) = 0, \quad (6.1)$$

$$\frac{1}{3}\Theta^2 + 2\frac{\dot{\phi}}{\phi}\Theta - \frac{\lambda}{2\xi}\phi^{n-2} - \frac{1}{4\xi}\frac{\dot{\phi}^2}{\phi^2} - \frac{\mu}{\xi\phi^2} + \frac{1}{2}{}^3R = 0, \quad (6.2)$$

$$\frac{\ddot{\phi}}{\phi} + \frac{\dot{\phi}}{\phi}\Theta - 2\xi\left(2\dot{\Theta} + \frac{4}{3}\Theta^2 + {}^3R\right) + n\lambda\phi^{n-2} = 0, \quad (6.3)$$

where the first is the cosmological equation for the acceleration, the second is the Hamiltonian constraint, i.e. the $\{0,0\}$ equation, and the third is the Klein-Gordon equation. We have also assumed standard matter to be a perfect fluid with a barotropic index w, so that the conservation equation yields

$$\dot{\mu} = -(1+w)\Theta\mu\,, \quad (6.4)$$

where μ is the the matter-energy density. In what follows, since we want to stress the role of a non minimally coupled scalar field in the modeling of dark energy, we will consider only $0 \leq w \leq 1$. Other values of these parameters, which can be associated with more exotic forms of matter energy densities, although interesting, will not be considered here.

The equations above can be converted into an autonomous system of first-order differential equations by defining the following set of expansion normalised variables:

$$x = \frac{3\dot{\phi}}{\phi\Theta}, \qquad y = \frac{3\lambda\phi^{n-2}}{2\xi\Theta^2},$$
$$z = \frac{3\mu}{\xi\phi^2\Theta^2}, \qquad K = \frac{3\,{}^3R}{2\Theta^2}, \quad (6.5)$$

from which we obtain

$$\begin{aligned}
x' &= \frac{1}{1+12\xi}\Big[12\xi\,(1+K+Kx)-2(1-6\xi)x-(5+24\xi)x^2+\left(1+\tfrac{1}{6\xi}\right)x^3 \\
&\quad -6\xi(n-2)y-(1+6n\xi)xy-6\xi(1+3w)z+\frac{1}{2}(1+3w)xz\Big], \\
y' &= \frac{2y}{1+12\xi}\left[1+24\xi+12\xi K-2x+\tfrac{1}{2}(1+12\xi)(n-2)x\right. \\
&\quad \left.+\left(1+\tfrac{1}{6\xi}\right)x^2-(1+6n\xi)y+\frac{1}{2}(1+3w)z\right], \qquad (6.6)\\
z' &= \frac{z}{1+12\xi}\left[12\xi-1-3w(1+12\xi)+24\xi K-6(1+4\xi)x\right. \\
&\quad \left.+2\left(1+\tfrac{1}{6\xi}\right)x^2-2(1+6n\xi)y+(1+3w)z\right], \\
K' &= \frac{2K}{1+12\xi}\left[12\xi(1+K)-2x+\left(1+\tfrac{1}{6\xi}\right)x^2-(1+6n\xi)y+\frac{1}{2}(1+3w)z\right],
\end{aligned}$$

where primes denote derivatives with respect to a new evolution variable $\tau=\ln a$ and the dynamical variables are constrained by

$$1+2x-\tfrac{1}{12\xi}x^2-y+K-z=0. \qquad (6.7)$$

The associated phase-space is 4-dimensional and the evolution is constrained by (6.7). The task is now to study the structure of such a space: this means finding the stability of the fixed points, and then to analyse the evolution of trajectories [88]. We will consider two cases: the vacuum case ($\mu=0$) and the matter case ($\mu\neq 0$).

6.2 The vacuum case

When we consider the vacuum case ($\mu=0$), the set of dynamical equations (6.6) reduces to

$$\begin{aligned}
x' &= \frac{1}{1+12\xi}\Big[12\xi\,(1+K+Kx)-2(1-6\xi)x-(5+24\xi)x^2+\left(1+\tfrac{1}{6\xi}\right)x^3 \\
&\quad -6\xi(n-2)y-(1+6n\xi)xy\Big], \\
y' &= \frac{2y}{1+12\xi}\left[1+24\xi+12\xi K-2x+\tfrac{1}{2}(1+12\xi)(n-2)x\right. \qquad (6.8)\\
&\quad \left.+\left(1+\tfrac{1}{6\xi}\right)x^2-(1+6n\xi)y\right], \\
K' &= \frac{2K}{1+12\xi}\left[12\xi(1+K)-2x+\left(1+\tfrac{1}{6\xi}\right)x^2-(1+6n\xi)y\right],
\end{aligned}$$

with the constraint equation given by

$$1 + 2x - \tfrac{1}{12\xi}x^2 - y + K = 0\,. \tag{6.9}$$

In this case, the phase-space is 3-dimensional.

6.2.1 Finite analysis

We can further simplify the system (6.8) by implementing the constraint (6.9):

$$\begin{aligned} x' &= -2x - 4x^2 + \tfrac{1}{6\xi}x^3 - \frac{y}{1+12\xi}\left[6\xi(n-4) + (6\xi(n-2)+1)x\right], \\ y' &= y\left[2 + (n-6)x + \tfrac{1}{3\xi}x^2 - \frac{2(6\xi(n-2)+1)}{1+12\xi}y\right]. \end{aligned} \tag{6.10}$$

From these equations, it is clear that the x axis ($y = 0$), characterised by the absence of a potential for the scalar field, is an invariant submanifold. This tells us that there is no orbit for which the potential of the scalar field can become exactly zero and that if the potential is initially set to zero, it will remain zero.

The fixed points can be obtained by setting $x' = 0$ and $y' = 0$. For the system (6.10) we obtain five fixed points (see Table 6.1). The coordinate of the point $\mathcal{A}$ is independent of ξ and n and the ones of $\mathcal{B}$ and $\mathcal{C}$ are independent of n. The point $\mathcal{D}$ is a finite fixed point for $n \neq 2$ and $\mathcal{E}$ a finite fixed point for $n \neq -\frac{(1+4\xi)}{2\xi}$.

Merging occurs for the points $\mathcal{E}$ and $\mathcal{B}$, and $\mathcal{E}$ and $\mathcal{C}$ for $n = 4 \pm \frac{\sqrt{3}\sqrt{\xi(1+12\xi)}}{\xi}$ respectively. The point $\mathcal{E}$ also merges with $\mathcal{D}$ for $n = 4 \mp \sqrt{\frac{1+12\xi}{\xi}}$.

All the fixed points except $\mathcal{A}$ and $\mathcal{D}$ are associated with flat spatial geometry. Point $\mathcal{A}$ is associated with an open spatial geometry and for $\mathcal{D}$ the sign of the space curvature depends on ξ and n: $K_{\mathcal{D}}$ is positive for $n \neq 2$, $n \in \left(4 - \sqrt{\frac{1+12\xi}{\xi}}\,, 4 + \sqrt{\frac{1+12\xi}{\xi}}\right)$ and negative otherwise.

The stability of the fixed points can be determined by evaluating the eigenvalues of the Jacobian matrix associated with the system (6.10) (see Table 6.3), as prescribed by the Hartman-Grobman Theorem [119] [1].

The fixed point $\mathcal{A}$ is a saddle for every value of the parameters ξ and n. The point $\mathcal{B}$ can either be a stable node or a saddle node whereas $\mathcal{C}$ is either an unstable node or a saddle node, depending on the values of ξ and n. The eigenvalues of $\mathcal{D}$ and $\mathcal{E}$ are both dependent on ξ and n so that the stability varies over the different ranges

[1] The values of the parameter for which the eigenvalues are zero are bifurcations for the dynamical system. In this chapter we will not give an analysis of the bifurcations referring the reader to the specific literature for more details.

of ξ and n. The stability of these fixed points have been summarised in Table 6.4.

The coordinates of the fixed points may be used to determine exact cosmological solutions at the fixed points themselves. In fact, when evaluated at these points, the Friedmann and the Klein-Gordon equations can be written as:

$$\dot{\Theta} = -\frac{\Theta^2}{3\alpha}, \qquad \alpha = \left[1 - 2x_i + \tfrac{1}{6\xi}x_i^2 - \left(\tfrac{6\xi(n-2)+1}{1+12\xi}\right) y_i\right]^{-1}, \tag{6.11}$$

$$\frac{\ddot{\phi}}{\phi} = -\frac{\beta}{9}\,\Theta^2\,, \qquad \beta = 3x_i + x_i^2 + \tfrac{6\xi(n-4)}{1+12\xi}y_i, \tag{6.12}$$

where (x_i, y_i) represent the coordinates of the fixed points. Integrating (6.11) and substituting into (6.12) gives

$$\frac{\ddot{\phi}}{\phi} + \frac{\alpha^2\beta}{(t-t_0)^2} = 0, \tag{6.13}$$

which has a Cauchy-Euler form. If the terms α and β are different from zero, equations (6.11) and (6.13) can be easily integrated, giving

$$a = a_0\,(t-t_0)^{\alpha}\,, \tag{6.14}$$

and

$$\phi = \begin{cases} (t-t_0)^{1/2}\left[\phi_0\,(t-t_0)^m + \phi_1\,(t-t_0)^{-m}\right]\,, & \text{if } \alpha^2\beta < \frac{1}{4}\,, \\ (t-t_0)^{1/2}\,(\phi_0 + \phi_1 \ln t)\,, & \text{if } \alpha^2\beta = \frac{1}{4}\,, \\ (t-t_0)^{1/2}\,(\phi_0 \sin\left[m\ln\left(t-t_0\right)\right] + \phi_1 \cos\left[m\ln\left(t-t_0\right)\right])\,, & \text{if } \alpha^2\beta > \frac{1}{4}\,, \end{cases} \tag{6.15}$$

where

$$m = \frac{1}{2}\sqrt{1 - 4\alpha^2\beta}. \tag{6.16}$$

In the case of point $\mathcal{A}$, we have a Milne evolution and a constant scalar field

$$\alpha_{\mathcal{A}} = 1, \qquad \phi_{\mathcal{A}} = \phi_0. \tag{6.17}$$

The above solution (as well as some others that will follow) is quite interesting because the scalar field is *constant*. This implies that $\mathcal{A}$ represents a state in which G_{eff} is constant and the potential of the scalar field acts as a cosmological constant. In other words, at this point, scalar tensor gravity is indistinguishable from standard GR plus cosmological constant.

For the point $\mathcal{B}$ the solutions are given by (6.14) and (6.15) with

$$\alpha_{\mathcal{B}} = \frac{1}{3(1+8\xi) - 4\sqrt{3\xi(1+12\xi)}}\,, \qquad m_{\mathcal{B}} = \frac{3}{6(1+8\xi) - 8\sqrt{3\xi(1+12\xi)}}\,, \quad (6.18)$$

and for point $\mathcal{C}$

$$\alpha_{\mathcal{C}} = \frac{1}{3(1+8\xi) + 4\sqrt{3\xi(1+12\xi)}}\,, \qquad m_{\mathcal{C}} = \frac{3}{6(1+8\xi) + 8\sqrt{3\xi(1+12\xi)}}\,. \quad (6.19)$$

Note that, for $\xi > 0$, the value of α for the above two solutions is always positive and less than 1 i.e. these two solution always represent two Friedmann-like solutions. In addition, $\mathcal{B}$ represents a solution in which the scalar field is growing, while at $\mathcal{C}$, ϕ is dissipating. If $n \neq 2$, the point $\mathcal{D}$ is associated with

$$\alpha_{\mathcal{D}} = 1, \qquad m_{\mathcal{D}} = \frac{n+2}{2(n-2)}, \quad (6.20)$$

which represents another Milne solution, while the scalar field is decreasing for $n < 2$ and increasing for $n > 2$. It is interesting that, unlike the Milne solution in GR, this linear solution for a is not necessarily a spatially hyperbolic one. The constant a_0 can be related to the parameters ξ and n for non-flat solutions:

$$a_0^2 = \frac{k(n-2)^2\xi}{1-[4+n(n-8)]\xi}. \quad (6.21)$$

When $n = 2$, $\mathcal{D}$ becomes an asymptotic fixed point and merges with $\mathcal{D}_\infty$ (its solution will be presented within the asymptotic analysis). Finally, for point $\mathcal{E}$ we have

$$\alpha_{\mathcal{E}} = \frac{2(n+2)\xi + 1}{(n-4)(n-2)\xi}, \qquad m_{\mathcal{E}} = \frac{n+2}{2(n-2)} \quad (6.22)$$

for all $n \neq 2,\ 4$. This solution represent an expansion for $n \in \left(-\frac{(1+4\xi)}{2\xi}, 2\right)$ and $n > 4$ and was already found in other contexts [97, 99, 164–166]. In particular, in [166] it is shown that for $n \in (2, 4)$ the scale factor associated to this point evolves towards a superinflating state (also called "Big Rip" singularity) without including any exotic feature like ghosts or non standard fluids. When $n = 2$ and $n = 4$, using the cosmological equations we obtain the solutions

$$a = a_0\,, \qquad \phi = \phi_0\ (\lambda = 0)\,, \quad (6.23)$$

$$a = a_0 e^{C(t-t_0)}, \qquad \phi = \phi_0 = \pm\sqrt{\tfrac{6\xi C^2}{\lambda}}\,, \quad (6.24)$$

which represent a static universe and a de Sitter evolution respectively. In both

Table 6.1: The coordinates and scale factor solutions of the fixed points for the vacuum case. We only show the exponent α of the solutions (6.14).

Point	Coordinates (x, y)	K	α
$\mathcal{A}$	$(0,\ 0)$	-1	1
$\mathcal{B}$	$\left(2(6\xi - \sqrt{3\xi(1+12\xi)}),\ 0\right)$	0	$\frac{1}{3(1+8\xi)-4\sqrt{3\xi(1+12\xi)}}$
$\mathcal{C}$	$\left(2(6\xi + \sqrt{3\xi(1+12\xi)}),\ 0\right)$	0	$\frac{1}{3(1+8\xi)+4\sqrt{3\xi(1+12\xi)}}$
$\mathcal{D}$	$\left(-\frac{2}{n-2},\ \frac{2+24\xi}{3\xi(n-2)^2}\right)$	$\frac{1-[4+n(n-8)]\xi}{(n-2)^2\xi}$	$1,\ \left(a_0^2 = \frac{k(n-2)^2\xi}{1-[4+n(n-8)]\xi}\right)$
$\mathcal{E}$	$\left(\frac{2(4-n)\xi}{1+2(n+2)\xi},\ \frac{(1+12\xi)[3-(n-10)(n+2)\xi]}{3(1+2(n+2)\xi)^2}\right)$	0	$\begin{cases} \frac{2(n+2)\xi+1}{(n-4)(n-2)\xi}, & n \neq 2,\ 4 \\ a = a_0, & n = 2 \\ a = a_0 e^{C(t-t_0)}, & n = 4 \end{cases}$

these cases an effective cosmological constant is present, whose value depends on the effective gravitational constant (via ϕ_0) and the coupling constant λ of the self-interaction of the scalar field. Again, since the scalar field is constant in these cases, these solution are indistinguishable from the GR solutions. The difference with point $\mathcal{A}$ is that the solution does not occur in "pure" GR and can also be stable. This is particularly interesting in the second case ($n = 4$) in which a de-Sitter solution able to mimic an inflationary or dark energy phase in a Λ GR cosmology is a semi-global attractor. The possibility that scalar tensor gravity could converge to GR has been proposed within the context of extended inflation both with the aid of numerical techniques [167] and a more formal proof [168]. The dynamical system approach allows one to see this phenomenon in a very clear way, even in the more general case of a non-zero potential. It turns out that the nature of the potential, determined in our case by the value of n, together with the value of the coupling plays a critical role in the realisation of this mechanism.

It is useful to define the deceleration parameter q in terms of the dynamical variables:

$$q = -2x_i + \tfrac{1}{6\xi}x_i^2 - \left(\tfrac{1-12\xi+6\xi n}{1+12\xi}\right) y_i. \tag{6.25}$$

This equation represents a parabola in the state space that divides the accelerating ($-1 < q < 0$) expansion phases from the decelerating ($q > 0$) ones. De Sitter and static solutions are represented by $q = -1$. Points $\mathcal{A}$ and $\mathcal{D}$ lie on the curve (6.25) as expected by the form of their scale factor solutions. On the other hand $\mathcal{B}$ and $\mathcal{C}$ always lie on the decelerated expansion side of the curve. Instead, for $\mathcal{E}$ we have accelerated expansion for $n \in \left(-\frac{(1+4\xi)}{2\xi}, 4 - \sqrt{\frac{1+12\xi}{\xi}}\right)$ or $n > 4 + \sqrt{\frac{1+12\xi}{\xi}}$ and a decelerated one

Table 6.2: Values of the parameter m and the corresponding scalar field solutions for the fixed points in vacuum.

Point	m	Solutions
$\mathcal{A}$	$\frac{1}{2}$	$\phi = \phi_1, \qquad \phi_0,\ \lambda = 0$
$\mathcal{B}$	$\frac{3}{6(1+8\xi)-8\sqrt{3\xi(1+12\xi)}}$	$\phi = \phi_0(t-t_0)^{1/2+m},\ \ \phi_1,\ \lambda = 0$
$\mathcal{C}$	$\frac{3}{6(1+8\xi)+8\sqrt{3\xi(1+12\xi)}}$	$\phi = \phi_1(t-t_0)^{1/2-m},\ \ \phi_0,\ \lambda = 0$
$\mathcal{D}$	$\frac{n+2}{2(n-2)}$	$\begin{cases} \phi = \phi_0^{\mathcal{D}}(t-t_0)^{1/2}, & n = -2 \\ \phi = \phi_1^{\mathcal{D}}(t-t_0)^{1/2-m}, & n \neq -2,\ 2 \\ \phi_0^{\mathcal{D}} = \pm\left(\frac{4\lambda}{1+12\xi}\right)^{\frac{1}{4}}, & \phi_1^{\mathcal{D}} = \left(\frac{4(1+12\xi)}{\lambda(n-2)^2}\right)^{\frac{1}{n-2}} \end{cases}$
$\mathcal{E}$	$\frac{n+2}{2(n-2)}$	$\begin{cases} \phi = \phi_0^{\mathcal{E}}(t-t_0)^{1/2}, & n = -2 \\ \phi = \phi_1^{\mathcal{E}}(t-t_0)^{1/2-m}, & n \neq -2,\ 2,\ 4 \\ \phi_0^{\mathcal{E}} = \pm 2\left(\frac{6\lambda\xi}{1+12\xi}\right)^{\frac{1}{4}}, & \\ \phi_1^{\mathcal{E}} = \left(\frac{2(1+12\xi)[3+(n-10)(n+2)\xi]}{\lambda\xi(n-2)(n-4)}\right)^{\frac{1}{n-2}} & \end{cases}$

Table 6.3: The eigenvalues associated with the fixed points in the vacuum model.

Point	Eigenvalues
$\mathcal{A}$	$[-2, 2]$
$\mathcal{B}$	$\left[4(1+12\xi) - 8\sqrt{3\xi(1+12\xi)},\ 6 + 2(n+2)\left(6\xi - \sqrt{3\xi(1+12\xi)}\right)\right]$
$\mathcal{C}$	$\left[4(1+12\xi) + 8\sqrt{3\xi(1+12\xi)},\ 6 + 2(n+2)\left(6\xi + \sqrt{3\xi(1+12\xi)}\right)\right]$
$\mathcal{D}$	$\left[\frac{(4-n)\xi - \sqrt{\xi\{3(8-n)n\xi+4\}}}{(n-2)\xi},\ \frac{(4-n)\xi + \sqrt{\xi\{3(8-n)n\xi+4\}}}{(n-2)\xi}\right]$
$\mathcal{E}$	$\left[\frac{(n-10)(n+2)\xi-3}{1+2(n+2)\xi},\ \frac{2(4+(n-8)n))\xi-2}{1+2(n+2)\xi}\right]$

Table 6.4: Stability of the fixed points in the vacuum case. The parameters are $N_\pm = 4 \pm \sqrt{3(1+12\xi)/\xi}$ and $Q_\pm = 4 \pm \sqrt{(1+12\xi)/\xi}$.

	Range of n			
Points	$(-\infty, -\frac{(1+4\xi)}{2\xi})$	$[-\frac{(1+4\xi)}{2\xi}, N_-)$	(N_-, Q_-)	$(Q_-, 2)$
$\mathcal{A}$	saddle	saddle	saddle	saddle
$\mathcal{B}$	repeller	repeller	repeller	repeller
$\mathcal{C}$	saddle	saddle	repeller	repeller
$\mathcal{D}$	attractor	attractor	attractor	saddle
$\mathcal{E}$	attractor	repeller	saddle	attractor

	$(2, Q_+)$	(Q_+, N_+)	(N_+, ∞)
$\mathcal{A}$	saddle	saddle	saddle
$\mathcal{B}$	repeller	repeller	saddle
$\mathcal{C}$	repeller	repeller	repeller
$\mathcal{D}$	saddle	attractor	attractor
$\mathcal{E}$	attractor	saddle	repeller

for $n < -\frac{(1+4\xi)}{2\xi}$ or $n \in \left(4 - \sqrt{\frac{1+12\xi}{\xi}}, 4 + \sqrt{\frac{1+12\xi}{\xi}}\right)$.

6.2.2 Asymptotic analysis

Since the dynamical system (6.10) is not compact, it might admit an asymptotic structure that is relevant for the global dynamics. In order to analyse the asymptotic features of the phase space, we use the Poincaré projection [97, 169]. This method consists of transforming to the polar coordinates

$$x = \bar{r}\cos\psi, \qquad y = \bar{r}\sin\psi \tag{6.26}$$

and setting $\bar{r} = \frac{\sqrt{r}}{1-r}$. In this way, the asymptotic regime is achieved for $r \to 1$. Using the Poincaré projection, the asymptotic form of the dynamical equations (6.10) read

$$r' = \frac{\cos^2\psi\ (3 - \cos 2\psi)}{12\xi}, \tag{6.27}$$

$$\psi' = \frac{\cos^3\psi\ \sin\psi}{6\xi(1-r)^2}. \tag{6.28}$$

Note that the radial equation does not depend on the radial coordinate. This means that the fixed points can be obtained by only considering the equation for ψ'. Setting $\psi' = 0$ we obtain the four fixed points listed in Table 6.5.

The equilibrium points at infinity corresponds to $\Theta \to 0$, i.e. static behaviours.

Table 6.5: Coordinates, behaviour of the scale factor and stability of the asymptotic fixed points in the vacuum model.

Point	ψ	Stability	Range of n
$\mathcal{A}_\infty$	0	saddle	all
$\mathcal{B}_\infty$	$\frac{\pi}{2}$	$\begin{cases} \text{saddle} \\ \text{attractor} \end{cases}$	$\begin{cases} n < 2 - \frac{1}{6\xi}, (n = 2) \\ n > 2 - \frac{1}{6\xi}, (n \neq 2) \end{cases}$
$\mathcal{C}_\infty$	π	saddle	all
$\mathcal{D}_\infty$	$\frac{3\pi}{2}$	$\begin{cases} \text{attractor} \\ \text{saddle} \end{cases}$	$\begin{cases} n < 2 - \frac{1}{6\xi} \\ n > 2 - \frac{1}{6\xi} \end{cases}$

As pointed out in the previous chapters, these solutions only satisfy the coordinates of the equilibrium points but do not satisfy all the evolution equations, and are therefore unphysical.

The stability of the asymptotic fixed points is summarised in Table 6.5. The points $\mathcal{A}_\infty$ and $\mathcal{C}_\infty$ are saddles for every value of n and ξ. The points $\mathcal{B}_\infty$ and $\mathcal{D}_\infty$ are non-hyperbolic and they can be shown to represent saddle-nodes. This means that they behave like saddles or nodes depending on which direction the orbits approach them and that a local separatrix exists to divide the different stability domains. In our specific case this separatrix corresponds to the equator of the Poincaré sphere (i.e. our "infinity"), so that effectively $\mathcal{B}_\infty$ behaves as a saddle if $n < 2 - 1/6\xi$ or $n = 2$ and an attractor if $n > 2 - 1/6\xi$ $(n \neq 2)$, and $\mathcal{D}_\infty$ behaves like a saddle if $n > 2 - 1/6\xi$ (including $n = 2$) and an attractor if $n < 2 - 1/6\xi$. For both these point the separatrix (i.e. our unitary circle) is always attractive so that orbit may bounce off the saddle and then approach the point along the unitary circle (see for example Figure 6.1). A summary of the stability of the asymptotic fixed points is summarised in Table 6.5.

Since the state space is two dimensional we can easily draw phase space diagrams for the vacuum case. Here we will limit ourselves to four examples representing the global state space [2] for four specific values of (n, ξ) (see Figures 6.1-6.4) that includes the two cases in which the theory admits s a GR attractor.

[2]By "global state space" we mean the projection of the $\theta > \pi/2$ part of the Poincaré sphere on the plane that contains its equator.

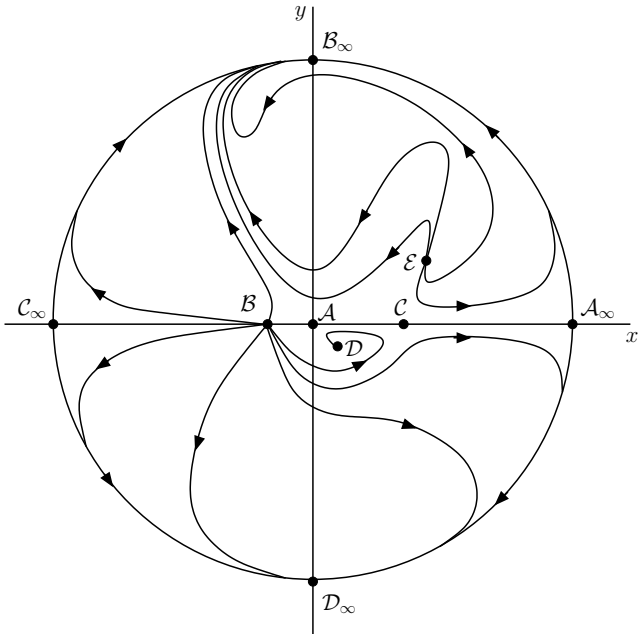

Figure 6.1: Global state space for $n \in \left(-\frac{(1+4\xi)}{2\xi}, 4-\sqrt{\frac{3(1+12\xi)}{\xi}}\right)$ (e.g. $n=-3$ and $\xi=0.35$). Note that the non hyperbolic point $\mathcal{B}_\infty$ correspond to a saddle everywhere but on the border of the circle in which it behaves as an attractor (see the text for details).

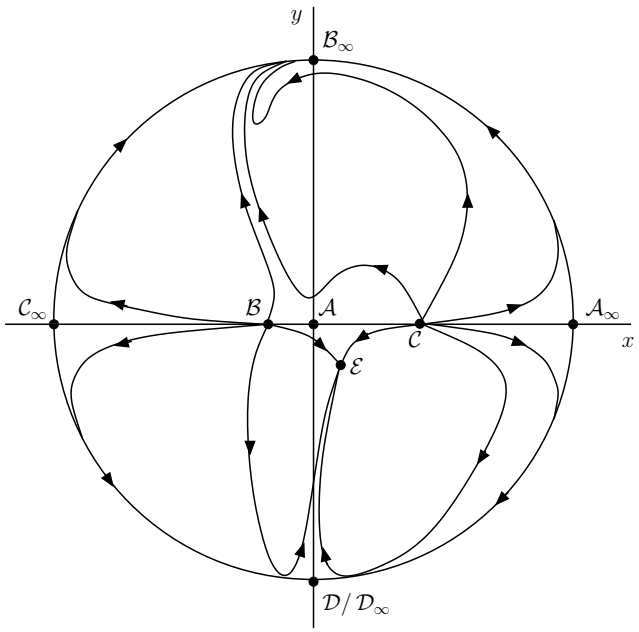

Figure 6.2: Global state space for $n=2$ with $\xi=1$.

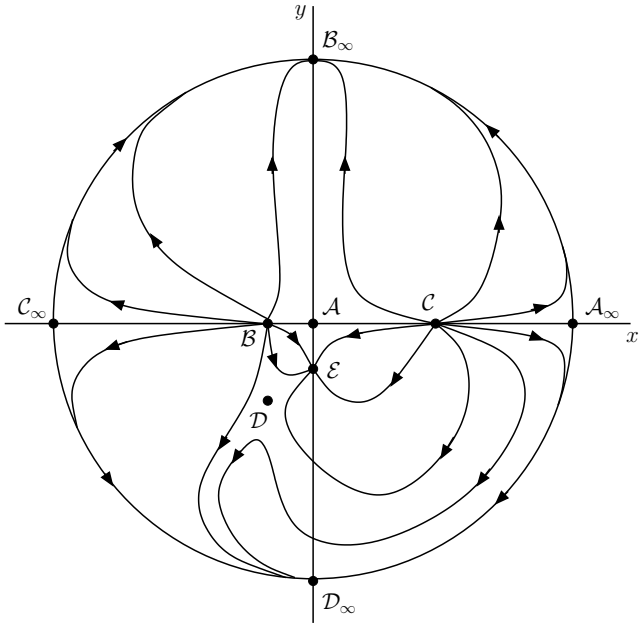

Figure 6.3: Global state space for $n \in \left(2\,, 4+\sqrt{\frac{1+12\xi}{\xi}}\right)$ (e.g. $n=4$ and $\xi=1$).

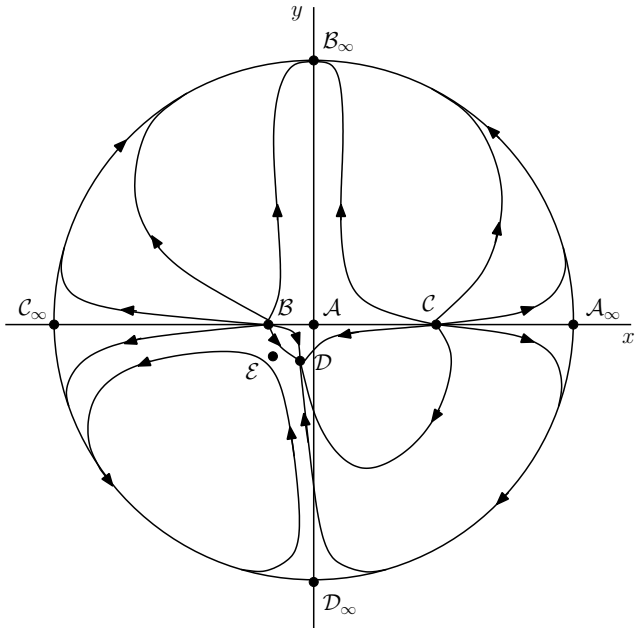

Figure 6.4: Global state space for $n \in \left(4-\sqrt{\frac{1+12\xi}{\xi}}\,, 4+\sqrt{\frac{3(1+12\xi)}{\xi}}\right)$ (e.g. $n=8$ and $\xi=1$).

6.3 The matter case

As we have seen in the system (6.6), the presence of matter in the dynamical system equations implies the introduction of another variable: z. Since μ is defined to be positive, the definition of the dynamical variables tells us that only negative values of z are compatible with attractive gravity. For this reason we will restrict the following analysis only to the physically relevant case $z \leqslant 0$.

As in the vacuum case, we can use the constraint (6.7) to eliminate one of the dynamical variables. The system (6.6) then reduces to:

$$\begin{aligned} x' &= \frac{-1}{1+12\xi}\left[2(1+12\xi)x + 4(1+12\xi)x^2 - \left(2+\tfrac{1}{6\xi}\right)x^3 + 6\xi(n-4)y \right. \\ &\quad \left. +(1+6\xi(n-2))xy + \tfrac{1}{2}(1+3w+24\xi)xz - 6\xi(1-3w)z\right], \\ y' &= \frac{y}{1+12\xi}\left[2(1+12\xi) + (1+12\xi)(n-6)x + 2\left(2+\tfrac{1}{6\xi}\right)x^2 \right. \\ &\quad \left. -2(1+6\xi(n-2))y + (1+3w+24\xi)z\right], \\ z' &= \frac{z}{1+12\xi}\left[-(1+3w)(1+12\xi) - 6(1+12\xi)x \right. \\ &\quad \left. +2\left(2+\tfrac{1}{6\xi}\right)x^2 - 2(1+6\xi(n-2))y + (1+3w+24\xi)z\right]. \end{aligned} \tag{6.29}$$

Since $y' = 0$ and $z' = 0$ are zero for $y = 0$ and $z = 0$, the two planes $y = 0$ and $z = 0$ corresponds to two invariant submanifolds. The first plane represents classes of theories in which the potential is zero, the second one classes of theories for which $z = 0$ and constitutes part of a vacuum invariant submanifold. The structure of the total vacuum invariant submanifold can be derived by writing the energy density in terms of the dynamical variables [82, 87]:

$$\mu \propto z y^{\frac{2}{n-2}} \Theta^{\frac{2n}{n-2}}. \tag{6.30}$$

It is clear that when $z = 0$ and $y \neq 0$ the energy density is zero. However when $y = 0$ and $z \neq 0$ the behaviour of μ depends on the value of n: the energy density is zero when $n > 2$, but it is divergent when $n < 2$. When both y and z are equal to zero, we can conclude that $\mu = 0$ only if $n > 2$. For $n < 2$ (6.30) is divergent and μ can only be obtained by directly solving the field equations.

6.3.1 Finite analysis

Setting $x' = 0$, $y' = 0$ and $z' = 0$ we obtain eight fixed points (see Table 6.6). The first five ($\mathcal{A}$, $\mathcal{B}$, $\mathcal{C}$, $\mathcal{D}$ and $\mathcal{E}$) sit in the $z = 0$ plane and have the same (x, y) coordinates of the corresponding vacuum fixed points. The coordinates of $\mathcal{F}$ and $\mathcal{G}$ are independent

of n and are finite for all ξ; $\mathcal{H}$ is a finite fixed point for $n \neq 0$ and merges with the asymptotic fixed subspace $\mathcal{L}_\infty$ for $n = 0$.

Merging occurs between the points $\mathcal{B}$, $\mathcal{C}$, $\mathcal{D}$, $\mathcal{E}$, $\mathcal{G}$ and $\mathcal{H}$. The first four points merge in the same way and for the same values of the parameters given in the vacuum case. Point $\mathcal{H}$ merges with $\mathcal{E}$ for $n = \frac{1}{2}\left(7 + 3w + \sqrt{\frac{\xi(9w^2+66w+73)+6(w+1)}{\xi}}\right)$; and with $\mathcal{G}$ when $n = \frac{3(w+1)(8\xi+1-w)}{4\xi(3w-1)}$.

All the fixed points but $\mathcal{A}$, $\mathcal{D}$, $\mathcal{F}$ are associated with flat solutions. $\mathcal{A}$ is associated with negative curvature and the sign of the spatial curvature for point $\mathcal{D}$ and $\mathcal{F}$ depends on the value of n and ξ.

The stability of the fixed points may be determined using the Hartman-Grobman theorem as in the vacuum case. The point $\mathcal{A}$ is a saddle for every value of w. Point $\mathcal{B}$ keeps the same stability found in the vacuum case for $w = 0$ and $1/3$, but it is always a saddle when $w = 1$. Instead, the stability of points $\mathcal{C}$ and $\mathcal{D}$ is the same as in the vacuum case for every value of w. Point $\mathcal{E}$ varies its stability with ξ, n, w and can behave like an attractor, a repeller or a saddle as shown in Table 6.10. On the other hand, the fixed points $\mathcal{F}$ and $\mathcal{G}$ are saddles for every value of the parameters. Finally, $\mathcal{H}$ is a saddle or a saddle focus for $w = 0$ and $w = 1/3$, while for $w = 1$ it can also be a repeller or an anti-spiral. Its stability is summarised in Table 6.11.

As in the vacuum case the coordinates of the fixed points can be used to find exact solutions for the evolution of the scale factor. From (6.1) and (6.3) we have

$$\dot{\Theta} + \frac{\Theta^2}{3\alpha} = 0, \qquad \alpha = \left[1 - 2x_i + \tfrac{1}{6\xi}x_i^2 - \left(\tfrac{1-12\xi+6\xi n}{1+12\xi}\right) y_i + \left(\tfrac{1+3w+24\xi}{2+24\xi}\right) z_i\right]^{-1} , \quad (6.31)$$

$$\frac{\ddot{\phi}}{\phi} + \frac{\alpha_m^2 \beta}{(t-t_0)^2} = 0, \qquad \beta = 3x_i + x_i^2 + \tfrac{6\xi(n-4)}{1+12\xi} y_i - \tfrac{6\xi(1-3w)}{1+12\xi} z_i \ , \quad (6.32)$$

where (x_i, y_i, z_i) represents the coordinates of the fixed points. For α and β different from zero, these equations have solutions of the form (6.14) and (6.15).

The points $\mathcal{A}$, $\mathcal{B}$, $\mathcal{C}$, $\mathcal{D}$ and $\mathcal{E}$ have the same solutions as in the vacuum case, since for these points $z = 0$. In particular the convergence mechanism of scalar tensor gravity towards GR is preserved when matter is present. Such a result was expected since in [167] and [168] this phenomenon is described when matter is present. The point $\mathcal{F}$ is associated to the Milne evolution and a constant scalar field

$$\alpha_{\mathcal{F}} = 1 \qquad \phi_{\mathcal{F}} = \phi_0 \ , \quad (6.33)$$

the value of the constant a_0 being influenced by the parameters ξ and w for non-zero

spatial curvature

$$a_0^2 = \frac{16k\xi}{w(3w-2)-1-16\xi}. \tag{6.34}$$

However, a direct check of the equations reveals that this solution is valid only for $w = -1/3$, which is outside the Zel'dovich interval. For point $\mathcal{G}$ we have

$$\alpha_{\mathcal{G}} = \frac{2(8\xi+1-w)}{32\xi+3(1-w^2)}, \qquad m_{\mathcal{G}} = \frac{3(1-w^2)+16\xi(1+3w)}{2\left(3(1-w^2)+32\xi\right)}\,. \tag{6.35}$$

This solution represents a Friedmann like expansion with the exponent depending on both ξ and w. Direct comparison with the cosmological equations reveals that this solution is physical only for $w > 2/3$ and $w \neq 1$.

Finally, point $\mathcal{H}$ with $n \neq 2$ is linked to a solution that a first glance resembles a well known Friedmann GR one:

$$\alpha_{\mathcal{H}} = \frac{2n}{3(n-2)(1+w)}, \qquad m_{\mathcal{H}} = \frac{n+2}{2(n-2)}\,. \tag{6.36}$$

This solution represents a Friedmann-like expansion for $n < 0$ and $n > \frac{6(w+1)}{3w+1}$ and power-law inflation when $n \in \left(2\,,\frac{6(w+1)}{3w+1}\right)$. Note that this point is not physical for $n \in (0\,,2)$ since (6.36) represents a contracting universe for which our time variable is not defined. When $n = 2$ we obtain a solution of the form

$$a = a_0\,, \qquad \phi = \phi_0, \qquad \lambda = 0, \tag{6.37}$$

which corresponds to a static universe with cosmological constant. Also this solution represent an effective "GR state" for the scalar tensor cosmology but in this case it is not a stable one. This means that in our model of non-vacuum scalar tensor cosmology no stable non vacuum GR like solutions are allowed.

Using (6.30) and the cosmological equations it is easy to conclude that the points $\mathcal{F}$ and $\mathcal{G}$ both admit vacuum solutions. This is not true for $\mathcal{H}$, for which the energy density is

$$\mu = \mu_0 t^{-\frac{2n}{n-2}}, \tag{6.38}$$

when $n \neq 2$, where

$$\mu_0 \;=\; z_{\mathcal{H}}\left(\frac{2y_{\mathcal{H}}}{\lambda}\right)^{\frac{2}{n-2}}\left[\frac{4\xi n^2}{3(n-2)^2(1+w)^2}\right]^{\frac{n}{n-2}},$$

and $y_{\mathcal{H}}$ and $z_{\mathcal{H}}$ are the y and z coordinates of $\mathcal{H}$ respectively. It is clear from the expression above that this point does not represent a physical solution for all values

Table 6.6: The coordinates and the sign of the spatial curvature of the non vacuum fixed points.

Point	Coordinates (x, y, z)	K
$\mathcal{A}$	$(0,\ 0,\ 0)$	-1
$\mathcal{B}$	$\left(2(6\xi - \sqrt{3\xi(1+12\xi)}),\ 0,\ 0\right)$	0
$\mathcal{C}$	$\left(2(6\xi + \sqrt{3\xi(1+12\xi)}),\ 0,\ 0\right)$	0
$\mathcal{D}$	$\left(-\frac{2}{n-2},\ \frac{2+24\xi}{3\xi(n-2)^2},\ 0\right)$	$\frac{1-[4+n(n-8)]\xi}{(n-2)^2\xi}$
$\mathcal{E}$	$\left(-\frac{2(n-4)\xi}{1+2(n+2)\xi},\ \frac{(1+12\xi)[3-(n-10)(n+2)\xi]}{3(1+2(n+2)\xi)^2},\ 0\right)$	0
$\mathcal{F}$	$\left(-\frac{(1+3w)}{2},\ 0, -\frac{(1+12\xi)(1+3w)}{12\xi}\right)$	$\frac{w(3w-2)-1-16\xi}{16\xi}$
$\mathcal{G}$	$\left(\frac{4\xi(1-3w)}{8\xi+1-w},\ 0,\ \frac{(1+12\xi)\{3(w-1)^2+16\xi(2-3w)\}}{3(8\xi+1-w)^2}\right)$	0
$\mathcal{H}$	$\left(-\frac{3(1+w)}{n}, \frac{3(1-w^2)+4\xi\{6(1+w)+n(1-3w)\}}{4n^2\xi}, \frac{2\xi\{n^2-6(1+w)-n(7+3w)\}-3(1+w)}{2n^2\xi}\right)$	0

of n and ξ since μ_0 and therefore μ can, in principle, be negative. In order for us to determine the values of n and ξ for which $\mathcal{H}$ is physical, we have to solve the inequality $\mu_0 > 0$. We obtain

$$n \in \left(\tfrac{1}{2}(7+3w) - \sqrt{\tfrac{\xi\left(9w^2+66w+73\right)+6(w+1)}{4\xi}}\,, \tfrac{1}{2}(7+3w) + \sqrt{\tfrac{\xi\left(9w^2+66w+73\right)+6(w+1)}{4\xi}}\right). \tag{6.39}$$

When $n = 2$ the cosmological equations reveal that $\mathcal{H}$ is instead associated with a vacuum ($\mu = 0$) solution.

As in the vacuum case we can write the deceleration parameter q in terms of the dynamical variables via

$$q = -2x_i + \tfrac{1}{6\xi}x_i^2 - \left(\tfrac{1-12\xi+6\xi n}{1+12\xi}\right)y_i + \left(\tfrac{1+3w+24\xi}{2(1+12\xi}\right)z_i. \tag{6.40}$$

The surface defined above divides the state space in two volumes representing the region in which the expansion is accelerated and the region in which it is decelerated. The fixed points $\mathcal{A}$, $\mathcal{B}$, $\mathcal{C}$, $\mathcal{D}$ and $\mathcal{E}$ behave like their vacuum counterparts, since they all satisfy $z = 0$. Point $\mathcal{F}$ lies on this surface consistently with the fact that it corresponds to Milne evolution. The point $\mathcal{G}$ always lies in the region in which the expansion is decelerating. The behaviour of $\mathcal{H}$ depends on the barotropic factor w

Table 6.7: The exponent α of the scale factor solutions and the energy density for the non vacuum case.

Point	α	Matter density
$\mathcal{A}$	1	$\mu = 0$
$\mathcal{B}$	$\frac{1}{3(1+8\xi)-4\sqrt{3\xi(1+12\xi)}}$	$\mu = 0$
$\mathcal{C}$	$\frac{1}{3(1+8\xi)+4\sqrt{3\xi(1+12\xi)}}$	$\mu = 0$
$\mathcal{D}$	$1,\ \left(a_0^2 = \frac{k(n-2)^2\xi}{1-[4+n(n-8)]\xi}\right)$	$\mu = 0$
$\mathcal{E}$	$\begin{cases} \frac{2(n+2)\xi+1}{(n-4)(n-2)\xi}, & n \neq 2,\ 4 \\ a = a_0 e^{C_0(t-t_0)}, & n = 2,\ 4 \end{cases}$	$\mu = 0$
$\mathcal{F}$	$1,\ \left(a_0^2 = \frac{16k\xi}{w(3w-2)-1-16\xi+}\right)$	$\mu = 0$
$\mathcal{G}$	$\frac{2(8\xi+1-w)}{32\xi+3(1-w^2)}$	$\mu = 0$
$\mathcal{H}$	$\begin{cases} \frac{2n}{3(n-2)(1+w)}, & n \neq 2 \\ a = a_0, & n = 2 \end{cases}$	$\begin{cases} \mu = \mu_0 t^{-\frac{2n}{n-2}} \\ \mu = 0 \end{cases}$

Table 6.8: The parameter m and the corresponding scalar field solutions for the non vacuum case. The integration constants have been calculated by direct substitution in the cosmological equations.

Point	m	Solutions
$\mathcal{A}$	$\frac{1}{2}$	$\phi = \phi_1, \qquad \lambda = 0$
$\mathcal{B}$	$\frac{3}{6(1+8\xi)-8\sqrt{3\xi(1+12\xi)}}$	$\phi = \phi_0(t-t_0)^{1/2+m},\ \ \lambda = 0$
$\mathcal{C}$	$\frac{3}{6(1+8\xi)+8\sqrt{3\xi(1+12\xi)}}$	$\phi = \phi_1(t-t_0)^{1/2-m},\ \ \lambda = 0$
$\mathcal{D}$	$\frac{n+2}{2(n-2)}$	$\begin{cases} \phi = \phi_0^{\mathcal{D}}(t-t_0)^{1/2}, & n = -2 \\ \phi = \phi_1^{\mathcal{D}}(t-t_0)^{1/2-m}, & n \neq -2,\ 2 \end{cases}$
$\mathcal{E}$	$\frac{n+2}{2(n-2)}$	$\begin{cases} \phi = \phi_0^{\mathcal{E}}(t-t_0)^{1/2}, & n = -2 \\ \phi = \phi_1^{\mathcal{E}}(t-t_0)^{1/2-m}, & n \neq -2,\ 2 \end{cases}$
$\mathcal{F}$	$\frac{1}{2}(3w+2)$	$\phi = \phi_1\ (w = -1/3), \quad \lambda = 0$
$\mathcal{G}$	$\frac{3(1-w^2)+16\xi(1+3w)}{2(3(1-w^2)+32\xi)}$	$\phi = \phi_1^{\mathcal{G}}(t-t_0)^{1/2-m}, \quad \lambda = 0,\ (w > 2/3,\ w \neq 1\ )$
$\mathcal{H}$	$\frac{n+2}{2(n-2)}$	$\begin{cases} \phi = \phi_0^{\mathcal{H}}(t-t_0)^{1/2}, & n = -2 \\ \phi = \phi_1^{\mathcal{H}}(t-t_0)^{1/2-m}, & n \neq -2,\ 2 \\ \phi_0^{\mathcal{H}} = \pm 2\left(\frac{24\lambda(1+w)^2}{3(1-w^2)+16\xi(1+3w)}\right)^{\frac{1}{4}}, \\ \phi_1^{\mathcal{H}} = \left(\frac{2(3+4(n+6)\xi-12(n-2)\xi w-3w^2)}{3\lambda(n-2)^2(1+w)^2}\right)^{\frac{1}{n-2}} \end{cases}$

Table 6.9: The eigenvalues associated with the non vacuum fixed points.

Point	Eigenvalues
$\mathcal{A}$	$[-2, 2, -1-3w]$
$\mathcal{B}$	$\left[4(1+12\xi)-8\sqrt{3\xi(1+12\xi)},\ 6+2(n+2)\left(6\xi-\sqrt{3\xi(1+12\xi)}\right),\right.$ $\left.3(1+8\xi)-\sqrt{3\xi(1+12\xi)}-3w\right]$
$\mathcal{C}$	$\left[4(1+12\xi)+8\sqrt{3\xi(1+12\xi)},\ 6+2(n+2)\left(6\xi+\sqrt{3\xi(1+12\xi)}\right),\right.$ $\left.3(1+8\xi)+\sqrt{3\xi(1+12\xi)}-3w\right]$
$\mathcal{D}$	$\left[\frac{(4-n)\xi-\sqrt{\xi\{3(8-n)n\xi+4\}}}{(n-2)\xi},\ \frac{(4-n)\xi+\sqrt{\xi\{3(8-n)n\xi+4\}}}{(n-2)\xi},\ \frac{6-n}{n-2}-3w\right]$
$\mathcal{E}$	$\left[\frac{-3+(n-10)(n+2)\xi}{1+2(n+2)\xi},\ \frac{-2+2\{4+(n-8)n\}\xi}{1+2(n+2)\xi},\ \frac{-3+2\{-6+(n-7)n\}\xi}{1+2(n+2)\xi}-3w\right]$
$\mathcal{F}$	$\left[\frac{1}{2}\left(4+(2-n)(1+3w)\right),\ \frac{2\xi(3w-1)-\sqrt{2\xi\{18\xi(1+w)^2+(1-w)(1+3w)^2\}}}{4\xi},\right.$ $\left.\frac{2\xi(3w-1)+\sqrt{2\xi\{18\xi(1+w)^2+(1-w)(1+3w)^2\}}}{4\xi}\right]$
$\mathcal{G}$	$\left[\frac{16\xi+(1-w)(1+3w)}{8\xi+1-w},\ \frac{16\xi(3w-2)-3(1-w)^2}{2(8\xi+1-w)},\ \frac{3(1-w^2)+2\xi\{6+n+3(2-n)w\}}{8\xi+1-w}\right]$
$\mathcal{H}$	$\left[\frac{-4+(n+2)(1+3w)}{n},\ \frac{3(w-1)(n+2)+12-\sqrt{S(n,\xi,\omega)}}{4n},\ \frac{3(w-1)(n+2)+12+\sqrt{S(n,\xi,w)}}{4n}\right]$
	$S(n,\xi,w)=3\xi^{-1}(1+12\xi)^{-1}\left\{-36(w-1)(1+w)^2-3\xi\left[4(1+w)^2(12w-37)\right.\right.$ $\left.+n^2\left(7+(2-9w)w\right)+4n(1+w)\left(w(19+6w)-17\right)\right]+4\xi^2\left[324(1+w)^2$ $\left.\left.+8n^3(-1+3w)+12n(1+w)(29+3w)+n^2\left(17-21w(10+3w)\right)\right]\right\}$

Table 6.10: Stability of the fixed point $\mathcal{E}$ for the matter case. The parameters are $N_\pm = 4\pm\sqrt{3}\sqrt{(1+12\xi)/\xi}$, $P^w_\pm = \frac{1}{2}(7+3w)\pm\sqrt{\frac{\xi(9w^2+66w+73)+6(1+w)}{4\xi}}$ and $Q_\pm = 4\pm\sqrt{(1+12\xi)/\xi}$.

	Range of n			
w	$\left(-\infty,-\frac{(1+4\xi)}{2\xi}\right)$	$\left(-\frac{(1+4\xi)}{2\xi},N_-\right)$	(N_-,P_-)	(P_-,Q_-)
0, 1/3	attractor	repeller	saddle	saddle
1	attractor	repeller	saddle	saddle
	(Q_-,Q_+)	(Q_+,P_+)	(P_+,N_+)	(N_+,P^1_+)
0, 1/3	attractor	saddle	saddle	repeller
1	attractor	saddle	saddle	saddle
	(P^1_+,∞)			
0, 1/3	repeller			
1	repeller			

Table 6.11: Stability of the fixed point $\mathcal{H}$ of the matter case. The parameters are $P^w_\pm = \frac{1}{2}(7+3w) \pm \sqrt{\frac{\xi(9w^2+66w+73)+6(1+w)}{4\xi}}$ and S_i, which are the real roots of the polynomial $S(n,\xi,w)$ given in Table 6.9, for the given value of w.

	Range of n			
w	$(-\infty, P^1_+)$	$(P^1_+, 6)$	$(6,\infty)$	bifurcations
0	saddle	saddle	saddle	$-\frac{3(1+8\xi)}{4\xi}, 0, 6, P^0_\pm$
1/3	saddle	saddle	saddle	$0, 4, P^{1/3}_\pm$
1	saddle	repeller	saddle	$0, 3, P^1_-$

and the parameter n: it lies in the accelerated evolution region when $n \in \left(2\,, \frac{6(1+w)}{1+3w}\right)$ for range of w considered here. Otherwise it lies in the decelerated evolution region.

6.3.2 Asymptotic analysis

We next study the asymptotic behaviour of the system (6.29) using the Poincaré projection. The compactification of the state space can be achieved by transforming to spherical coordinates

$$x = \bar{r}\sin\theta\cos\psi, \qquad y = \bar{r}\sin\theta\sin\psi, \qquad z = \bar{r}\cos\theta, \tag{6.41}$$

where $\bar{r} = \frac{\sqrt{r}}{1-r}$ and $\bar{r} \in [0,\infty)$, $\theta \in [0,\pi]$ and $\psi \in [0, 2\pi]$. In the limit $r \to 1$ ($\bar{r} \to \infty$), equations (6.29) become

$$r' = \frac{\cos^2\psi\ \sin^2\theta}{24\xi}\left[(\cos 2\psi - 3)\sin^2\theta - 4\cos^2\theta\right], \tag{6.42}$$

$$\theta' = -\frac{\cos\theta\ \sin^3\theta\ \cos^4\psi}{6\xi(1-r)^2}, \tag{6.43}$$

$$\psi' = \frac{\sin^2\theta\ \cos^3\psi\ \sin\psi}{6\xi(1-r)^2}. \tag{6.44}$$

As in the vacuum case the radial equation does not contain the radial coordinate, so that the fixed points can be obtained using only the angular equations. Setting $\psi' = 0$ and $\theta' = 0$, we obtain four fixed points and a fixed subspace which are listed in Table 6.12.

The equilibrium points at infinity, as in the vacuum case, are unphysical.

The points $\mathcal{A}_\infty$ and $\mathcal{B}_\infty$ lie on the plane $z = 0$ and therefore their solutions are the same as the vacuum points $\mathcal{A}_\infty$ and $\mathcal{C}_\infty$, respectively. Points $\mathcal{C}_\infty$ and $\mathcal{D}_\infty$ represent the poles of the Poincaré sphere and it is easy to prove that they are linked to the

same solutions at $\mathcal{A}_\infty$ and $\mathcal{B}_\infty$.

In addition to the fixed points above, we found two fixed subspaces $\mathcal{L}_1$ and $\mathcal{L}_2$, that contains all the points with $\psi = \pi/2$ and $\psi = 3\pi/2$, respectively. The stability of these asymptotic fixed points can be deduced by analysing the stability with respect to the angular coordinates, and from the sign of r'. The points $\mathcal{A}_\infty$ and $\mathcal{B}_\infty$ are stable nodes for all values of n and ξ. Points $\mathcal{C}_\infty$ and $\mathcal{D}_\infty$ represent the poles of the Poincaré sphere and it is easy to prove that they represent the same scale factor solution at $\mathcal{A}_\infty$ and $\mathcal{B}_\infty$.

All the other points including the fixed subspaces $\mathcal{L}_1$ and $\mathcal{L}_2$, have both eigenvalues equal to zero. In order to derive the stability of these points we have to analyse the effect of the non-linear contributions have on dynamical equations. This can be done by developing the R.H.S using a Taylor expansion of the dynamical equations around the fixed point up to the first non-zero order and then directly solving the system obtained.

For the points $\mathcal{C}_\infty$ and $\mathcal{D}_\infty$ we obtain the solutions:

$$\psi_{C_\infty} = c_2, \qquad \theta_{C_\infty} = -\frac{6\xi}{\tau \sin(\psi_0)\cos^3(\psi_0) + 6\xi c_1}, \tag{6.45}$$

$$\psi_{D_\infty} = c_2, \qquad \theta_{D_\infty} = \pi - \frac{6\xi}{\tau \sin(\psi_0)\cos^3(\psi_0) + 6\xi c_1}. \tag{6.46}$$

This result tells us that when we choose initial conditions around these points, the evolution of the universe will follow an orbit with constant ψ, with τ increasing [3] and θ approaching 0 or π. If we also consider the behaviour of the radial equation we conclude that these points behave like saddles.

For the fixed subspaces $\mathcal{L}_1$ and $\mathcal{L}_2$, we find

$$\psi(\tau) = \frac{\sqrt[3]{-2\xi}}{\sqrt[3]{\tau \cos\theta_0 \sin^3\theta_0 + 96\xi c_1}} \pm \frac{\pi}{2}\,, \tag{6.47}$$

$$\theta(\tau) = \theta_0 - \frac{\tan\theta_0}{2} + c_2\left[\tau\left(\sin 4\theta_0 - 2\sin 2\theta_0\right) - 768\xi c_1)\right]^{\frac{2}{3}\csc^2\theta_0}\,. \tag{6.48}$$

It is clear that, for τ increasing, the solution for ψ approaches $\pi/2$ for $\mathcal{L}_1$ and $3\pi/2$ for $\mathcal{L}_2$, while θ increases. The radial behaviour is very complicated and depends critically on the value of the coordinate θ_0, w, n and ξ (we will not show this dependence here). We may however conclude that this subspace is a saddle or an attractor depending on the value of θ_0.

[3] This behaviour is reversed in case of a contracting cosmology because in this case τ effectively changes sign when a is decreasing.

Table 6.12: Coordinates, behaviours and stability of the asymptotic fixed points in the non vacuum case.

Point	(θ, ψ)	Stability
$\mathcal{A}_\infty$	$(\frac{\pi}{2}, 0)$	attractor
$\mathcal{B}_\infty$	$(\frac{\pi}{2}, \pi)$	attractor
$\mathcal{C}_\infty$	$(0, 0)$	saddle
$\mathcal{D}_\infty$	(π, π)	saddle
$\mathcal{L}_1$	$(\theta_0, \frac{\pi}{2})$	
$\mathcal{L}_2$	$(\theta_0, \frac{3\pi}{2})$	

The state space in the matter case is 3-dimensional and therefore cannot be visualised as easily as its vacuum counterpart. For this reasons we will not give here any sketch of the state space and we refer the reader to the next section for an analysis of the results derived above.

6.4 Discussion and conclusions

In this chapter, the dynamics of STG FLRW cosmological models has been studied using a DS analysis. We have considered a generic non–minimally coupled theory of gravity where the coupling and the potential are powers of the scalar field, both in a vacuum and in presence of a perfect fluid. The set of parameters characterising the cosmological models are $\{\xi, \lambda, n, w\}$, i.e. the coupling constant, a constant parameter, the power of the self-interacting potential and the barotropic index of the perfect matter fluid, respectively. The phase-space is 3-dimensional in absence of matter while it is 4-dimensional in presence of matter, but in both cases the FLRW Hamiltonian constraint allows one to reduce their dimensionality. Our investigation considered the existence and local stability of critical points (finite analysis) and the asymptotic analysis via the Poincaré projection.

We identified 5 finite fixed points in the vacuum case and 8 in the matter case. In the vacuum case, there are 4 asymptotic stability points corresponding to the four intersections of the axes with the unitary Poincaré circle. In the matter case, we have to consider a unitary 3-sphere and on top of the vacuum asymptotic points we find two more points and two "fixed subspaces". The stability of fixed points strictly depends on the values of the above parameters and in particular on ξ and n, i.e. the coupling and the power of self–interacting potential.

In the vacuum case, the two dimensional state space is divided in two halves by the invariant submanifold associated with $V(\phi) = 0$. Of the nine fixed points we found,

five of them ($\mathcal{A}, \mathcal{B}, \mathcal{C}, \mathcal{A}_\infty, \mathcal{C}_\infty$) are permanently on this invariant submanifold, two of them $\mathcal{B}_\infty, \mathcal{C}_\infty$ do not change their position and the other two "move" in the phase plane depending on the values of the parameters. In particular, $\mathcal{D}$ is characterised by $q = 0$ and its position is on the curve described by the equation given in (6.25) and $\mathcal{E}$ is associated with a flat spatial geometry and always lies on the curve described by the constraint (6.9) with $K = 0$. Even if matter is not present the scalar field is able to induce an expanding Friedmann-like evolution. However, the value of α in (6.18) and (6.19) reveals that at these fixed points the scale factor cannot grow faster than $t^{1/2}$. In addition, these solutions are unstable for every value of the parameters. The point $\mathcal{E}$ admits the widest spectrum of behaviours. Depending on the values of n and ξ its solution can represent an inflationary phase, a Friedmann-like phase or a contraction. A comparison with the stability analysis reveals that $\mathcal{E}$ is an attractor only when it corresponds to contracting solutions or power law inflation. This has two consequences: (i) in the scalar field dominated regime our model of scalar tensor cosmology admits an inflationary phase as an attractor even if this attractor is not global and not unique; (ii) since there is no value of the parameters for which the $\mathcal{E}$ is a saddle, this model does not admit a transient inflationary phase and cannot solve the graceful exit problem.

The case $n = 4$ is particularly interesting because, for this value of n, $\mathcal{E}$ is associated with a GR ($\phi = const.$) de Sitter solution and is an attractor. This fact has two main consequences: (i) it shows that with a non–minimally coupled scalar field with quartic potential, the early time cosmology evolves towards an inflationary phase which is indistinguishable from a GR one; and (ii) it gives us an independent confirmation of the idea that a scalar tensor theory of gravity can evolve towards GR. The difference is that when a potential is present, the realisation of such mechanism is strictly related to the form of the potential.

In the matter case, we found three new finite fixed points which are physical only for specific values of the parameters. In particular, $\mathcal{F}$ is never physical because it satisfies the cosmological equations only for a negative w. Point $\mathcal{G}$ represents a physical vacuum solution only for $w > 2/3$ and $w \neq 1$. For these values of w, this point is associated with an expansion whose rate cannot be higher than the radiation dominated GR-FLRW solution. Point $\mathcal{H}$ is associated to a non-vacuum solution which resembles a well known Friedmann-GR solution. As n varies, this solution can represent power law inflation, a decelerated Friedmann solution and a contraction. For $n = 2$, this point is linked to a GR-like state, but since it is unstable for every value of the parameters, we conclude that there is no way for this class of scalar tensor

cosmologies to approach a stable non-vacuum GR state. In fact, a quick look to the table above reveals that there is no value of the parameters for which any of the finite fixed points are stable. This means that the only non-vacuum attractors for this class of theories are the asymptotic fixed points and their associated Lemaître solution. Therefore we can conclude that the class of cosmologies we treated are doomed either to approach an effectively vacuum state (probably corresponding to thermal death) that corresponds to one of the vacuum attractors or to recollapses towards a Big Crunch.

The most interesting orbits are the ones that "travel" between point $\mathcal{E}$ and $\mathcal{H}$. This is because they could represent cosmic histories in which a Friedmann-like cosmology enters naturally in a phase of accelerated expansion or cosmic histories in which an unstable inflationary phase is followed by a second inflationary phase. The first type of orbits is interesting because they can in principle help solve the incompatibility between the evolution towards a Dark Energy era and the formation of large scale structure. The second ones are interesting because they potentially unify "dark" scalar fields and the inflaton within a single scheme.

Since the state space is three dimensional it is not easy to check if such orbits actually exist without the use of numerical techniques. However, our results allow one to give some necessary condition for these orbits to exist and to rule out some of them. For example, it is easy to see that there is no value of the parameters for which $\mathcal{E}$ can represent an unstable Friedmann solution and $\mathcal{H}$ an inflationary phase. On the other hand, for $n \in (4, Q_+)$ and $w = 0, 1/3$ we have that $\mathcal{H}$ corresponds to an unstable decelerated expansion, $\mathcal{E}$ correspond to a stable power law inflation and these points are not separated by any invariant submanifold. This means that, in principle cosmic histories exist for which a transient Friedmann evolution approaches to a power law inflationary phase in a natural way.

If $n \in (4, 6(1+w)/(3w+1))$ and $w = 0, 1/3$ another interesting set of cosmic histories is possible in which we have two inflationary phases, a first one which is unstable associated with $\mathcal{H}$ and a second one which is stable associated with $\mathcal{E}$. Although only a detailed analysis of these cosmic histories can reveal if this last group of cosmic histories also include the deceleration phase necessary for the realisation of standard cosmology, this scenario is interesting because it shows that in STG the non–minimally coupled scalar field can act as *both* the inflaton and dark energy. Such a behaviour has been also found in a class of higher order gravity models [105] and definitely deserves a more careful investigation. Such a study, will be the topic of a forthcoming paper.

As final comment, it is worth stressing the connection between the model presented above and the String-Dilaton action. Using the transformation (2.29), which is only a reparametrisation for the scalar field, we can pass from the action (2.22) to (2.30). This means that all the exact solutions for the scale factor that we have derived together with their stability are also solutions for the String-Dilaton action. Therefore, our analysis also allows us to give details of the dynamics of low-energy string cosmology which could be of great interest in the quest for finding observational constraints for this theory.

Chapter 7

Tensor anisotropies in the CMB from scalar-tensor gravity

A possible testing ground for alternative theories such as STG, is the cosmic microwave background (CMB). The high precision measurements provided by experiments such as WMAP allow us to constrain the parameters of specific models in STG and may also provide a means to distinguish between various models. The spectrum of density (scalar) perturbations and gravitational waves (tensor perturbations) can be determined from the CMB.

In [170] a formalism was developed for determining CMB anisotropies from gravitational waves in the 1+3 covariant framework. This method was also successfully used in the braneworld scenario [171]. In this chapter we will extend the formalism of [170, 171] to models with STG. We compute the tensor perturbations for a general STG and obtain solutions for specific class of theories. These solutions together with a modified CMB code (based on CMBFAST [172] or CAMB [173]) will then be used to compute the tensor anisotropies. This work is currently in progress.

7.1 Tensor perturbation equations

7.1.1 The background

In order to obtain a description of the tensor perturbations we need to choose a suitable background. Current observations seem to indicate that the Universe appears to be isotropic and homogeneous on large scales, and thus a FLRW background is a

logical candidate. Homogeneity an isotropy imply that

$$\sigma = \omega = 0, \quad \tilde{\nabla}_a f = 0,$$

where f is any scalar quantity; in particular

$$\tilde{\nabla}_a \mu = \tilde{\nabla}_a p = 0 \;\Rightarrow\; \dot{u}_a = 0.$$

The evolution equations (1.16), (1.35) and (1.22) given in §1.3, respectively reduce to

$$\dot{\Theta} + \tfrac{1}{3}\Theta^2 + \tfrac{1}{2}(\tilde{\mu} + 3\tilde{p}) = 0, \tag{7.1}$$

$${}^3R = \frac{6K}{a^2} = 2\tilde{\mu} - \tfrac{2}{3}\Theta^2, \tag{7.2}$$

$$\dot{\tilde{\mu}} + \Theta(\tilde{\mu} + \tilde{p}) = 0. \tag{7.3}$$

In the 1+3 –covariant approach to cosmology [85], we can describe small deviation from the FLRW spacetime by taking all the quantities that are zero in the background as being first order and retain in the equations given in §1.3 only the terms that are linear in these quantities, that is all second-order terms are dropped. This *linearisation* allows us to decouple the scalar, vector and tensor parts of the perturbations, so that we may treat them separately.

In this chapter we will focus only on the tensor perturbations for which the scalar and vector contributions of the 1+3 variables vanish, i.e.

$$f,\, \tilde{\nabla}_a f,\, \tilde{\nabla}_a \tilde{\nabla}_b f = 0, \quad \forall\ f \ \ \text{(scalar)}, \tag{7.4}$$

and

$$\bar{V}_a,\, \tilde{\nabla}_a \bar{V}_b = 0, \quad \forall\ \bar{V}_a \ \ \text{(solenoidal vector)}. \tag{7.5}$$

7.1.2 The general linear tensor perturbation equations

A description of the tensor perturbations [174] can be obtained by applying (7.4) and (7.5) to the evolution equations (1.18), (1.27) and (1.28) to give

$$\dot{\sigma}_{ab} + \tfrac{2}{3}\Theta\sigma_{ab} + E_{ab} - \tfrac{1}{2}\tilde{\pi}_{ab} = 0, \tag{7.6}$$

$$\dot{E}_{ab} + E_{ab}\Theta - \operatorname{curl} H_{ab} + \tfrac{1}{2}(\tilde{\mu} + \tilde{p})\sigma_{ab} + \tfrac{1}{6}\Theta\tilde{\pi}_{ab} + \tfrac{1}{2}\dot{\tilde{\pi}}_{ab} = 0, \tag{7.7}$$

$$\dot{H}_{ab} + H_{ab}\Theta + \operatorname{curl} E_{ab} - \tfrac{1}{2}\operatorname{curl}\tilde{\pi}_{ab} = 0, \tag{7.8}$$

together with the conditions

$$\tilde{\nabla}_b H^{ab} = 0, \quad \tilde{\nabla}_b E^{ab} = 0, \quad H_{ab} = \mathrm{curl}\, \sigma_{ab}. \tag{7.9}$$

The equations above may be reduced to a system of ordinary differential equations by making use of a standard harmonic analysis. This can be done by expanding the transverse traceless quantities into electric ($Q^{(k)}_{ab}$) and magnetic ($\bar{Q}^{(k)}_{ab}$) parity tensor harmonics [170], with dimensionless coefficients:

$$\begin{aligned} E_{ab} &= \sum_k \left(\frac{k}{a}\right)^2 [E_k Q^{(k)}_{ab} + \bar{E}_k \bar{Q}^{(k)}_{ab}], \\ H_{ab} &= \sum_k \left(\frac{k}{a}\right)^2 [H_k Q^{(k)}_{ab} + \bar{H}_k \bar{Q}^{(k)}_{ab}], \\ \sigma_{ab} &= \sum_k \left(\frac{k}{a}\right) [\sigma_k Q^{(k)}_{ab} + \bar{\sigma}_k \bar{Q}^{(k)}_{ab}], \\ \tilde{\pi}_{ab} &= \sum_k [\tilde{\pi}_k Q^{(k)}_{ab} + \bar{\pi}_k \bar{Q}^{(k)}_{ab}]. \end{aligned} \tag{7.10}$$

Using $H_{ab} = \mathrm{curl}\, \sigma_{ab}$, we arrive at the coupled equations

$$\frac{k}{a^2}[\sigma_k' + \mathcal{H}\sigma_k] + \frac{k^2}{a^2} E_k - \tfrac{1}{2}\tilde{\pi}_k = 0 \tag{7.11}$$

$$\frac{k^2}{a^2}[E_k' + \mathcal{H}E_k] + \frac{k}{a^2}\left(\mathcal{H}^2 - k^2 - 2K + \frac{a^2}{6}(\tilde{\mu} + 3\tilde{p})\right)\sigma_k = -\tfrac{1}{2}[\tilde{\pi}_k' + \mathcal{H}\tilde{\pi}_k], \tag{7.12}$$

where primes denote the conformal time variable τ: $\frac{d\tau}{dt} = \frac{1}{a}$, and $\mathcal{H} = \frac{a'}{a} = \frac{a}{3}\Theta$. Taking the time derivative of (7.11) gives

$$\sigma_k'' + 2\mathcal{H}\sigma_k' + \left[k^2 + 2K - \frac{a^2}{3}(\tilde{\mu} + 3\tilde{p})\right]\sigma_k = \frac{a^2}{k}[\tilde{\pi}_k' + 2\mathcal{H}\tilde{\pi}_k]. \tag{7.13}$$

7.1.3 Perturbations equations for scalar-tensor gravity

In chapter 2 we showed how an extended theory of gravity like STG (see §2.2), can be treated like standard GR, but where the source is composed of two fluids. In other words by recasting the field equations in the form (2.34), we can easily generalise the perturbation equations given above, to obtain the tensor perturbations for STG.

An important step in this procedure is the choice of frame since from (2.34) it is not clear which choice of u_a (matter or scalar field) is more convenient. We shall choose the frame associated with standard matter, i.e. $u_a = u^m_a$. The reason for this choice is that real observers are situated in galaxies and these galaxies follow standard

matter geodesics. The kinematical components can then be decomposed according to (2.37) and substituted into the relevant equations.

Because we are making use of conformal time, we need to rewrite the scalar field components (2.36) as

$$\begin{aligned}
\mu^{\phi} &= \frac{1}{F(\phi)}\left[\tfrac{1}{2}V(\phi)+\frac{1}{4a^2}\phi'^2-3\frac{\mathcal{H}}{a^2}F'(\phi)\right],\\
p^{\phi} &= \frac{1}{F(\phi)}\left[\frac{1}{4a^2}\phi'^2-\tfrac{1}{2}V(\phi)+\frac{\mathcal{H}}{a^2}F'(\phi)+\frac{1}{a^2}F''(\phi)\right], \qquad (7.14)\\
q_c^{\phi} &= \frac{1}{a^2}\frac{F'(\phi)}{F(\phi)}u_c',\\
\pi_{ab}^{\phi} &= -\frac{1}{a}\frac{F'(\phi)}{F(\phi)}\sigma_{ab}.
\end{aligned}$$

The evolution equations for μ, μ^{ϕ} and q_c^{ϕ} can be found from the twice contracted Bianchi equations:

$$\mu' + 3(\mu+p)\mathcal{H} = 0, \qquad (7.15)$$

$$\mu^{\phi'} + \tilde{\nabla}^c q_c^{\phi} + 3(\mu^{\phi}+p^{\phi})\mathcal{H} + 2(u^{c'}q_c^{\phi}) + \sigma^{ab}\pi_{ba}^{\phi} = \mu\frac{\phi'}{F^2}\frac{\partial F}{\partial\phi}. \qquad (7.16)$$

where the ϕ subscripts indicate the scalar field component of the effective fluid.

Using the identities (2.37) and (7.14) in equations (7.11)-(7.13), we can obtain the tensor perturbation equations for scalar tensor gravity [68]. These are:

$$\frac{k}{a^2}\left[\sigma_k' + \left(\mathcal{H}+\frac{F'}{2F}\right)\sigma_k\right] + \frac{k^2}{a^2}E_k - \frac{1}{2F}\pi_k = 0 \qquad (7.17)$$

$$\begin{aligned}
&\frac{k^2}{a^2}\left[E_k' + \left(\mathcal{H}+\frac{F'}{2F}\right)E_k\right] + \frac{k}{a^2}\left\{\frac{a^2}{6F}\left(\mu+3p-V(\phi)\right)+\mathcal{H}^2-k^2-2K\right.\\
&\left.+\frac{1}{6F}\phi'^2+\frac{F'}{F}\mathcal{H}+\frac{3}{4}\left(\frac{F'}{F}\right)^2\right\}\sigma_k = -\frac{1}{2F}\left[\pi_k' + \left(\mathcal{H}-\frac{3F'}{2F}\right)\pi_k\right], \qquad (7.18)
\end{aligned}$$

and

$$\begin{aligned}
&\sigma_k'' + \left(2\mathcal{H}+\frac{F'}{F}\right)\sigma_k' + \left[k^2+2K-\frac{a^2}{3F}\left\{\mu+3p-V(\phi)\right\}-\frac{1}{3F}\phi'^2-\left(\frac{F'}{F}\right)^2\right]\sigma_k\\
&= \frac{a^2}{kF}\left[\pi_k' + \left(2\mathcal{H}-\frac{F'}{F}\right)\pi_k\right]. \qquad (7.19)
\end{aligned}$$

7.2 CMB tensor power spectra

Assuming that the photon anisotropic stress is negligible (i.e. $\pi_{ab} = 0$) [170], we can define the variable $u_k \equiv a\ F(\phi)^{1/2}\sigma_k$ which satisfies the equation of motion

$$u_k'' + \left[k^2 + 2K - \mathcal{H}^2 - \frac{a^2}{6F}\left\{\mu + 3p - V(\phi)\right\} - \frac{F'}{F}\mathcal{H} - \frac{3}{4}\left(\frac{F'}{F}\right)^2 - \frac{1}{6F}\phi'^2\right] u_k = 0 \tag{7.20}$$

It is useful to relate the covariant variables used above to the Bardeen metric perturbation variable H_T, via

$$(k^2 + 2K)H_{Tk} = \frac{\sigma_k'}{k} + 2E_k, \tag{7.21}$$

whose evolution equation is given by

$$H_{Tk}'' + \left(2\mathcal{H} + \frac{F'}{F}\right)H_{Tk}' + (k^2 + 2K)H_{Tk} = 0, \tag{7.22}$$

from which it is clear that H_T is conserved on large scales.

7.2.1 The case $F(\phi) = \xi\phi^2$ and $V(\phi) = \lambda\phi^{2n}$

We will consider the class of scalar-tensor theories where the non-minimal coupling and self-interaction potential have the forms:

$$F(\phi) = \xi\phi^2, \qquad V(\phi) = \lambda\phi^{2n}, \tag{7.23}$$

where $\xi > 0$. In chapter 6 [104] the following exact solution was found

$$a(\tau) = a_0\,\tau^{\frac{2n}{n(1+3w)-3(1+w)}}, \qquad \phi(\tau) = \phi_0\,\tau^{-\frac{3(1+w)}{n(1+3w)-3(1+w)}}. \tag{7.24}$$

This solution assumes that standard matter behaves like a perfect fluid with barotropic index w, so that the energy density is given by

$$\mu = \mu_0\,\tau^{-\frac{6n(1+w)}{n(1+3w)-3(1+w)}}, \tag{7.25}$$

and the pressure by $p = w\mu$.

The parameters ϕ_0 and μ_0 is given by

$$\phi_0 = \left(\frac{3\left\{3(1-w^2) + 8\xi(n+3) - 24w\xi(n-1)\right\}}{2a_0^2\lambda\left(n(1+3w) - 3(1+w)\right)^2}\right)^{\frac{1}{2(n-1)}}, \tag{7.26}$$

and

$$\mu_0 = \left(-3(1+w) + 4\xi(2n^2-7n-3) - 12\xi w(n+1)\right) \times \left(\frac{3}{2a_0^2\left(n(1+3w)-3(1+w)\right)^2}\right)^{\frac{n}{n-1}} \left(\frac{3(1-w^2)+8\xi(n+3)-24w\xi(n-1)}{\lambda}\right)^{\frac{1}{n-1}}. \tag{7.27}$$

We can recover GR in the limit $\xi \to 1/2$ and $n \to \pm\infty$.

Using these solutions, we can solve (7.20) for a flat FLRW model, to find the following solutions: For the matter dominated regime ($w = 0$), we have

$$u_k(\tau) = \sqrt{k\tau}\left[C_1 J\left(\tfrac{1}{2}\left(\tfrac{5n-9}{n-3}\right), k\tau\right) + C_2 Y\left(\tfrac{1}{2}\left(\tfrac{5n-9}{n-3}\right), k\tau\right)\right], \tag{7.28}$$

and in the radiation dominated regime ($w = 1/3$) we have

$$u_k(\tau) = \sqrt{k\tau}\left[C_3 J(\tfrac{3}{2}, k\tau) + C_4, Y(\tfrac{3}{2}, k\tau)\right], \tag{7.29}$$

where J and Y are Bessel functions of the first and second kind respectively.

We can then determine the solutions for σ_k, E_k and H_{Tk} in the radiation regime, straightforwardly:

$$\sigma_k(\tau) = \frac{A}{k^2\tau^2}\left[(C_3\, k\tau + C_4)\cos(k\tau) + (C_4\, k\tau - C_3)\sin(k\tau)\right], \tag{7.30}$$

$$E_k(\tau) = \frac{A}{k^3\tau^3}\left[(C_3\, k\tau + C_4(1-k^2\tau^2))\cos(k\tau) + (C_4\, k\tau - C_3(1-k^2\tau^2))\sin(k\tau)\right], \tag{7.31}$$

$$H_{Tk}(\tau) = \frac{A}{k\tau}\left[C_3\sin(k\tau) - C_4\cos(k\tau)\right], \tag{7.32}$$

where

$$A = -\sqrt{\frac{2}{\pi a_0^2\xi}}\left(\frac{a_0^2(n-2)^2\lambda}{1+12\xi}\right)^{\frac{1}{2(n-1)}}. \tag{7.33}$$

These solutions are of the same form as their GR counterparts, apart from the scaling factor A which depends on the parameters of the given model.

Performing a series expansion, we arrive at the appropriate initial conditions for large-scale modes in the radiation era:

$$\sigma_k = -\frac{nk\tau}{3n-4} + \frac{n^2(k\tau)^3}{2(3n-4)(5n-4)} + \mathcal{O}[(k\tau)^5], \tag{7.34}$$

$$E_k = \frac{2(n-1)}{3n-4} + \frac{4n(2n-1)(k\tau)^2}{(3n-4)(5n-4)} + \mathcal{O}[(k\tau)^4], \tag{7.35}$$

$$H_{Tk} = 1 - \frac{n(k\tau)^2}{2(3n-4)} + \frac{n^2(k\tau)^4}{8(3n-4)(5n-4)} + \mathcal{O}[(k\tau)^6]. \tag{7.36}$$

In the limit $n \to \pm\infty$, we recover the GR results.

Numerical Evaluation

The initial conditions, (7.34)–(7.36), can now be used in a modified version of CMBFAST [172] or CAMB [173], to obtain the tensor temperature and polarisation power spectra. This work is currently underway and should be finished in the next few months. Once we obtain the results we can compare them to the known GR results [172, 175].

7.3 Conclusions

Our main aim in this chapter was to study tensor anisotropies in the CMB in a general STG. Using the 1 + 3–covariant framework, we obtained the tensor perturbation equations. We chose to work in conformal time so that the relevant quantities are dimensionless. We considered a class of STG where the non-minimal coupling and self-interacting potential are of the form $F(\phi) = \xi\phi^2$ and $V(\phi) = \lambda\phi^{2n}$, respectively. For this class of models we found the solutions (7.30)–(7.32) as well as the initial conditions (7.34)–(7.36). These solutions only differ from the ones found in GR by a scaling factor A. One would therefore expect the profile of the temperature power spectrum to have the same form as GR but with the peaks being rescaled.

Currently, we are modifying the CMB code using these results, so that the tensor anisotropies can be analysed and possible constraints to the physical parameters can be found.

Chapter 8

Final Remarks

A large portion of this thesis was dedicated to the application of the theory of dynamical systems (DS). In the context of alternative theories of gravity, this tool has proven to be extremely useful for studying the dynamical behaviour of cosmological models. Due to the highly complex nature of these type of theories, it is not easy to gain an understanding of the stability and global behaviour of the underlying cosmological models. The DS approach [88, 89] addresses some of these problems, since it provides one with exact solutions through the determination of equilibrium points and a (qualitative) description of the global dynamics of the system. In this thesis we have employed this method to study the cosmologies associated with two types of ETG, namely R^n–gravity and STG. Cosmological behaviours such as late time acceleration, isotropisation, and static and bounce behaviours, to name but a few, were identified. Some of the exact solutions found using DS, have been used to study observational consequences of these theories (e.g. chapter 7).

Lagrangians of the type $f(R) = R^n$ were first considered as toy models mainly due to their simplicity. However, because of this they have proven useful as a first investigation of HOTG. Many of the properties, such as a stable isotropic past attractor found in chapter 3, have been recovered in more general theories [83, 84]. The addition of the linear term, i.e. $f(R) = R+\alpha R^n$ Lagrangians, significantly complicate the evolutions equations. In [83], eight variables were required (as apposed to three in chapter 3) to obtain a closed system of equations so that a dynamical systems analysis could be performed. They only considered the vacuum case and their variables were non-compact (expansion normalised).

The effect of spatial curvature on the isotropisation of cosmological models in the

presence of R^n-gravity was investigated in chapter 4. We found that as in GR, later time behaviour with spatial curvature will lead to a growth in anisotropies. Thus isotropisation for these models, imply cosmological behaviours which evolve towards flat spacetimes.

The use of compact expansion normalised variables in chapter 4, allowed us to investigate static solutions and bounce behaviours. Although no exact Einstein static solutions were found in this analysis, we do find bounce behaviours (see chapter 5).

The advantages and disadvantages of using compact and non-compact variables were discussed in chapter 5. We showed that when ever possible, it is advisable to use compact expansion normalised variables. We illustrated this by making use of two examples; an LRS Bianchi I model and a FRW model, both in the presence of R^n-gravity. We stress that this result is also valid for more general theories of gravity.

In chapters 6 and 7 we looked at a class of STG where quadratic non-minimal couplings to gravity and self-interacting power law potentials are assumed. A dynamical system analysis is performed on a FRW model in the presence of this STG in chapter 6. We found promising cosmic histories where a Friedmann-like cosmology is followed by a phase of accelerated expansion, so that both large scale structure formation and the dark energy era can in principle be compatible. Cosmic histories were also found in which one unstable inflationary phase is followed by a secondary inflationary phase. In this case we potentially have the same scalar field being responsible for the inflaton and quintessence fields.

In chapter 7 the ground work was done for analysing tensor anisotropies in the CMB. Solutions and initial conditions for the shear (σ_k), electric part of the Weyl tensor (E_k), and the Bardeen perturbation variable (H_{Tk}) were found. These are currently being used in a modified CMB code to analyse the tensor anisotropies.

In conclusion, in this thesis we investigated cosmological models with R^n-gravity and STG. The results we found for R^n-gravity are promising and further investigation into more general HOTG would be justified. Interesting features such as the isotropic initial conditions requires further investigation, especially in the context of inflation. Similarly, the class of STG considered here, had many attractive features. Current work, such as chapter 7, are looking at the observational consequences of these types of theories and should in practise allow us to distinguish between various models and theories of gravity.

Bibliography

[1] S. Weinberg, Gravitation and Cosmology (New York: Wiley, 1972).

[2] M. Milgrom, Astrophys. J. 270 (1983) 365.

[3] R.H. Sanders, Astron. Astrophys. 136 (1984) L21.

[4] R.H. Sanders, Lect. Notes Phys. 720 (2007) 375, astro-ph/0601431.

[5] J.W. Moffat and I.Y. Sokolov, Phys. Lett. B378 (1996) 59, astro-ph/9509143.

[6] P.D. Mannheim, Astrophys. J. 479 (1997) 659, astro-ph/9605085.

[7] M.D. Roberts, Gen. Rel. Grav. 36 (2004) 2423, astro-ph/0209456.

[8] J.R. Brownstein and J.W. Moffat, Astrophys. J. 636 (2006) 721, astro-ph/0506370.

[9] J.R. Brownstein and J.W. Moffat, Mon. Not. Roy. Astron. Soc. 367 (2006) 527, astro-ph/0507222.

[10] J.D. Bekenstein, Phys. Rev. D70 (2004) 083509, astro-ph/0403694.

[11] M.K. Mak and T. Harko, Phys. Rev. D70 (2004) 024010, gr-qc/0404104.

[12] T. Harko and K.S. Cheng, Astrophys. J. 636 (2005) 8, astro-ph/0509576.

[13] C.G. Böhmer and T. Harko, Class. Quant. Grav. 24 (2007) 3191, arXiv:0705.2496 [gr-qc].

[14] T. Harko and K.S. Cheng, Phys. Rev. D76 (2007) 044013, arXiv:0707.1128 [gr-qc].

[15] P. Brax and C. van de Bruck, Class. Quant. Grav. 20 (2003) R201, hep-th/0303095.

[16] Y. Fujii and K.i. Maeda, The scalar-tensor theory of gravity (Cambridge: Cambridge University Press, 2003).

[17] S.M. Carroll et al., Phys. Rev. D70 (2004) 043528, astro-ph/0306438.

[18] S.M. Carroll et al., Phys. Rev. D71 (2005) 063513, astro-ph/0410031.

[19] S. Nojiri and S.D. Odintsov, Phys. Rev. D68 (2003) 123512, hep-th/0307288.

[20] S. Capozziello, Int. J. Mod. Phys. D11 (2002) 483, gr-qc/0201033.

[21] V. Faraoni, Phys. Rev. D72 (2005) 124005, gr-qc/0511094.

[22] M.L. Ruggiero and L. Iorio, JCAP 0701 (2007) 010, gr-qc/0607093.

[23] A. de la Cruz-Dombriz and A. Dobado, Phys. Rev. D74 (2006) 087501, gr-qc/0607118.

[24] N.J. Poplawski, Phys. Rev. D74 (2006) 084032, gr-qc/0607124.

[25] N.J. Poplawski, Class. Quant. Grav. 24 (2007) 3013, gr-qc/0610133.

[26] A.W. Brookfield, C. van de Bruck and L.M.H. Hall, Phys. Rev. D74 (2006) 064028, hep-th/0608015.

[27] Y.S. Song, W. Hu and I. Sawicki, Phys. Rev. D75 (2007) 044004, astro-ph/0610532.

[28] B. Li, K.C. Chan and M.C. Chu, Phys. Rev. D76 (2007) 024002, astro-ph/0610794.

[29] X.H. Jin, D.J. Liu and X.Z. Li, (2006), astro-ph/0610854.

[30] T.P. Sotiriou and S. Liberati, Annals Phys. 322 (2007) 935, gr-qc/0604006.

[31] T.P. Sotiriou, Class. Quant. Grav. 23 (2006) 5117, gr-qc/0604028.

[32] R. Bean et al., Phys. Rev. D75 (2007) 064020, astro-ph/0611321.

[33] I. Navarro and K. Van Acoleyen, JCAP 0702 (2007) 022.

[34] A.J. Bustelo and D.E. Barraco, Class. Quant. Grav. 24 (2007) 2333, gr-qc/0611149.

[35] G.J. Olmo, Phys. Rev. D75 (2007) 023511, gr-qc/0612047.

[36] J. Ford, S. Giusto and A. Saxena, Nucl. Phys. B790 (2008) 258, hep-th/0612227.

[37] F. Briscese et al., Phys. Lett. B646 (2007) 105, hep-th/0612220.

[38] S. Baghram, M. Farhang and S. Rahvar, Phys. Rev. D75 (2007) 044024, astro-ph/0701013.

[39] D. Bazeia et al., Phys. Lett. B649 (2007) 445, hep-th/0701106.

[40] P.J. Zhang, Phys. Rev. D76 (2007) 024007, astro-ph/0701662.

[41] B. Li and J.D. Barrow, Phys. Rev. D75 (2007) 084010, gr-qc/0701111.

[42] T. Rador, Phys. Rev. D75 (2007) 064033, hep-th/0701267.

[43] T. Rador, Phys. Lett. B652 (2007) 228, hep-th/0702081.

[44] L.M. Sokolowski, Class. Quantum Grav. 24 (2007) 3391, gr-qc/0702097.

[45] V. Faraoni, Phys. Rev. D75 (2007) 067302, gr-qc/0703044.

[46] O. Bertolami et al., Phys. Rev. D75 (2007) 104016, arXiv:0704.1733 [gr-qc].

[47] S.K. Srivastava, (2007), arXiv:0706.0410 [hep-th].

[48] S. Capozziello, V.F. Cardone and A. Troisi, JCAP 0608 (2006) 001.

[49] A.A. Starobinsky, JETP Lett. 86 (2007) 157, arXiv:0706.2041 [astro-ph].

[50] A.Y. Kamenshchik, U. Moschella and V. Pasquier, Phys. Lett. B511 (2001) 265, gr-qc/0103004.

[51] H. Sandvik et al., Phys. Rev. D69 (2004) 123524, astro-ph/0212114.

[52] M. Visser, Class. Quant. Grav. 21 (2004) 2603, gr-qc/0309109.

[53] P. Jordan, Schwerkraft und Weltall (Braunschwig: Frierich Vieweg und sohn, 1955).

[54] C. Brans and R.H. Dicke, Phys. Rev. 124 (1961) 925.

[55] I.L. Buchbinder, S.D. Odintsov and I.L. Shapiro, Effective Action in Quantum Gravity (Bristol: IOP Publishing, 1992).

[56] A.H. Guth, Phys. Rev. D23 (1981) 347.

[57] D. La and P.J. Steinhardt, Phys. Rev. Lett. 62 (1989) 376.

[58] D. La, P.J. Steinhardt and E.W. Bertschinger, Phys. Lett. B231 (1989) 231.

[59] P.J.E. Peebles and B. Ratra, Rev. Mod. Phys. 75 (2003) 559, astro-ph/0207347.

[60] V.F. Cardone, A. Troisi and S. Capozziello, Phys. Rev. D72 (2005) 043501, astro-ph/0506371.

[61] B. Boisseau et al., Phys. Rev. Lett. 85 (2000) 2236, gr-qc/0001066.

[62] A. Riazuelo and J.P. Uzan, Phys. Rev. D66 (2002) 023525, astro-ph/0107386.

[63] M. Demianski et al., Astron. Astrophys. 454 (2006) 55, astro-ph/0604026.

[64] M. Demianski et al., (2007), arXiv:0711.1043 [astro-ph].

[65] S. Capozziello et al., (2007), arXiv:0706.2615 [astro-ph].

[66] C.A. Clarkson, A.A. Coley and E.S.D. O'Neill, Phys. Rev. D64 (2001) 063510, gr-qc/0105026.

[67] S. Carloni, P.K.S. Dunsby and C. Rubano, Phys. Rev. D74 (2006) 123513, gr-qc/0611113.

[68] S. Carloni and P.K.S. Dunsby, Phys. Rev. D75 (2007) 064012, gr-qc/0612133.

[69] S. Nojiri and S.D. Odintsov, Phys. Rev. D74 (2006) 086005, hep-th/0608008.

[70] S. Capozziello, V.F. Cardone and A. Troisi, Mon. Not. Roy. Astron. Soc. 375 (2007) 1423, astro-ph/0603522.

[71] C.G. Böhmer, T. Harko and F.S.N. Lobo, arXiv:0709.0046 [gr-qc].

[72] S. Nojiri and S.D. Odintsov, Phys. Lett. B652 (2007) 343, arXiv:0706.1378 [hep-th].

[73] A.S. Eddington, The Mathematical Theory of Relativity (Cambridge: Cambridge University Press, 1952).

[74] N.H. Barth and S.M. Christensen, Phys. Rev. D28 (1983) 1876.

[75] H. van Elst, J.E. Lidsey and R.K. Tavakol, Class. Quant. Grav. 11 (1994) 2483, gr-qc/9404044.

[76] A.A. Starobinsky, Sov. Astron. Lett. 9 (1983) 302.

[77] J.D. Barrow and A.C. Ottewill, J. Phys. A16 (1983) 2757.

[78] A. Berkin, Phys. Rev. D42 (1990) 1016.

[79] G.J. Olmo, Phys. Rev. D72 (2005) 083505.

[80] S. Capozziello, S. Carloni and A. Troisi, Recent Res. Dev. Astron. Astrophys. 1 (2003) 625, astro-ph/0303041.

[81] T. Clifton and J.D. Barrow, Phys. Rev. D72 (2005) 103005, gr-qc/0509059.

[82] J.A. Leach, S. Carloni and P.K.S. Dunsby, Class. Quant. Grav. 23 (2006) 4915, gr-qc/0603012.

[83] J.D. Barrow and S. Hervik, Phys. Rev. D74 (2006) 124017, gr-qc/0610013.

[84] J.D. Barrow and J.D. Middleton, Phys. Rev. D75 (2007) 123515, gr-qc/0702098.

[85] G.F.R. Ellis and H. van Elst, Cosmological models (Cargése Lectures 1998) (Dordrect: Kluwer, 1998) pp. 1–116, gr-qc/9812046.

[86] G.F.R. Ellis, Relativistic cosmology, Cargése Lectures in Physics vol. 6, edited by E. Scatzman, pp. 1 – 59, NewYork: Gordon and Breach, 1973.

[87] S. Carloni et al., Class. Quant. Grav. 22 (2005) 4839, gr-qc/0410046.

[88] J. Wainwright and G.F.R. Ellis, editors, Dynamical Systems in Cosmology (Cambridge: Cambridge University Press, 1997).

[89] A.A. Coley, Dynamical systems and cosmology (Dordrecht: Kluwer Academic Publishers, 2003).

[90] J. Wainwright and W.C. Lim, J. Hyperbol. Diff. Equat. 2 (2005) 437, gr-qc/0409082.

[91] A.B. Burd and J.D. Barrow, Nucl. Phys. B308 (1988) 929.

[92] S.J. Kolitch and D.M. Eardley, Ann. Phys. 241 (1995) 128, gr-qc/9405016.

[93] S.J. Kolitch, Ann. Phys. 246 (1996) 121, gr-qc/9409002.

[94] C. Santos and R. Gregory, Annals Phys. 258 (1997) 111, gr-qc/9611065.

[95] D.J. Holden and D. Wands, Class. Quant. Grav. 15 (1998) 3271, gr-qc/9803021.

[96] S. Foster, Class. Quant. Grav. 15 (1998) 3485, gr-qc/9806098.

[97] L. Amendola, M. Litterio and F. Occhionero, Int. J. Mod. Phys. A5 (1990) 3861.

[98] A. Billyard, A. Coley and J. Ibanez, Phys. Rev. D59 (1999) 023507, gr-qc/9807055.

[99] D.J. Holden and D. Wands, Phys. Rev. D61 (2000) 043506, gr-qc/9908026.

[100] E. Gunzig et al., Class. Quant. Grav. 17 (2000) 1783.

[101] E. Gunzig et al., Phys. Rev. D63 (2001) 067301, gr-qc/0012085.

[102] A. Saa et al., Int. J. Theor. Phys. 40 (2001) 2295, gr-qc/0012105.

[103] V. Faraoni, Ann. Phys. 317 (2005) 366, gr-qc/0502015.

[104] S. Carloni et al., Class. Quantum Grav. 25 (2008) 035008, gr-qc/0701009.

[105] M. Abdelwahab, S. Carloni and P.K.S. Dunsby, (2007), arXiv:0706.1375 [gr-qc].

[106] N. Goheer, J.A. Leach and P.K.S. Dunsby, Class. Quant. Grav. 24 (2007) 5689, arXiv:0710.0814 [gr-qc].

[107] L. Amendola et al., Phys. Rev. D75 (2007) 083504, gr-qc/0612180.

[108] L. Amendola, D. Polarski and S. Tsujikawa, Phys. Rev. Lett. 98 (2007) 131302, astro-ph/0603703.

[109] G. Cognola, M. Gastaldi and S. Zerbini, (2007), gr-qc/0701138.

[110] N. Agarwal and R. Bean, (2007), arXiv:0708.3967 [astro-ph].

[111] K.N. Ananda and M. Bruni, Phys. Rev. D74 (2006) 023523, astro-ph/0512224.

[112] K.N. Ananda and M. Bruni, Phys. Rev. D74 (2006) 023524, gr-qc/0603131.

[113] A. Campos and C.F. Sopuerta, Phys. Rev. D63 (2001) 104012, hep-th/0101060.

[114] A. Campos and C.F. Sopuerta, Phys. Rev. D64 (2001) 104011, hep-th/0105100.

[115] A. Coley, Class. Quant. Grav. 19 (2002) L45, hep-th/0110117.

[116] A.A. Coley, Phys. Rev. D66 (2002) 023512, hep-th/0110049.

[117] P. Dunsby et al., Phys. Rev. D69 (2004) 101303, hep-th/0312174.

[118] N. Goheer et al., Phys. Rev. D70 (2004) 123517, hep-th/0408092.

[119] P. Hartman, Ordinary Differential Equations (New York: Wiley, 1964).

[120] D. Lovelock and H. Rund, Tensors Differential Forms and Variational Principles (New York: Dover, 1989).

[121] S. Rippl et al., Gen. Rel. Grav. 28 (1996) 193, gr-qc/9511010.

[122] S. Capozziello and R. de Ritis, Class. Quant. Grav. 11 (1994) 107.

[123] S. Capozziello, R. de Ritis and C. Rubano, Phys. Lett. A177 (1993) 8.

[124] S. Capozziello, S. Nojiri and S.D. Odintsov, Phys. Lett. B634 (2006) 93, hep-th/0512118.

[125] S. Capozziello et al., Phys. Lett. B639 (2006) 135, astro-ph/0604431.

[126] V. Faraoni, E. Gunzig and P. Nardone, Fund. Cosmic Phys. 20 (1999) 121, gr-qc/9811047.

[127] E.E. Flanagan, Class. Quant. Grav. 21 (2004) 3817, gr-qc/0403063.

[128] L.M. Sokolowski, Class. Quant. Grav. 24 (2007) 3391 , gr-qc/0702097.

[129] T. Padmanabhan, Highlights in Gravitation and Cosmology, edited by B. Iyer et al., p. 156, Cambridge: Cambridge University Press, 1988.

[130] K. Yano, Integral Formulas in Riemannian Geometry(Pure and Applied Mathematics: A Series of Monographs) (New York: Marcel Dekker Inc., 1970).

[131] J.D. Barrow and S. Cotsakis, Phys. Lett. B214 (1988) 515.

[132] K.i. Maeda, Phys. Rev. D39 (1989) 3159.

[133] E. Kasner, Trans. Am. Math. Soc. 27 (1925) 101.

[134] J.D. Barrow and T. Clifton, Class. Quant. Grav. 23 (2006) L1, gr-qc/0509085.

[135] T. Clifton and J.D. Barrow, Class. Quant. Grav. 23 (2006) 2951, gr-qc/0601118.

[136] R. Maartens and D.R. Taylor, Gen. Rel. Grav. 26 (1994) 599.

[137] G.F.R. Ellis, J. Math. Phys. 8 (1967) 1171.

[138] J.M. Stewart and G.F.R. Ellis, J. Math. Phys. 9 (1968) 1072.

[139] H. van Elst and G.F.R. Ellis, Class. Quant. Grav. 13 (1996) 1099, gr-qc/9510044.

[140] S.W. Goode and J. Wainwright, Class. Quant. Grav. 2 (1985) 99.

[141] E.F. Bunn, P. Ferreira and J. Silk, Phys. Rev. Lett. 77 (1996) 2883, astro-ph/9605123.

[142] A. Kogut, G. Hinshaw and A.J. Banday, Phys. Rev. D55 (1997) 1901, astro-ph/9701090.

[143] T.R. Jaffe et al., Astrophys. J. 629 (2005) L1, astro-ph/0503213.

[144] C.B. Collins and S.W. Hawking, Astrophys. J. 180 (1973) 317.

[145] S.H. Strogatz, Nonlinear Dynamics and Chaos (Cambridge, Massachusetts: Perseus Books, 1994).

[146] R.W. Wald, Phys. Rev. D28 (1983) 2118.

[147] M. Goliath and G.F.R. Ellis, Phys. Rev. D60 (1999) 023502, gr-qc/9811068.

[148] T. Clifton and J.D. Barrow, Phys. Rev. D72 (2005) 123003, gr-qc/0511076.

[149] C.G. Böhmer, L. Hollenstein and F.S.N. Lobo, Phys. Rev. D76 (2007) 084005, arXiv:0706.1663 [gr-qc].

[150] J.D. Barrow et al., Class. Quant. Grav. 20 (2003) L155, gr-qc/0302094.

[151] R.C. Tolman, Relativity Thermodynamics and Cosmology (Oxford University Press, 1934; Dover, 1987).

[152] S. Carloni, P.K.S. Dunsby and D.M. Solomons, Class. Quant. Grav. 23 (2006) 1913, gr-qc/0510130.

[153] T. Clifton, Class. Quant. Grav. 24 (2007) 5073, gr-qc/0703126.

[154] D.M. Solomons, P. Dunsby and G. Ellis, Class. Quant. Grav. 23 (2006) 6585, gr-qc/0103087.

[155] S. Carloni, A. Troisi and P.K.S. Dunsby, (2007), arXiv:0706.0452 [gr-qc].

[156] H. Poincaré, J. Mathématiques 7 (1881) 375.

[157] L. Perko, Differential equations and dynamical systems (New York: Springer Verlag, 1996).

[158] N. Goheer, J.A. Leach and P.K.S. Dunsby, Class. Quantum Grav. 25 (2008) 035013, arXiv:0710.0819 [gr-qc].

[159] C.B. Collins, Commun. Math. Phys. 23 (1971) 137.

[160] S. Capozziello and R. de Ritis, Int. J. Mod. Phys. D2 (1993) 367.

[161] S. Capozziello et al., Riv. Nuovo Cimento 19N4 (1996) 1.

[162] N.D. Birrell and P.C.W. Davies, Quantum Fields in Curved Space (Cambridge: Cambridge University Press, 1982).

[163] S. Capozziello, R. de Ritis and A.A. Marino, Class. Quant. Grav. 14 (1997) 3243, gr-qc/9612053.

[164] L. Amendola, Phys. Rev. D60 (1999) 043501, astro-ph/9904120.

[165] J.D. Barrow and K.i. Maeda, Nucl. Phys. B341 (1990) 294.

[166] R. Gannouji et al., JCAP 0609 (2006) 016, astro-ph/0606287.

[167] J. Garcia-Bellido and M. Quiros, Phys. Lett. B243 (1990) 45.

[168] T. Damour and K. Nordtvedt, Phys. Rev. D48 (1993) 3436.

[169] S. Capozziello, F. Occhionero and L. Amendola, Int. J. Mod. Phys. D1 (1993) 615.

[170] A. Challinor, Class. Quant. Grav. 17 (2000) 871, astro-ph/9906474.

[171] B. Leong et al., Phys. Rev. D66 (2002) 104010, astro-ph/0208015.

[172] U. Seljak and M. Zaldarriaga, Astrophys. J. 469 (1996) 437, astro-ph/9603033.

[173] A. Lewis, A. Challinor and A. Lasenby, Astrophys. J. 538 (2000) 473, astro-ph/9911177.

[174] P.K.S. Dunsby, B.A.C.C. Bassett and G.F.R. Ellis, Class. Quant. Grav. 14 (1997) 1215, gr-qc/9811092.

[175] U. Seljak and M. Zaldarriaga, Phys. Rev. Lett. 78 (1997) 2054, astro-ph/9609169.